Electronics and Computer Science
Faculty of Engineering and Physical Sciences
University of Southampton

Yi Farn Lim
yfl1f18@soton.ac.uk
20/04/2022

Improving Robotic Grasping using Iterative Learning Control

Project supervisor: Professor Christopher Freeman
Second examiner: Doctor Nicolas Green

A project report submitted for the award of
MEng Electrical and Electronics Engineering

Abstract

Over millions of years of evolution, nature has perfected one of the most widely used features of humans. Hands, particularly fingers allow humans to grasp and manipulate everyday object. As such, the environment has been adapted to suits human's operation. Therefore, to allow robots to operate effectively, they have to behave like humans in some way such as able to walk up fleets of stairs, grasp and manipulate object. Many research has been carried out focusing on the hardware aspect of robotic gripper such as flexible, multiple fingers, suction. However, research into the controller side of robotic grasping is limited. This causes most industrial sized robots to operate slowly, with a low mean grasp per hour, only able to operate in a tightly controlled environment while doing specific tasks. To fully exploit the potential of robots assisting human, robotic grasping has to at least be on par with humans capability.

Due to the large potential of robotics, there has been significant investments brought into this area. It is expected that robotic market would experience a growth of 17.45% per annum [2]. This has encouraged further development into control and decision algorithm on selecting grasping task, methods, and performance the task accurately and reliably. This project will focus on designing an Iterative Learning Control (ILC) algorithm to allow the gripper to grasp and transport various objects securely and safely.

Most currently used grasping controllers uses Impedance Control which does not improves itself after each iteration. As grasping is a repetitive action, the performance of the controller can be improved by learning previous iterations errors, similar to a footballer practising shooting repetitively. There has been ONE well known research of robotic grasping utilising simple learning controllers. Therefore, a novel approach is taken to use an advance model-based (Norm-Optimal) ILC Controllers for robotic grasping. To evaluate the effectiveness of this new control algorithm, a simulation environment is designed to replicate the physical system. The performance of the new controller is compared against a conventional Impedance Controller.

This project has achieved strong results and improve robotic grasping in the following areas;

- Built an accurate and realistic simulation model of the actual physical system using MATLAB Simulink with Simscape Multibody toolbox.
- Increase mean grasp per hour.
- Ability to grasp object of different weight.
- Ability to correct itself after encountering numerous common disturbances
- Lower average grasping force compared to conventional Impedance Controller

This project offers the potential of using a low complexity learning controller for a very repetitive operation over conventional non-learning controller.

Statement of Originality

- I have read and understood the ECS Academic Integrity information and the University's Academic Integrity Guidance for Students.
- I am aware that failure to act in accordance with the Regulations Governing Academic Integrity may lead to the imposition of penalties which, for the most serious cases, may include termination of programme.
- I consent to the University copying and distributing any or all of my work in any form and using third parties (who may be based outside the EU/EEA) to verify whether my work contains plagiarised material, and for quality assurance purposes.

You must change the statements in the boxes if you do not agree with them.

We expect you to acknowledge all sources of information (e.g. ideas, algorithms, data) using citations. You must also put quotation marks around any sections of text that you have copied without paraphrasing. If any figures or tables have been taken or modified from another source, you must explain this in the caption and cite the original source.

I have acknowledged all sources, and identified any content taken from elsewhere.

If you have used any code (e.g. open-source code), reference designs, or similar resources that have been produced by anyone else, you must list them in the box below. In the report, you must explain what was used and how it relates to the work you have done.

I have not used any resources produced by anyone else.

You can consult with module teaching staff/demonstrators, but you should not show anyone else your work (this includes uploading your work to publicly-accessible repositories e.g. Github, unless expressly permitted by the module leader), or help them to do theirs. For individual assignments, we expect you to work on your own. For group assignments, we expect that you work only with your allocated group. You must get permission in writing from the module teaching staff before you seek outside assistance, e.g. a proofreading service, and declare it here.

I did all the work myself, or with my allocated group, and have not helped anyone else.

We expect that you have not fabricated, modified or distorted any data, evidence, references, experimental results, or other material used or presented in the report. You must clearly describe your experiments and how the results were obtained, and include all data, source code and/or designs (either in the report, or submitted as a separate file) so that your results could be reproduced.

The material in the report is genuine, and I have included all my data/code/designs.

We expect that you have not previously submitted any part of this work for another assessment. You must get permission in writing from the module teaching staff before re-using any of your previously submitted work for this assessment.

I have not submitted any part of this work for another assessment.

If your work involved research/studies (including surveys) on human participants, their cells or data, or on animals, you must have been granted ethical approval before the work was carried out, and any experiments must have followed these requirements. You must give details of this in the report, and list the ethical approval reference number(s) in the box below.

My work did not involve human participants, their cells or data, or animals.

ECS Statement of Originality Template, updated August 2018, Alex Weddell aiofficer@ecs.soton.ac.uk

Acknowledgements

I would like to acknowledge and thank my supervisor, Professor Christopher Freeman who made this project possible. His guidance and enthusiasm throughout the project stages has truly made it fun and enjoyable.

I would also like to thank my family for their constant support and encouragement during my time at the university as well as welfare check on my mental and physical health.

And finally, thank you to University of Southampton for making this journey special and memorable.

Contents

2149 -> 1758
1750 -> 1522
1354 -> 1109
2112 -> 1719
1549 -> 1075
2694 -> 2095
1424 -> 1216
514 -> 502
13546 -> 10996

1 Review of Robotic Gripping Controller

Humans are hard to pleased, we experience fatigue, emotions, demand higher pay and so on. Therefore, industry has adopted automation concept since early 1970s, during the Third Industrial Revolution [1]. Automation uses computers and robots to assist humans in repetitive, predictable tasks and could theoretically operate 24 hours a day, 7 days a week while keeping the long-term operating cost to the minimal.

From a simple Roomba vacuum cleaner to the state-of-the-art robotic arm assembly system found in car manufacturing, the demand for personal and industrial robots is on a rapid rise. As such the global robotics market was valued by Mordorintelligence to be at USD 27.73 billion in 2020 and is expected to grow to USD 74.1 billion by the end of 2026 [2].

There is a race to develop a robot that could 'do it all'. Amazon, one of the leading e-commerce giants has gone as far as hosting a yearly competition that challenges teams around the world to design and showcase robots that is capable of separating different types of objects ranging from soft toy to toothbrush and sort them according to the customer's order [3]. Not only that, recently an interview conducted by Tom Scott on Orcardo Grocery warehouse a 'Hive system' could be used for online grocery shopping, where an approximately 2300 robots are in charge of identified, picked, place and sort goods from the warehouse to each individual customer basket ready to be packed and delivered to the users around the UK in a 5-hour window [4].

Although robots have evolved massively since the early 1970s, it is still far from what humans are capable. There are numerous issues that hinders the performance of robots. These issues motivate this research to investigate and attempts to mitigate effect caused by the issues.

1.1 Problem Analysis

The advantageous of having robots to assist humans has only been realised about half a decade ago, but humans have been developing buildings, structures, system for centuries. It comes as no surprise that the biggest problem faced by robots is that the world around them is optimised for humans and not robots [4]. Humans have a few powerful tools at their disposal that current generation of robots are lacking, such as powerful processing power (Brain), the ability to move around freely and easily (Legs) and the ability to grasp and manipulate objects (Hands). AlphaGo has demonstrated the advancement in processing power while Boston Dynamics shows that robot can move freely with leg-like configuration, however, the development for grasping and ultimately manipulation is relatively slow.

For robots to interact with the world, they require the ability to grasp and manipulate object freely and effectively. To achieve this, it is crucial to develop both the hardware and software of a gripper.

One of the most advance grasping control system, Dex-Net 4.0 is capable of grasping 300 items per hour with a success rate of 95% [5]. On the contrary, an average human is capable of grasping between 400 to 600 items per hour [3]. To overcome this challenge, the repetitive nature of grasping and interaction behaviour between robots and environment need to be realised and thus the controller has to be able to fulfil a range of criteria:

- Learn from previous grasping error/mistakes.
- Able to correct itself from environmental disturbance.
- Ensure the deadtime between each operation is to the minimum.

- Uses least amount of force.
- Capable of grasping a range of objects.

1.2 Approach to Robotic Grasping

Robotic grasping research can be split into 2 categories, Hardware and Controller. Hardware deals with the physical structure of the gripper including what type of gripper to be used as well as what materials it should be made out of while controller plans and execute the action to complete the required task in a safe and secure manner.

Grasping requires the gripper to interact with the environment or object. Over the past decade, different gripper hardware has been developed and tested. All gripper has one feature in common – a finger-like structure. These fingers come in various shapes and sizes depending on the task requirement such as a simple parallel 2-plate gripper (Fig. 1.1a), fingers aligned in a claw structure for a more stable grasp (Fig. 1.1b), suction cup gripper controlled by pressurised air to handle delicate objects by spreading the pressure out evenly (Fig. 1.1c) and incorporating 'softness' to gripper by exploiting compliance properties which is capable of curling and straightening by adjusting the pressurised air sent to the fingers (Fig. 1.1d). [3]

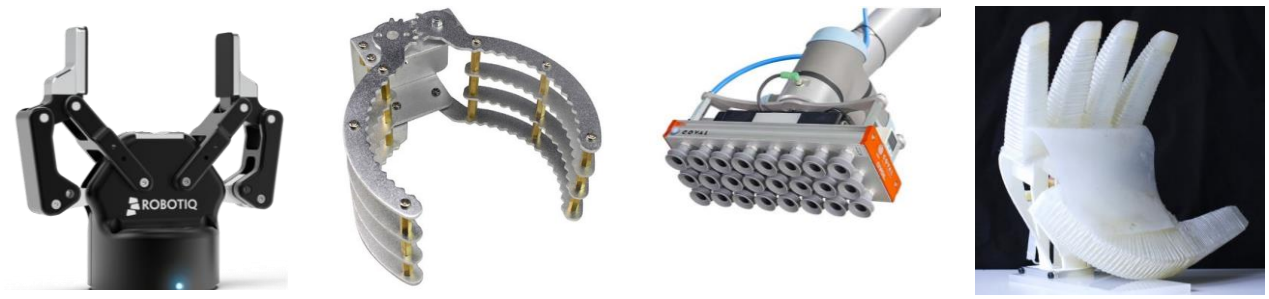

(a) Parallel Plate Gripper (b) Crawl Gripper (c) Suction cup Gripper (d) Compliance Gripper

Figure 1.1: Common types of Grippers

Control process of grasping can be further split into 3 categories, Task selection, Motion planning and Motion Control. There are 3 different autonomy levels to realise the 3 tasks as identified by Ozawa [6] as illustrated in Figure 1.2. Master-Slave systems employs a 'dummy' small scale manipulator for the operators and the gripper would mimic the operation. Where shared autonomy includes the operator manually selecting the grasping tasks and provides a minimal correction on the gripper operation. Recently with the development of Machine Learning, the task of the operator reduces to as little as instructing the robot with general instructions such as move items from one location to another and the algorithm would autonomously decide on the grasping strategies [3, 11].

Task selection relates to how the gripper should grasp an object. The simplest way is for robots to 'copy' humans' grasping methods and actions known as grasp taxonomy. There have been extensive studies on this area, with some generalising human grasping into 6 ways [7, 8], while others into 16 ways [9]. Some studies have even gone as far as analysing how interaction forces are distributed during grasping action. But these different grasping methods can be further generalised based on the shape of grasp into 5 classes (non-grasp, grasp, positioning/orientation, regrasp, object interaction) illustrated in Figure 1.3 [6].

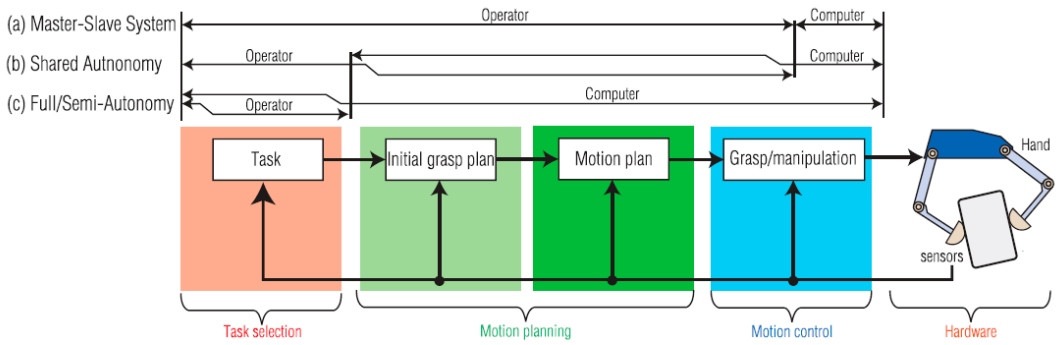

Figure 1.2: Autonomy of robotic gripper

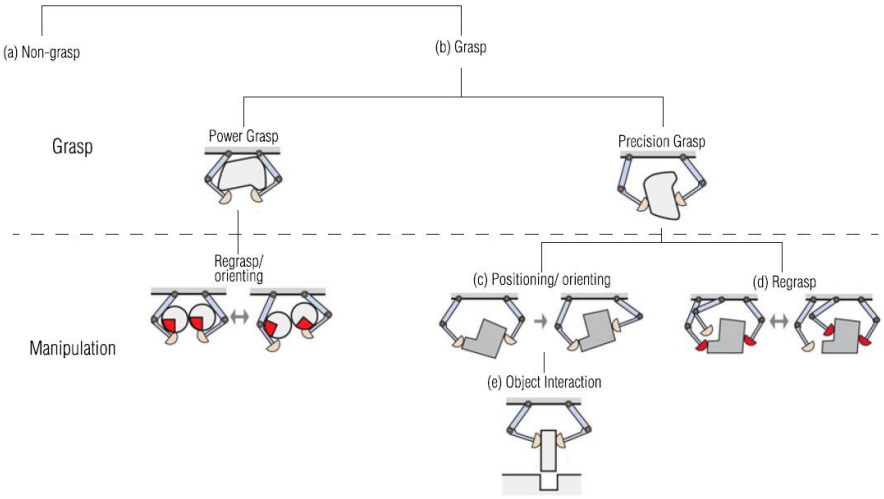

Figure 1.3: Grasp category

Motion planning plans initial grasping point and motion for a successfully grasp. The controller requires some information of the object such as size and orientation to deduce a safe grasp, manipulate and transport strategy. For the controller to work out a grasping strategy, contacts between gripper and object are modelled. There are a few widely used contacts modelling models, such as frictionless point contact which only models normal force, friction point contact which also models tangential force, and soft finger contact which also models torsional moment. Details of these basic contact model are explained by Ozawa [6].

Finally, motion control corrects any error to allow the gripper to realise the initial planned motion. The following section will investigate different types of motion control controller for robotic grasping in chronological order.

1.3 A History of Controllers for Robotic Grasping

The role of grasping controller is to ensure that the object is grasped securely to successfully complete the grasping task. Generally, this requires the control of finger movement.

Sequential controller is the simplest controller where it selects a certain grasping motion from a series of pre-programmed motions. In the experiment conducted by Tamashita [12], the controller is pre-programmed with 20 primary motions and the task of the controller is to follow the pre-programmed motion selected by the operator. This controller however lacks the ability to grasp the object optimally

as it is not able to produce the ‘overall best’ motion but rather the ‘best’ from the list of pre-programmed motions.

Reflexive controllers increase the grasping possibility to infinite and can be imagined by observing a young baby grasping an object. As an object gets in contact to the palm, the baby instinctively closes the fingers and grasp the object. If attempts are made to remove the object, the baby would grasp harder to oppose the motion. Commonly light or optical sensors are embedded inside each jaw of the gripper [13, 14] to detect contact between gripper and object. The flaw of the controller is its inability to detect the applied force which could damage the goods as excessive force is applied. This problem could be mitigated with some form of external sensors such as visual or force.

Hybrid controller that controls both the position and force simultaneously. Many hybrid controllers require the internal force to be dynamically decoupled from its motion by using model-based controller such as the one investigated by Shin and Lee [15]. Where the controller uses the error between the desired and actual position and force signal to alter the joint acceleration to reduce excessive force applied to the object.

Often, system dynamics are hard to be abstracted/modelled. Thus, adaptive controller is one of the non-model-based controllers. Adaptive controller is able to retain excellent motion tracking ability even when there is uncertainty (mass, inertia, centre of mass) while dynamically decoupling the internal force of the contact [16]. Other advantageous of adaptive controllers are its similar robustness, much higher tracking accuracy and performs well in high speed despite having uncertainties when compared to simple PD or hybrid controller [17]. Performing well when operated in high speed is desirable as this allows the gripper to be able to pick more items per hour.

Impedance controller on the other hand is simple, as it models the interaction force using mechanical impedance. Mass-spring-damper [18] structure is often used to model the interaction forces between the gripper and environment without the need to know the system dynamics or to decouple the internal forces. To reduce the complexity of controlling a multi-finger gripper, often multiple fingers involved in manipulation are combined together and be represented by a single mass and inertia structure [19]. Due to its simple structure, impedance control has been gaining a lot of attention in recent years and is currently one of the most used control schemes for grasping.

All controllers discussed above does not utilise errors from previous iteration which are often rich in information [20]. Therefore, this motivates learning controllers. Iterative learning controller (ILC) proposed by Nakayama [21] uses a non-model-based P-type controller to minimise the position and force error where after 30 iterations, the gripper trajectory was identical to the ideal trajectory. Nakayama also states that the convergence of position tracking would always lead to the convergence force applied. However, research into ILC is very limited.

A summary of the advantages and disadvantages of each controller discussed is shown in Table 1.1.

Table 1.1: Comparison between different grasping controllers

Name	Complexity	No. of grasping sequence	Force control	Decouple internal force?	Knowledge of system dynamics?	Use previous iteration error?
Sequential	Simple	Finite	No	N/A	N/A	No
Reflexive	Simple	Infinite	No	N/A	N/A	No
Hybrid position/force	Moderate	Infinite	Yes	Yes	Yes	No
Adaptive	Moderate	Infinite	Yes	Yes	No	No
Impedance	Simple	Infinite	Yes	No	No	No
Learning	Moderate	Infinite	Yes	No	Depends on scheme	Yes

1.4 Importance of Simulation

With the recent rapid development of computer hardware technology, simulation has become a crucial first step in product development and research. Simulation offers a platform where research, development and modification can be tested in a virtual environment within a short time frame with low budget commitment before building a prototype. On top of that, simulation is also capable of providing valuable glimpse at any potential system flaws in a risk-free and safe environment. [22]

2 Detailed Specification

In the literature review, strength and weakness of different grasping controller was identified. It was discussed that robotic grasping often operates in a repetitive environment and most development has not utilised previous iteration errors which are often information rich. The research conducted on ILC concludes that the actual trajectory of the gripper is able to match the ideal trajectory but converges relatively slow since it uses non-model method. The limitation of current generation grasping controller identified in chapter 1.1 still remains.

Therefore, a novel approach is to design a grasping controller that utilises the advantageous of controllers discussed in chapter 1.3 to solve the limitation discussed in chapter 1.1. As such, the following design requirements was identified.

2.1 Design Requirements

The following design requirements focus on the selection of simulation environment and model used to evaluate the controller.

DR1. Simulation model is chosen such that it is **closely relates to real industrial robotic configuration**. This ensures that the controller is tested on a representative system and the result can correlate to the industry.
DR2. Simulation should **model real world interaction dynamics/forces**. This allows minimal inaccuracy between simulation environment and real world thus ensures the results are representative.
DR3. The simulation should **contain visual models**. Visual models are crucial to not only showcase the achievement of the controller but also to assists in discovering any potentially 'hidden' issues that might not be captured by just analysing the data.

The following design requirements highlights the aim for the controller to eliminate or reduce limitations raised in chapter 1.1.

DR4. The robot (arm and gripper) shall be able to **reach and grasp the object accurately**. The normalised position error should be less than 0.01 within the first 15 iterations of operations. This ensures the robot has a fast start up time.
DR5. The robot (arm and gripper) shall be able to **reach and grasp the object quickly**. The complete reach-grasp-return trajectory should be completed within 5 to 7 seconds to gives the robot a 514 to 720 means pick per hour.
DR6. The gripper shall grasp the object with the **least amount of force**. It shall not exceed 25% of the ideal force within 20 iterations of grasping the object securely. This ensures minimal excessive force is applied while considering any uncertainties in the environment and object modelling.
DR7. The robot (arm and gripper) shall be capable of **grasping object of different mass**. The object would range between 0.2kg to 2kg. This ensures the robot is capable of grasping a range of objects.
DR8. The robot (arm and gripper) shall be capable of adjusting itself to **correct for a range of repetitive disturbances**. The robot will be subjected to the following disturbance scenarios (DS)

DS1. **Constant error**. The error shall have a magnitude of 5-10%. This arise when there is an initial state error due to inaccurate tuning or wear and tear while the robot is operating.
DS2. **Impulsive error**. The error shall have a magnitude of 5-10%. This arise when the robot bumps into items or massive wear and tear in certain isolated part of the system.

2.2 Overview of Iterative Learning Control (ILC)

Iterative learning control uses information rich errors from previous iterations and learn from it. ILC has been successfully implemented in numerous other applications with some notable advantageous such as the ability to control motion with high precision [23], to remove disturbances asymptotically [24] and high robustness where it is capable of converging even in situations where there are uncertainties in system parameters estimates [25].

Therefore, considering the success of ILC in other applications and exploiting the repetitiveness of grasping, there is a strong motivation to employ ILC as grasping controller to meet the design requirements set out in chapter 2.1.

ILC can be split into model based and non-model based, and the following 2 subsections will investigate them further.

2.2.1 Non-Model based ILC

2.2.1.1 D-Type

The earliest ILC controller was proposed by Arimoto [26] where the algorithm uses the error generated by the previous iteration to modify the next iteration input vector. Vectors are used to allow the algorithm to perform batch process between each iteration. The update equation was defined as

$$\boldsymbol{u}_{k+1}(t) = \boldsymbol{u}_k(t) + \beta(t)\dot{\boldsymbol{e}}_k(t) \tag{2.1}$$

and the error

$$\boldsymbol{e}_k(t) = \boldsymbol{r}(t) - \boldsymbol{y}_k(t) \tag{2.2}$$

where $\boldsymbol{u}_{k+1}(t)$ is the next iteration input vector, $\boldsymbol{u}_k(t)$ is the current iteration input vector, $\beta(t)$ is the learning gain matrix, $\dot{\boldsymbol{e}}_k(t)$ is the derivative of current iteration error $\boldsymbol{e}_k(t)$, $\boldsymbol{r}(t)$ is the reference trajectory, $\boldsymbol{y}_k(t)$ is the actual system trajectory and k is the iteration number.

The system will converge to 0 error when the iteration number goes infinite, and the convergence criteria is met. Otherwise, the system might experience divergence where the error increases.

2.2.1.2 P-Type

Some disadvantages of performing derivation of current iteration error includes the chance of amplifying small error and requiring more processing power. Therefore Arimoto [27] proposed a P-type ILC defined as follows

$$\boldsymbol{u}_{k+1}(t) = \boldsymbol{u}_k(t) + \beta(t)\boldsymbol{e}_k(t) \tag{2.3}$$

Since non-model-based algorithm converges slower than model-based counterpart due to not directly countering the system dynamics, other variations of non-model based ILC controllers such as PD, D-alpha, Higher order, etc that would be omit here.

2.2.2 Model Based ILC

Model based ILC requires the knowledge of the plant, particularly the system dynamics.

Plant models can be obtained through learning using data from multiple trails. Theoretically, if the abstracted model is identical to the actual plant, the system would converge in 1 iteration. However, it is impossible and unpractical to model an identical plant, therefore studies have shown if the plant is not accurate, the system will take more iterations to converge. As more iterations are conducted, the difference between the expected output and actual output can be used to tune the model to increase its accuracy [28].

2.2.2.1 Inverse Plant ILC

Inverse plant ILC directly counters the plant dynamics with its inverse.

The output of the system is

$$y_k(t) = G^0(u_k(t)) \tag{2.4}$$

where G^0 denotes the true plant. The error equation remains unchanged as denoted in Equation 2.2. As the plant is known, the optimal input sequence can be obtained as follows

$$u_k(t) = -G^0(r(t))^{-1} \tag{2.4}$$

where $G^0(.)^{-1}$ denotes the inverse of G^0.

The disadvantage of inverse plant method is any inaccuracy in the model or environmental disturbance can cause significant problems to the system. However, this method is acceptable even when there are uncertainties if the model updates the difference after each iteration [29].

2.2.2.2 Norm-Optimal ILC

Norm-optimal method works by optimising a cost function.

One such attempt is to minimise the tracking error described by Equation 2.5.

$$J(\boldsymbol{u}^*(k)) = \min_u J(\boldsymbol{u}(k)) \tag{2.5}$$

By using gradient descent, the optimal input that minimises the cost function can be obtained [30].

$$\nabla_u J = \left[\frac{\partial J}{\partial \boldsymbol{u}_i}\right] = 0 \tag{2.6}$$

To further improves the performance, the learning gain should change proportionally with error size. Thus, the gradient descent step size should be chosen automatically [31].

A new minimisation problem has been identified by Amann et al. [32] which is able to reduce each iteration normalised tracking error, automatically choose step size for cost function and improve robustness is described as follows

$$u_{k+1} = \arg\min_{u_{k+1}} \{J_{k+1}(u_{k+1})\} \tag{2.7}$$

where the cost function and error are defined as

$$J_{k+1}(u_{k+1}) = \|e_{k+1}\|_y^2 + \|u_{k+1} - u_k\|_u^2 \tag{2.8}$$

$$e_{k+1} = r - y_{k+1} \tag{2.9}$$

$$y_{k+1} = Gu_{k+1} \tag{2.10}$$

where spaces $\mathcal{U}$ and $\mathcal{Y}$ are ℓ_2-spaces.

Detailed calculation has been omitted but can be found at paper published by Amann et al. [32]. The final input sequence after solving the minimisation problem in Equation 2.7 is as follow

$$u_{k+1} = u_k + (R + QG^TG)^{-1}QG^Te_k \tag{2.11}$$

Where R and Q are diagonal matrices. R minimises the change in input sequence between iterations while Q minimises the tracking error. Careful tuning of the parameters ensures that the tracking error minimises quickly while ensuring excessive control effort is not injected to ensure smooth operation.

2.3 Overview of Impedance Control

To quantify the improvements ILC should make over conventional controllers, a baseline controller should be developed and subject to the same test. After reviewing Tabl3 1.1, impedance control is chosen as a baseline comparison controller due to its simple and easy implementation while giving promising result. This chapter will briefly introduce impedance control algorithm adopted in modern grasping control.

Impedance control can be regarded as mechanical impedance and is normally used to described complex system using a mass-spring-damper system shown in Figure 2.1. Causality is an important concept in impedance control. Typically, the robot would act as impedance where the environment would behave as admittance since the environment is often composed by inertia where it accepts effort and produce flow.

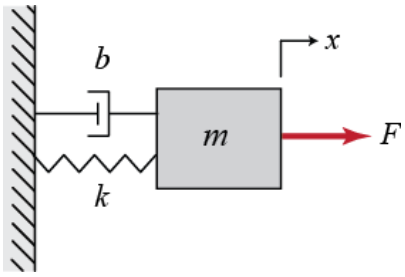

Figure 2.1: "Mass-spring-damper system" by ControlTutorialsForMatlab&Simulink is licensed under CC BY 4.0

This system can be described by the following equation

$$F = Ma + Cv + Kx \tag{2.12}$$

where M denotes the inertia, B denotes viscous damper, K denotes stiffness, a denotes acceleration, v denotes velocity and x denotes displacement.

Realising acceleration is double differentiation of displacement and velocity is the differentiation of displacement, by using the concept of Laplace transform, equation 2.12 can be written as

$$F(s) = (Ms^2 + Cs + K)X(s) \tag{2.13}$$

where it can be rearranged to form the following transfer function

$$\frac{X}{F}(s) = \frac{1}{Ms^2+Cs+K} \tag{2.14}$$

The two methods which are commonly used to implement the transfer function are integration and discretisation method [33]. In this project, integration method would only be considered as it is more widely used in grasping operation [34, 35]. Integration method was proposed by Caccavale et al. [36] to robot in the configuration presented in Figure 2.2.

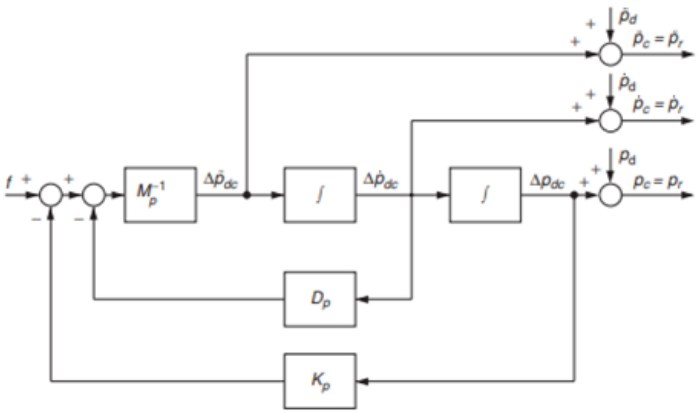

Figure 2.2: Block diagram for Impedance control using Integration method

The operator would be tasked to choose 3 values, namely inertia (M_p), damping (D_p) and stiffness (K_p). Intuitively there is a relationship between grasping force and gripper end factor location, the algorithm will calculate the difference between the desire and actual force and adjust the gripper grasping displacement, velocity, and acceleration accordingly. This method has been tested to perform exceptionally well under different environment (soft and stiff) [33].

3 Design Overview

This section will provide a high-level overview and general approach for 4 crucial parts of the project:

- **Simulation environment,** including simulation software selection, robot selection and modelling overview.
- Design of **robot (excluding gripper) controller** for moving the gripper to and from the desired location.
- Design of **gripper controller** including a baseline impedance controller and ILC controller that would fulfil the design requirements set out in chapter 2.1.
- Test and evaluate controller performance under different **disturbance** set out in chapter 2.1.

As the project is complex, each of the 4 parts of the project will be split further into multiple bite size subparts to ensure each feature is thoroughly tested, verified, and analysed. Project management techniques and plans can be found in Appendix A.

3.1 Simulation Environment

DR1 requires the simulation robot model to be representative of current industrial robot. There are 2 commonly used configuration in the industry, gantry robot and robotic arm. Gantry robot consists of 3 independent axis actuator that moves a gripper along the X, Y and Z axis and has a cuboid work volume while robotic arm combines multiple joints to moves the gripper and has a sphere work volume. Gantry robot is the simplest configuration and Ratcliffe [37] has identified the system dynamics of one such system shown in Figure 3.1. Therefore, this is an ideal robot to test the gripper controller algorithm before preceding to the more complicated robotic arm system.

Figure 3.1: Proposed gantry robot by Ratcliffe

According to chapter 1.2, parallel plate grippers are the simplest and most universal. Thus, to keep the complexity down, parallel plate grippers is chosen.

There is numerous simulation software out in the market. Some are open-source, others required licensing. Focusing on university subscribed and open-source software; 3 most promising software for robotics has been identified, Gazebo, Webots, and MATALB.

Gazebo is open-source and is considered to be one of the widely used robotics software, it allows the designer complete control over simulation since it is integrated into ROS framework and is programmed in C++. However, Gazebo lack good documentation active community and is challenging to learn.

Webots is a good alternative to Gazebo as it has simple and easy to use GUI, huge model database, has an active community as well as good documentation. Webots is mainly programmed using C++ but there is API for other programming language such as Java, Python and even MATLAB [38].

Although MATLAB is proprietary, the university has subscription for education use. MATLAB is commonly best known for data analysis as well as its ginormous collection of toolboxes including one of the most widely used control system design toolbox. Simulink is built on top of MATLAB and is an easy-to-use graphical based simulation environment utilising 'drag and drop' design. Simscape multibody is an add-on of Simulink which allows the user to add graphical model to the simulation. However, the learning curve can be steep despite good documentation as well as the high CPU demand.

All 3 software are capable of simulating interaction force and contains 3D visual models which fulfils DR2 and DR3. Keeping in mind the aim of the project is to design a controller for a robot and the pros and cons listed in table 3.1, it is decided that the good numerical computation and control system design toolbox that MATLAB offers is the best choice to design, test and analyse the controller performance.

Table 3.1: Features comparison between robotic simulation software

Software	License	Documentation	Programming language (main)	Robotic models (built-in)	Control toolbox
Gazebo	Apache 2.0	Fair	C++	Fair	N/A
Webots	Apache 2.0	Decent	C++	Decent	N/A
MATLAB	University subscriptions	Good	MATLAB	Limited	Good

The steps to model gantry robot and contact forces in Simulink are shown in Figure 3.2.

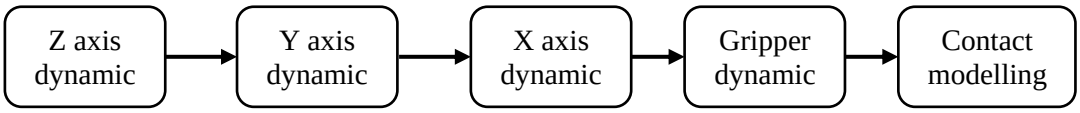

Figure 3.2: Steps on modelling gantry and environment dynamics in Simulink

3.2 Gantry Controller

After reviewing Ratcliff [37] thesis, it is concluded that Norm-Optimal ILC performs the best. Therefore, this project would use Norm-Optimal ILC to control the X, Y and Z axis of the gantry. Recall that equation 2.2 shows the equation for current iteration error while equation 2.11 shows the next iteration input vector update algorithm.

As this project focuses on motion controller, the ideal trajectory would be given by the operator and is predefined. Since each axis of the gantry robot are independent to each other, they are decoupled, and 3 separate controllers will be used. The R and Q values for each controller will be tuned to meet DR4 and DR5. The schematic for the controllers is shown in Figure 3.3.

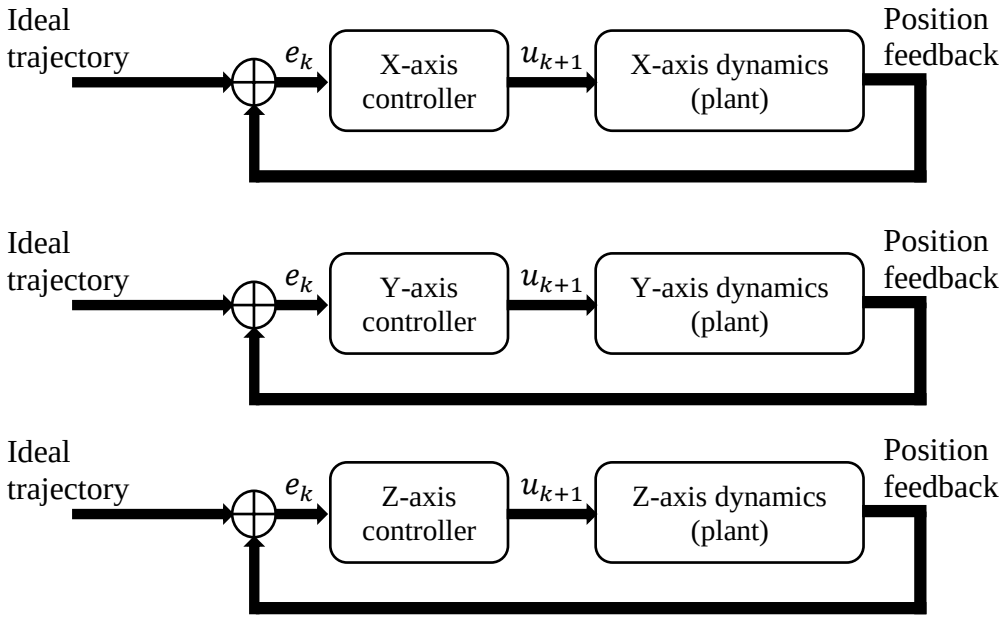

Figure 3.3: High-level schematic for X, Y and Z axis controllers

3.3 Gripper Controller

The following subsection will give an overview of the design schematic of Impedance and ILC controllers.

3.3.1 Impedance Control

Impedance controller focuses on minimising the force error between ideal and actual force by manipulating its grasping area, a position controller is needed to reduce position error [34]. Since ILC updates the input vector at the end of each iteration, it is not suitable to be used as impedance controller changes the grasping distance at each sampling time. A conventional PD controller is used instead, and the schematic is shown in Figure 3.4.

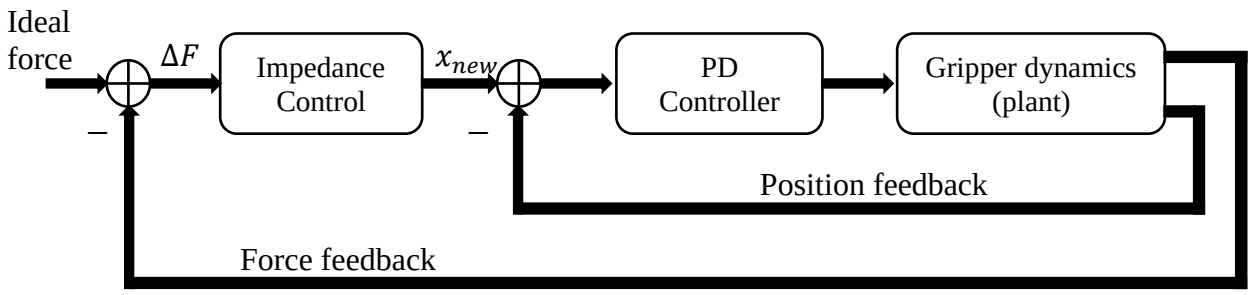

Figure 3.4: High-level schematic for impedance gripper controller

Where ΔF is force error and x_{new} is the new trajectory for the gripper to realise minimum force grasping. Upon digitising equation 2.12 and changing notation, the equation becomes

$$\Delta F(k) = M\Delta\ddot{x}(k) + B\Delta\dot{x}(k) + K\Delta x(k) \tag{3.2}$$

The equation can be rearranged to make $\Delta\ddot{x}(k)$ the subject as shown below

$$\Delta\ddot{x}(k) = M^{-1}(\Delta F(k) - K\Delta x(k) - B\Delta\dot{x}(k)) \tag{3.3}$$

Equation 3.3 is the impedance control update and can be represented in block diagram as shown in Figure 3.5.

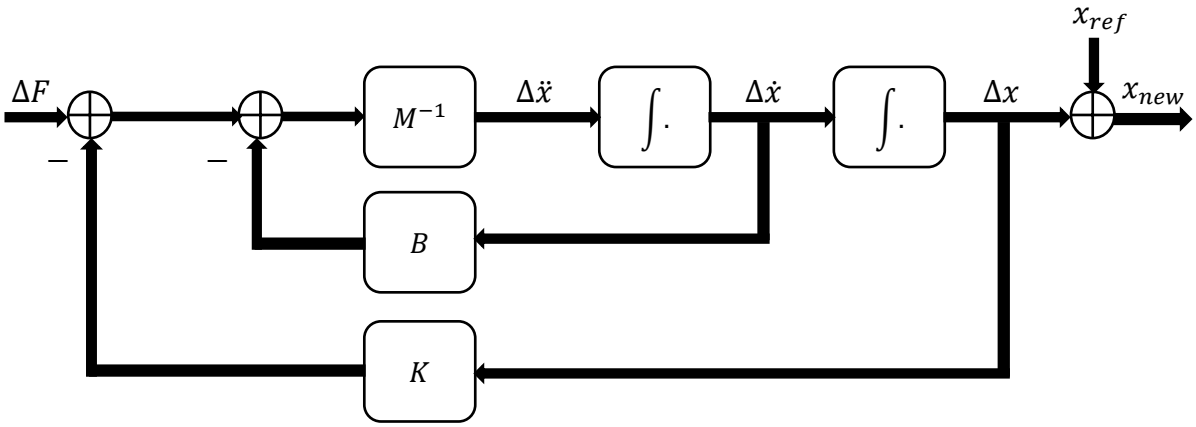

Figure 3.5: Impedance controller schematic

3.3.2 Iterative Learning Control

To realise DR4 to DR8 set out in chapter 2.1 and evaluating the advantageous and disadvantageous of each ILC scheme in chapter 2.2, norm-optimal ILC is decided to be the best.

However, since norm-optimal ILC requires minimising a cost function and Amann et al. [32] only minimises the tracking error, there is no single update equation that minimises both tracking and force error simultaneously. It is too complicated and time consuming for this project to evaluate equation that would produce a single update. Thus, it is decided that the position tracking of gripper would adopt norm-optimal approach described in equation 2.11, while force control will use a simple update shown in equation 3.4.

$$\boldsymbol{r}_{k+1}(t) = \boldsymbol{r}_k(t) + \beta(t)\Delta\boldsymbol{F}_k(t) \tag{3.4}$$

Where r_k denotes the last iteration reference trajectory, scalar gain β and $\Delta\boldsymbol{F}_k$ denotes the force error.

The schematic for ILC is shown in Figure 3.6.

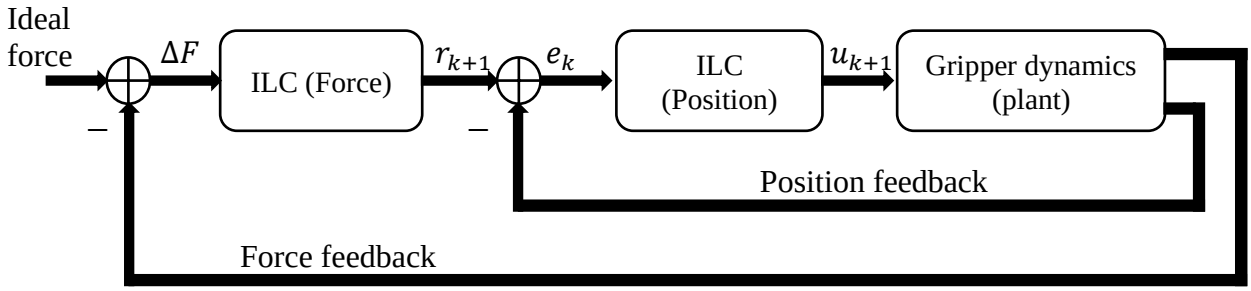

Figure 3.6: High-level schematic for ILC gripper controller

Where r_{k+1} denotes the new reference trajectory for the gripper.

3.4 Disturbance

Random disturbance/errors are unavoidable, and it is crucial that the robot can adapt itself without any humans intervention. Thus, the two most common disturbance that a robot would encounter is discussed in chapter 2.1 under Disturbance Scenario (DS).

As these two disturbances occurred in the environment that the robot situates in, one could model the disturbance as 'noise' added to the signal from the controller to the plant using the following equation.

$$\tilde{u} = u + d \tag{3.5}$$

Where d is the disturbance, u is the uncorrupted signal, and $\tilde{u}$ is the corrupted signal.

As such, the disturbance test schematic shown in Figure 3.7 can be used to test the performance of each controller when X, Y, Z axis and gripper encounter any disturbance.

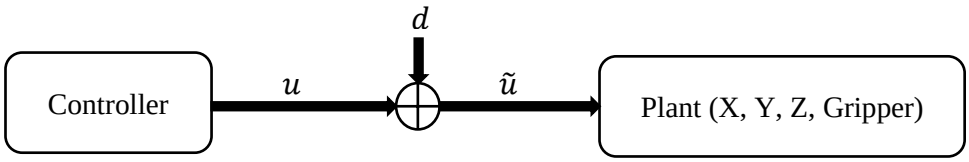

Figure 3.7: High-level schematic of controller output corrupted by disturbance

4 Simulation Model

This chapter will translate the simulation model design discussed in chapter 3.1 into MATLAB environment using Simulink and Simscape Multibody.

4.1 Gantry Modelling

Each axis of the gantry robot has a few important features that needs to be modelled,

1. It has mass and interacts with the environment; hence it has its own unique dynamics.
2. It is capable of moving in only one axis.

The goal is to model the dynamics of each axis as identified by Ratcliff [37] into the simulation environment.

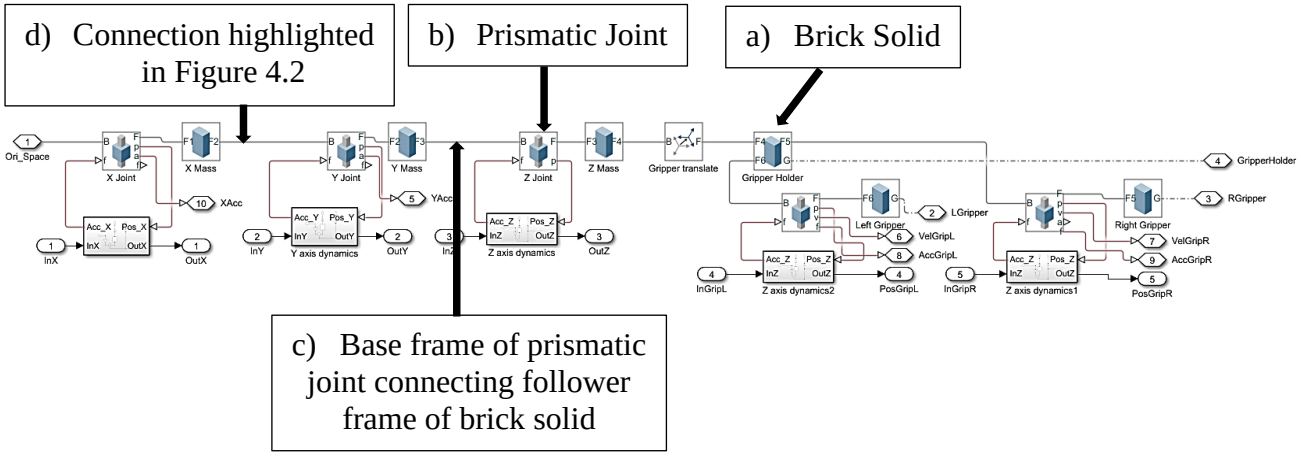

Figure 4.1: Schematic of proposed model in Simulink

The visual of each axis can be represented by 'Brick Solid' shown in Figure 4.1a, where the dimension and density of the object are defined for each axis as shown in Table 4.1.

Table 4.1: Values of Simulink model for each part of the gantry robot

Part	Dimension (mm)	Work area (mm)	Mass (kg)
X axis	520 × 25 × 25	640	4.32
Y axis	25 × 25 × 25	520	3.51
Z axis	25 × 25 × 100	100	0.169
Gripper	70 × 50 × 35	50	0.081

Since the X axis actuator is responsible in moving Y, Z, and gripper along the X axis, while Z and gripper are situated on top of Y structure; it can be imagine as 'moving' Y structure along X axis. Hence the X axis brick solid which moves in X direction will have the same dimension as Y structure. Same analogy can be applied to the rest of the brick solid. This can be seen in Figure 4.14.

'Prismatic Joint' shown in Figure 4.1b is able to move the 'brick solid' in Z direction. It accepts 'force' as input to move the object and can output a range of values including position, velocity, acceleration, and actuator force.

Frames are a very important concept when modelling using Simscape Multibody. There are 2 main crucial frames are base and follower frame. The frames have some important properties

1. Base frame of the subsequent prismatic joint will follow the orientation of the follower frame of the previous brick solid. Illustrated in Figure 4.1c.
2. The orientation of X, Y and Z axis of brick solid can be orientated so that the Z axis of the follower frame will be position at the intended travel direction, the base frame will have the same orientation of the previous 'object' follower frame to ensure it 'stacks' on top nicely. Illustrated in Figure 4.2.

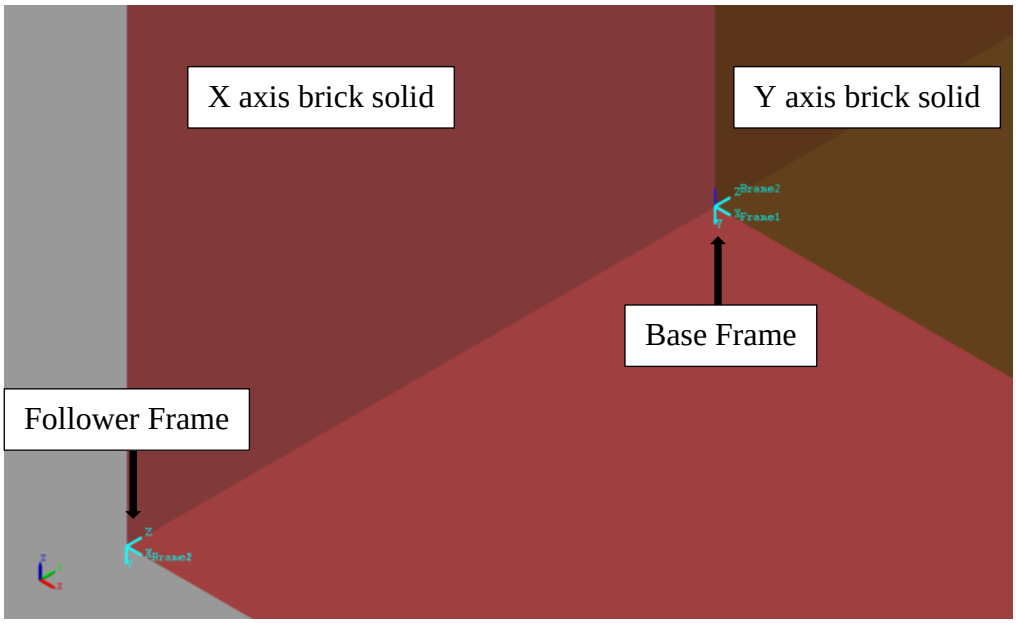

Figure 4.2: Visual representation of the base and follower frame connection (between X and Y axis) highlighted in Figure 4.1d

To ensure the model is as accurate as possible, it is crucial to model the dynamics experienced by each axis and gripper. A simple way of achieving this is to use a feedback loop PD controller to tune the dynamics of the system. An illustration of such system can be found in Figure 4.3.

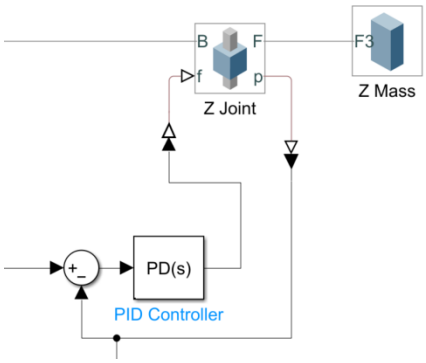

Figure 4.3: Proposed PD controller to model the dynamics of the system

Grouping prismatic joint and brick solid together and donate them as 'Plant, P' and PD controller as 'C', the transfer function of the proposed system is as follows

$$H(s) = \frac{PC}{1 + PC}$$

$$H(s) = \frac{P(k_p + k_d S)}{1 + P(k_p + k_d S)} = \frac{k_p + k_d S}{P^{-1} + k_p + k_d S} \tag{4.1}$$

The following sub-sections will explain issues encountered by such system, iterative of improvement and finally a proposed final solution.

4.1.1 Trial 1

The Laplace transform of the prismatic joint connected to brick solid can be represented using Equation 4.2 after conducting step response shown in Figure 4.4.

$$P(s) = \frac{1}{ms^2} \tag{4.2}$$

where m is the mass.

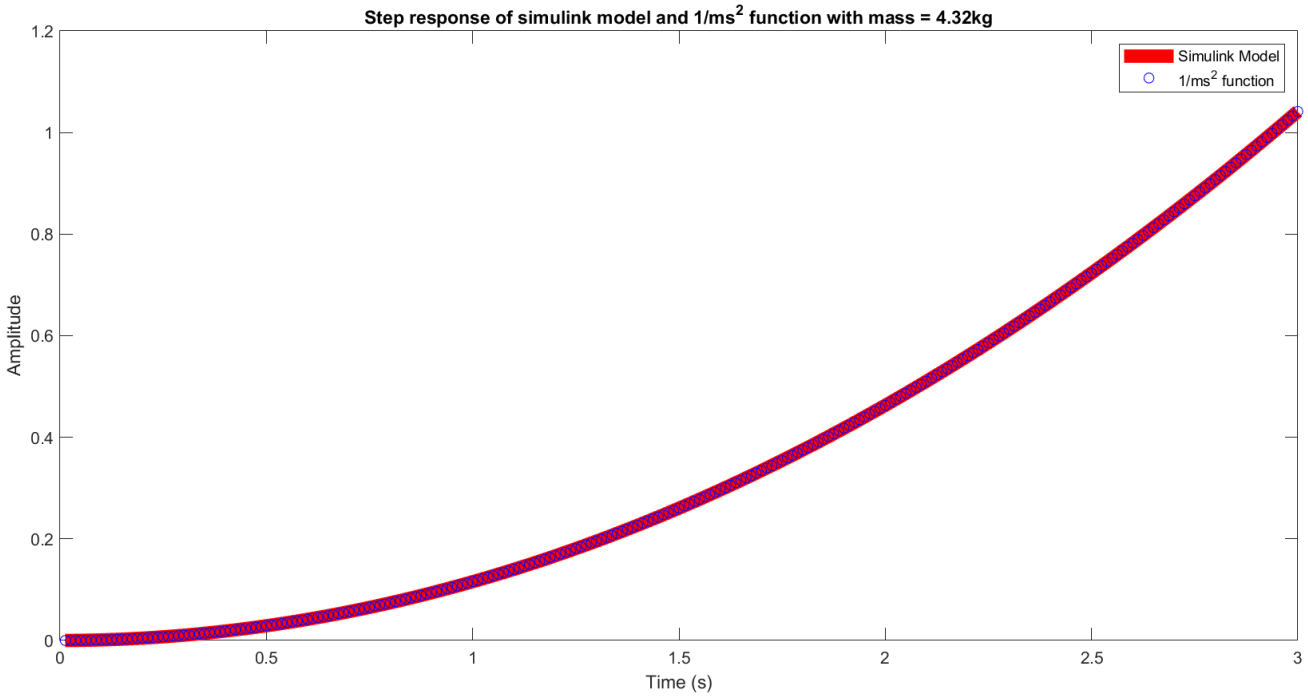

Figure 4.4: Step response for the prismatic and brick solid model VS the equivalent representation shown in Equation 4.1.

As the system expands, the total mass acted on the first part of the system is the sum of its own and all the following mass of the rest of the connected system. For example, total mass needed to be pushed by X axis prismatic joint is the sum of X, Y, Z and Gripper brick solid equating to 8.098kg.

Using the schematic proposed in Figure 4.3. The PD controller is tuned using a MATLAB built-in function, PID Tuner. PID Tuner has a graphical GUI where the user is able to change the parameter values typing or using a slider. The response of the resultant system can be seen instantly.

To model system dynamics, the impulse response of actual system transfer function (Figure 4.5) has to match with the step response of the model schematic (Figure 4.6) by matching their peak response and transient time as closely as possible. The best values are $k_p = 33634.3806$ and $k_d = 163.3421$.

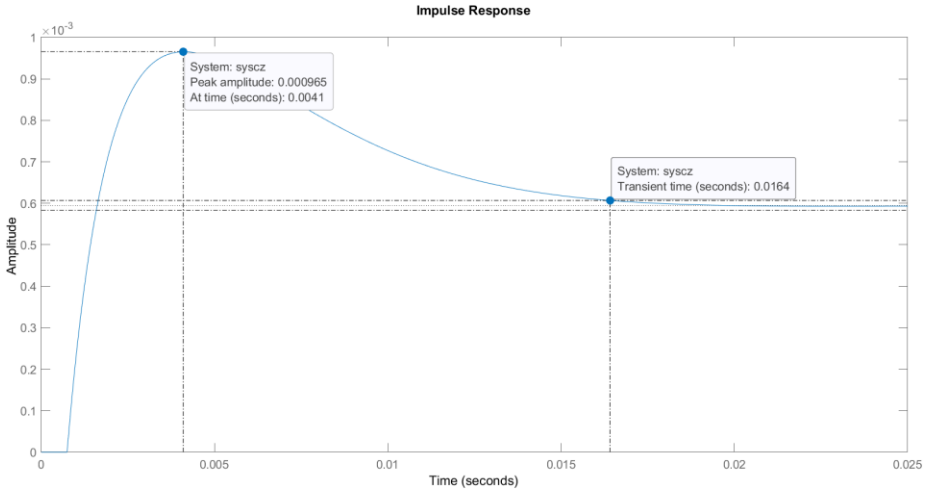

Figure 4.5: Impulse response of Z axis actual transfer function

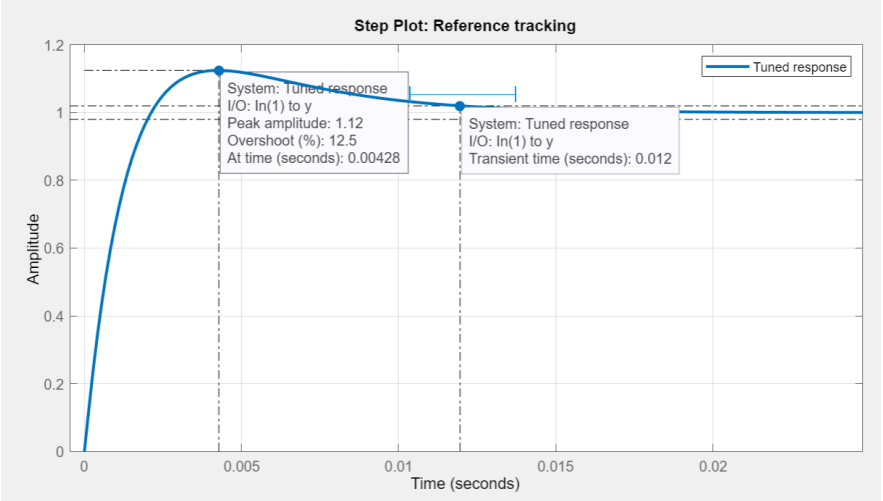

Figure 4.6: Step response of Simulink model using schematic proposed in Figure 4.3

The difference between impulse and step response is small (in terms of few milliseconds) thus is acceptable since the grasping operation is in seconds.

The step response of the modelled system denoted by Equation 4.1 and 4.2 can be denoted to as follow.

$$F(s) = \frac{1}{s} \cdot H(s) = \frac{1}{s}\left(\frac{k_p + k_d s}{ms^2 + k_p + k_d s}\right) \tag{4.3}$$

Figure 4.7 places the 2 responses together and it can be seen that the steady state amplitude is different despite having similar peak response and transient time. Schematic proposed in Figure 4.3 has a downside where the steady state response is always equates 1 as shown by applying the Final Value Theorem to Equation 4.3.

$$\lim_{s \to 0} sF(s) = \frac{k_p}{k_p} = 1 \tag{4.4}$$

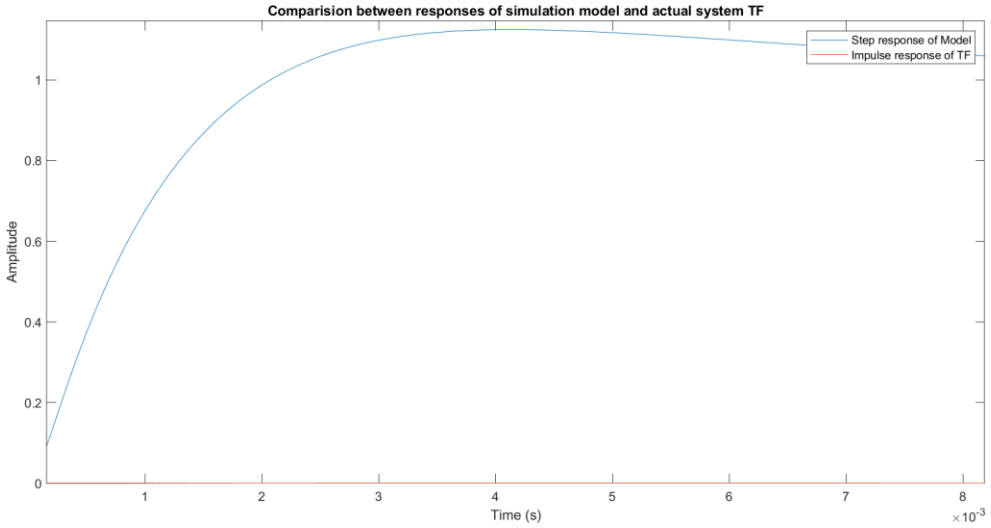

Figure 4.7: Comparison between step response of Simulink model and impulse response of actual system transfer function for Z axis

4.1.2 Trial 2

There are 2 potential solutions to solve the mismatch steady state response issue, the first is to move the PD controller and place it in the feedback loop as shown in Figure 4.8. The other option is to place a scalar gain to the input signal sent to the PD controller to scale down the steady state response accordingly as shown in Figure 4.9.

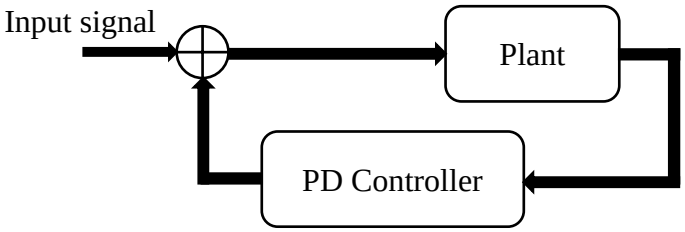

Figure 4.8: Proposed schematic where PD controller is located at the feedback loop with no scalar gain

The new transfer function to represent the system is as follows.

$$H(s) = \frac{P}{1 + PC}$$

$$H(s) = \frac{P}{1 + P(k_p + k_d S)} = \frac{1}{P^{-1} + k_p + k_d S} \tag{4.5}$$

Upon applying the final value theorem, the equation becomes

$$\lim_{s \to 0} sF(s) = \frac{1}{k_p} \tag{4.6}$$

where

$$F(s) = \frac{1}{s} \cdot H(s) = \frac{1}{s}\left(\frac{1}{ms^2 + k_p + k_d s}\right)$$

Therefore, the steady state value will be determined by the proportional gain value chosen to tune the PD controller and thus still be 'fixed' in some sense. On top of that, the PID tuner function assumes the PID controller is placed where it cascades with the plant, thus it is not possible to tune the dynamics directly using PID tuner.

4.1.3 Trial 3

With the problem encountered in the previous subsection, the other feasible option is to add a scalar gain to the input signal. As PID tuner does not work when the PD controller is placed in a feedback configuration, the following schematic is proposed.

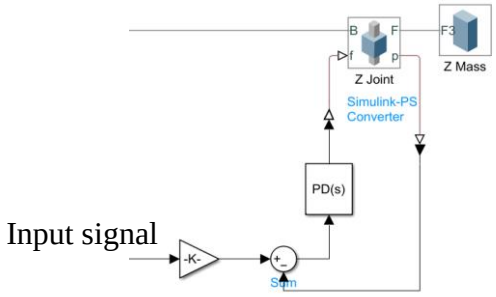

Figure 4.9: Proposed schematic for modelling gantry robot dynamics with PD controller and scalar gain

The transfer function of the system can be formulated as follows

$$H(s) = \frac{PC}{1 + PC}$$

$$H(s) = \alpha \frac{P(k_p + k_d s)}{1 + P(k_p + k_d s)} = \alpha \frac{(k_p + k_d s)}{P^{-1} + k_p + k_d s} = \alpha \frac{(k_p + k_d s)}{m s^2 + k_p + k_d s} \tag{4.7}$$

where α denotes scalar gain and is obtained visually using graph. According to figure 4.10, the steady state impulse response value for Z axis is 5.93×10^{-4}. Thus, to match this value to step response steady state value, α has to be 5.93×10^{-4} which is also $\frac{1}{1686.3406}$.

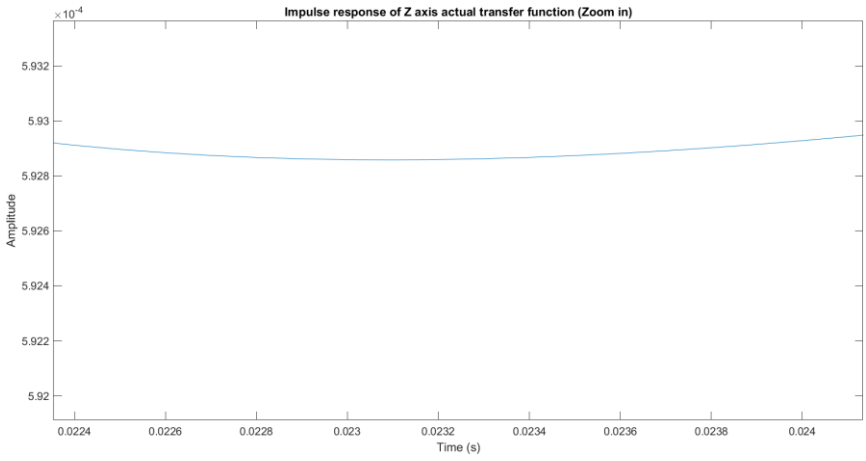

Figure 4.10: Zoom in impulse response of Z axis actual transfer function

Figure 4.11 shows the impulse response of Z axis transfer function and step response of Z axis model.

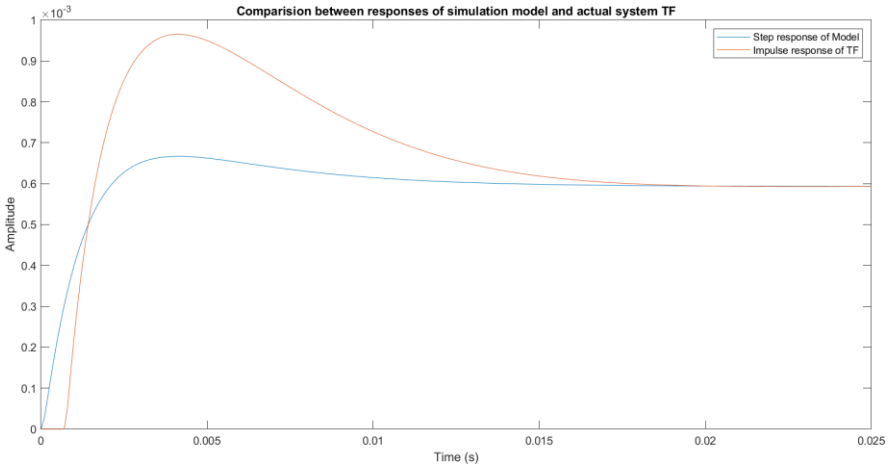

Figure 4.11: Comparison figure between step response of Simulink model with scalar gain and impulse response of actual Z axis transfer function

Although the peak amplitude is different, since the peak response and transient time are similar, and the difference is in milli scale, it is deemed to be acceptable.

With this, the dynamics modelling is complete and the model transfer function for each part of the system can be found using equation 4.7 by substituting the corresponding values shown in Table 4.2 and is now denoted as 'Apparent TF'. The below example is for Z axis.

$$H(s) = \alpha \frac{(k_p + k_d s)}{ms^2 + k_p + k_d s} = \frac{1}{1686.3406} \frac{(33734.3806 + 163.3421s)}{0.2498s^2 + 33734.3806 + 163.3421s} \tag{4.8}$$

Table 4.2: Values for Simulink models of each part of the gantry robot and gripper

Part	α	k_p	k_d	Sum masses
X axis	1/12.5	27146.67	1020.03	8.04
Y axis	1/500	131139.23	1480.58	3.72
Z axis	1/1686.3	33734.38	163.3421	0.2493
Gripper (each finger)	1/1550.7	33734.38	163.3421	0.0405

A step response of apparent transfer function is plotted along with the Simulink model step response to ensure the deduced apparent transfer function is accurate and is shown in figure 4.12. There are only minimal differences which could be caused by numerical inaccuracy.

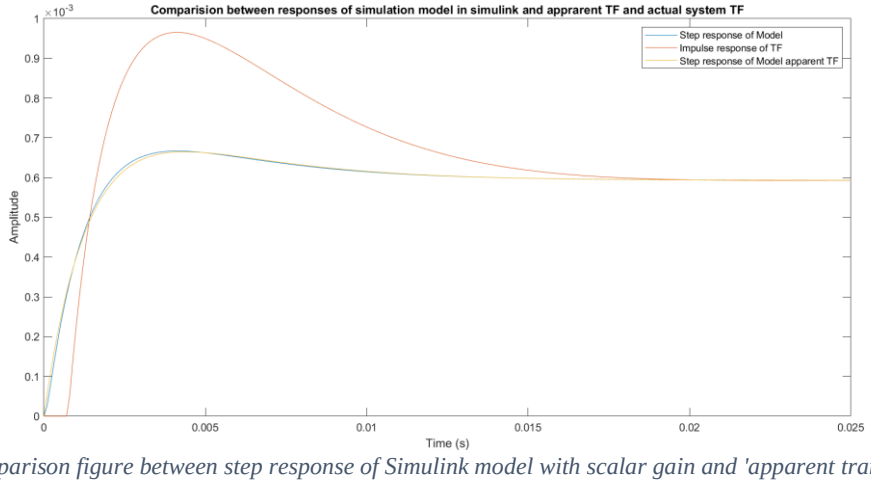

Figure 4.12: Comparison figure between step response of Simulink model with scalar gain and 'apparent transfer function' and impulse response of actual Z axis transfer function

The final schematic of the system in Simulink is shown in Figure 4.13 where the axis dynamics block follows Figure 4.9 schematic. While the visual aspect of the system is shown in Figure 4.14.

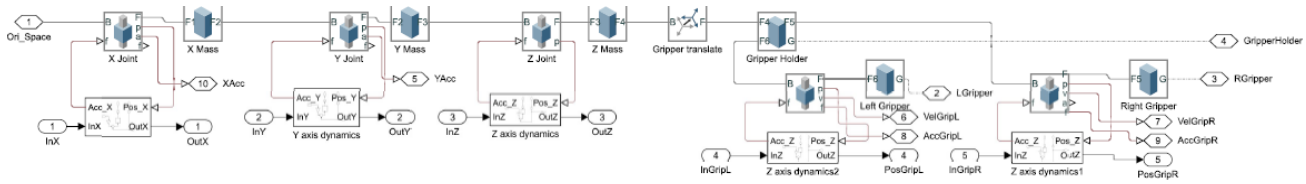

Figure 4.13: Overall schematic of gantry model

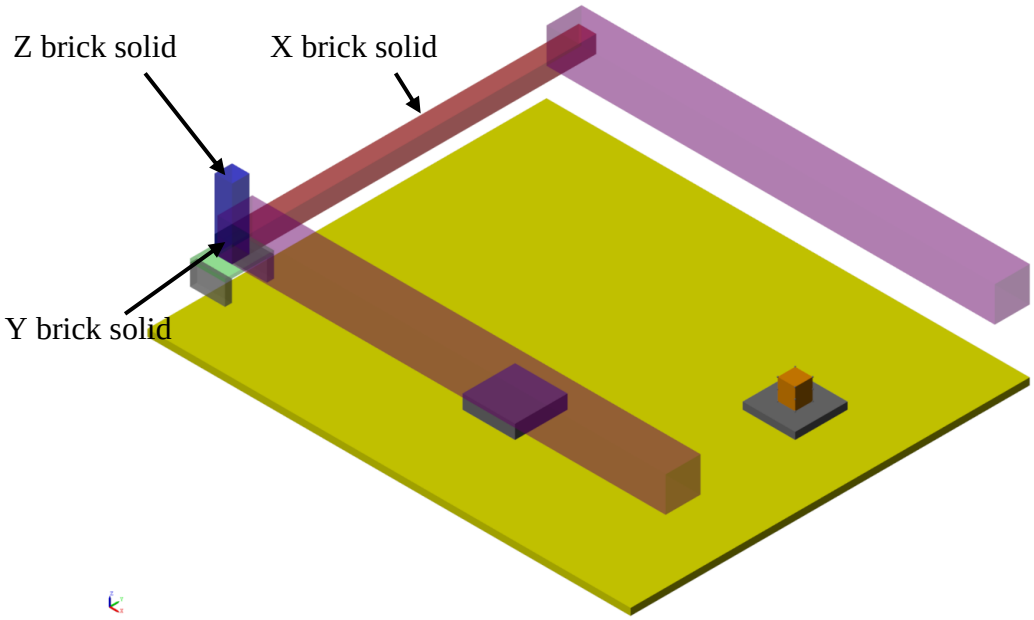

Figure 4.14: Visual view of gantry model

4.2 Contact Modelling

Simscape Multibody offers a range of blocks to model contact between two bodies. In this project the blocks that are used are ‘Solid Sphere’ and ‘Spatial Contact Force’.

Spatial contact force uses penalty force-based method to implement contact force. Penalty method allows the two-contacting object to overlap each other slightly to generate contact force as shown in figure 4.15. The block is capable of giving several parameters as output including normal and frictional force.

The amount of normal force generated when the two bodies are in contact are modelled using a mass-spring-damper system and can be adjusted by changing the stiffness and damping value. In this project, the damping is set to 0 for easier calculation while stiffness is set to 1000N/m.

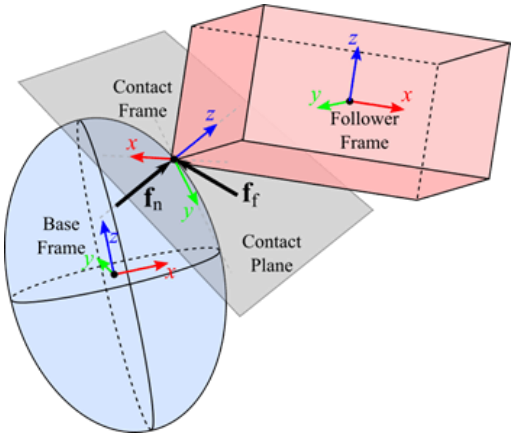

Figure 4.15: Simscape Multibody contact forces explanation diagram (adapted from MATLAB website)

The frictional force is computed using the built-in smooth stick-slip method, where the parameters of interest are coefficient of static and dynamic friction. Typically, the coefficient for dynamic friction is less than static, since the aim is for the object not to slip, the force is kept within the static region, hence it is fine to ignore the lower dynamic coefficient value and set both coefficients to 0.5.

To speed up modelling and improve performance, the gripper will be in contact with multiple strategically placed 1mm radius solid spheres instead of the whole object surface which can be seen at figure 4.17. This produces the contact force schematic shown in figure 4.16.

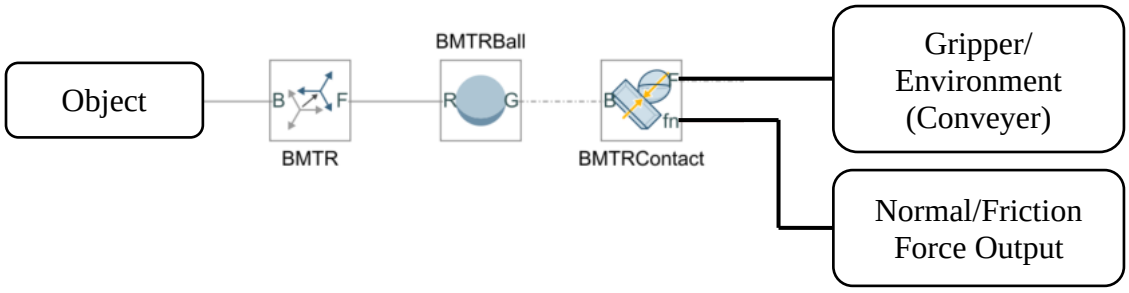

Figure 4.16: Schematic for modelling contact forces between two bodies

In total, the object will have 12 spheres spread around equally as shown in Figure 4.17. This ensures that there will be at least 4 spheres in contact with either the gripper fingers or the conveyer where the object is situated at to ensure that the object does not rotate in any direction while being grasp or placed on the conveyer.

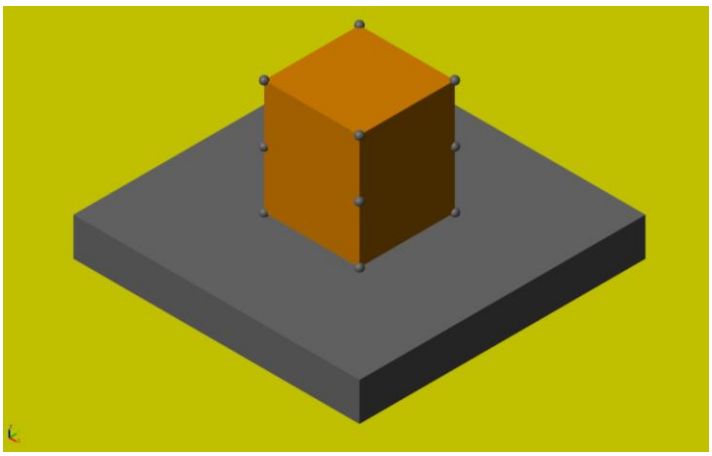

Figure 4.17: Diagram showing contact points (sphere) of the object to be grasped

4.2.1 Grasping Force Calculation

A free body diagram of an object being lifted can be seen in Figure 4.18.

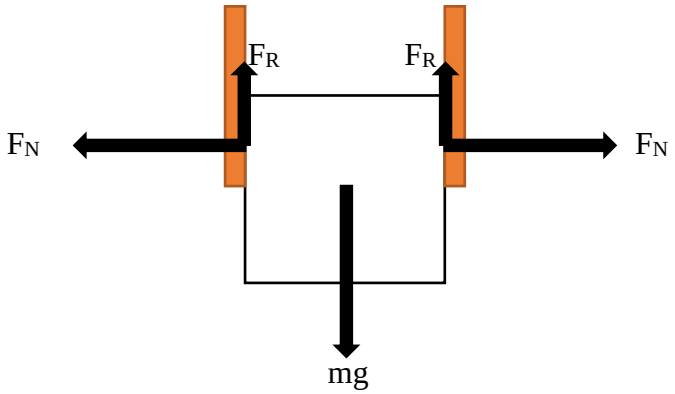

F_R = Frictional Force
F_N = Normal Force
m = Mass
g = gravitational acceleration

Figure 4.18: Free body diagram of grasping and lifting an object with two fingers parallel plate gripper

To ensure the object can be lifted,

$$2F_R \geq mg \tag{4.9}$$

recalling the friction force formula,

$$F_N = \mu F_R \tag{4.10}$$

where μ is the coefficient of friction is set to 0.5. Since the magnitude of the grasping force for one finger is the same as the normal force it experienced. Each gripper has to exert a force of

$$F_g = F_N = \frac{(0.5)m(9.81)}{2} \tag{4.11}$$

Therefore, the theoretical minimum force to grasp and lift the object securely can be calculated. This force is then spread evenly over all the spheres that it comes in contact with. In this project, each finger is in contact with 4 spheres as shown in figure 4.19.

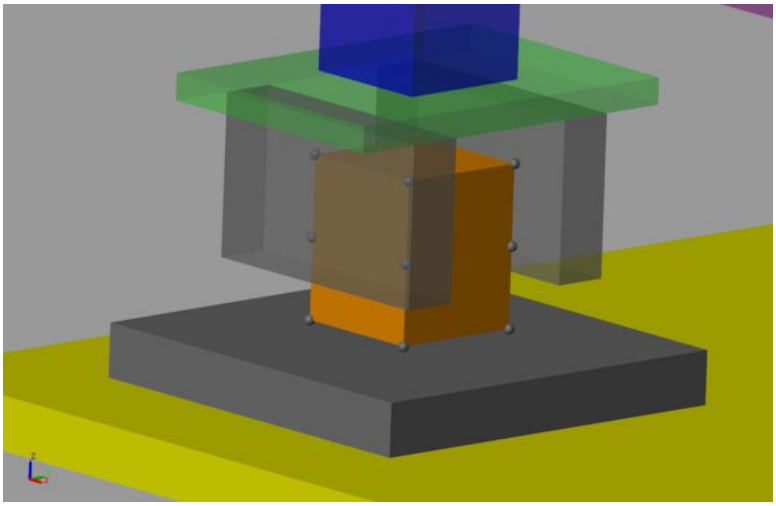

Figure 4.19: Diagram showing the contact between two bodies of interest (Object and Gripper, and Object and Conveyer)

For a mass of 2kg object, the frictional force of each gripper finger can be calculated using Equation 4.9 to be

$$F_R = \frac{mg}{2} = \frac{(2)(9.81)}{2} = 9.81$$

Since the finger is in contact with 4 spheres, the frictional force will be evenly distributed among the 4 spheres giving the force experienced by each sphere to be

$$F_{Rsphere} = \frac{9.81}{4} = 2.45N$$

while the minimum normal force is calculated as follows

$$F_g = \frac{(0.5)m(9.81)}{2} = 4.905N$$

Figure 4.20 shows the simulation value for $F_{Rsphere}$. Since the gripper did not grasp with minimal grasping distance, the normal force is not the same as F_g.

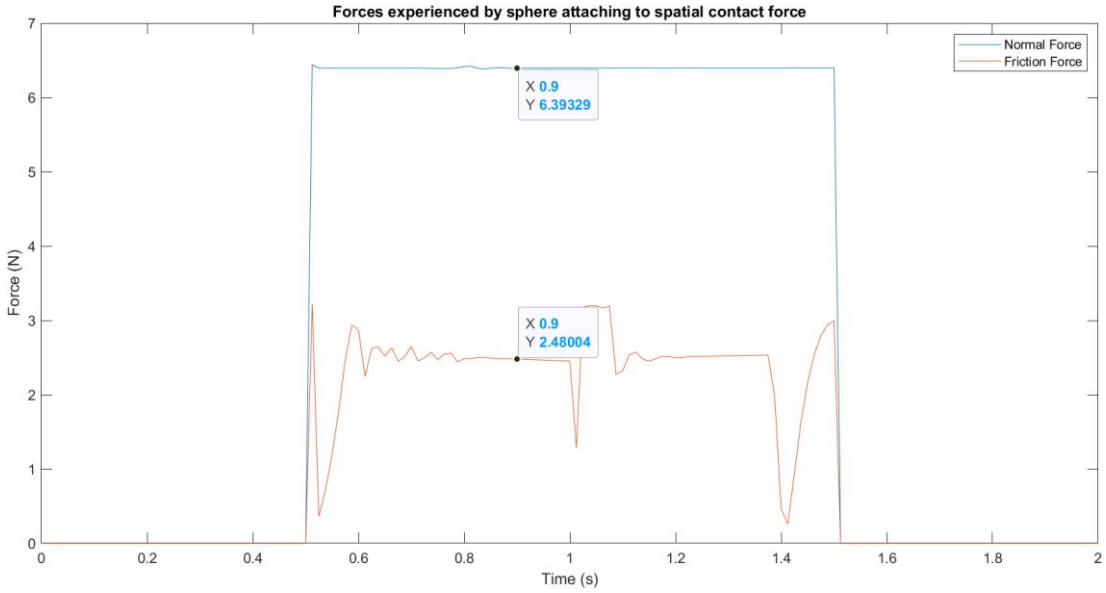

Figure 4.20: Graph showing the Normal and Frictional forces that the spatial contact force experience when grasping and lifting the object from conveyer

4.2.2 Normal Force while Accelerating

The gripper fingers are parallel to the X-axis as seen from figure 4.19. Therefore, the normal force experienced by each gripper changes due to the acceleration and deceleration when moved in Y direction as illustrated in figure 4.21.

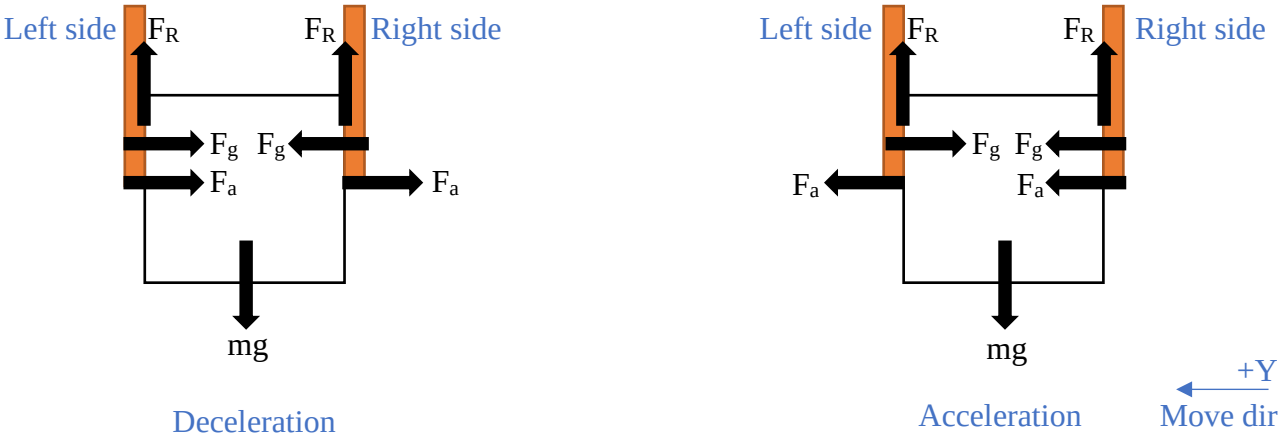

Figure 4.21: Free body diagram of forces acting on object and gripper due to acceleration and deceleration in Y direction

In the deceleration phase, the net normal force experience by each finger is,

$$F_{NetRight} = F_g - F_a$$

$$F_{NetLeft} = F_g + F_a$$

While in the acceleration phase,

$$F_{NetRight} = F_g + F_a$$

$$F_{NetLeft} = F_g - F_a$$

These changes can be seen in figure 4.22 when the gripper accelerates in Y direction, where right gripper initially experience more force due to acceleration and experience less in the second half due to deceleration.

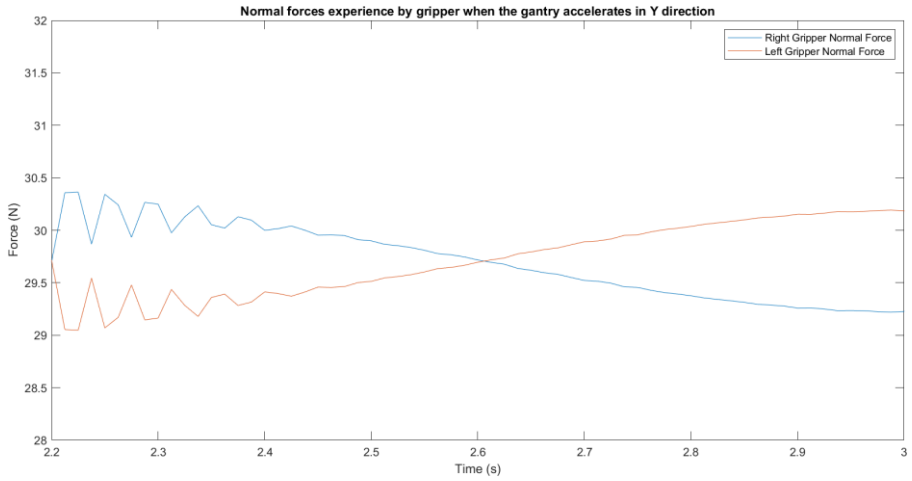

Figure 4.22: Graph showing the change in net force experienced by gripper finger due to acceleration and deceleration in Y direction

5 XYZ Position Controller Design

This chapter will design the Norm-Optimal ILC controllers discussed in chapter 3.1 for the 3-axis reach, grasp and return motion. A quick summary of requirements for the controller design is as follows.

1. Reach and grasp object within 15 iterations. Therefore, gantry controller should converge under 10 iterations to ensure grasping phase has sufficient iterations to learn and improve.
2. Reach and grasp operation should complete within 5 to 7 seconds.

As the controller is designed in discrete time, the duration of the whole reach and grasp trajectory is aimed to be completed in 4s with a sampling time of 0.01s giving 400 data points.

5.1 Trajectory profile generation 1

As discussed in chapter 3.1, each axis will be controlled by its own independent controller. These controllers will have the algorithm shown in Figure 5.1.

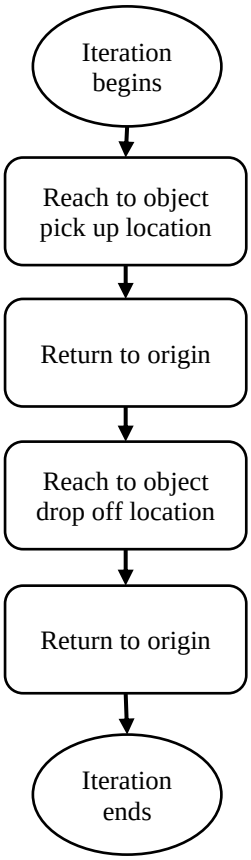

Figure 5.1: Basic control algorithm for 3 axes controllers

The object pick-up and drop-off location can be different as it is in real system. The pick-up location is located at $0.5m \times 0.3m$, while the drop-off location is at $0.3m \times 0.1m$.

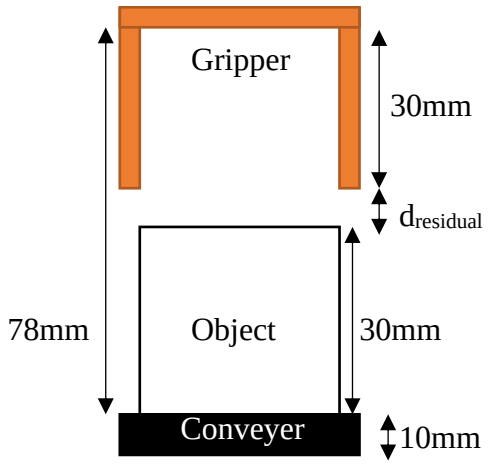

Initial conveyer height = 10m
Destination conveyer height = 20mm.

$$d_{residual} = 78 - 30 - 30 = 18mm$$

To ensure object is firmly grasped, it should grasp at least half of the object.

$$\begin{aligned} d_{zi} &= d_{residual} + obj_{mid} + margin \\ &= 18mm + 15mm + 5mm \\ &= 38mm \end{aligned}$$

Destination conveyer is 10mm higher thus $d_{zf} = 28mm$.

Figure 5.2: Z axis travel distance calculation

Figure 5.2 shows the configuration of gripper and object and calculation for Z axis travelling distance.

With the target X, Y and Z values known, it is possible to generate a profile for the gantry to follow. To ensure smooth operations, the trajectory profile should have a gentle rise and fall. Rising profile is calculated using the following equation

$$y = \frac{-A\cos\left(\frac{1}{d}\pi x\right)+A}{2} \tag{5.1}$$

where the falling profile is

$$y = \frac{A\cos\left(\frac{1}{d}\pi x\right)+A}{2} \tag{5.2}$$

where A denotes steady state amplitude, d denotes rise or fall time period, x denotes sampling instance.

To ensure the trajectory can be completed in the shortest time, the deadtime for each axis should be as low as possible. This can be achieved by moving multiple axis together such as X and Y. However, one of the top priorities is to transport the object safely, therefore Z axis should only be moved when X and Y axis are within grasping region to avoid knocking the object over prematurely. Unfortunately, that means introducing deadtime for Z axis while X and Y axis moves and additional deadtime for X and Y axis to ensure Z axis completes its operation.

The profiles for the 3-axis are shown in Figure 5.3.

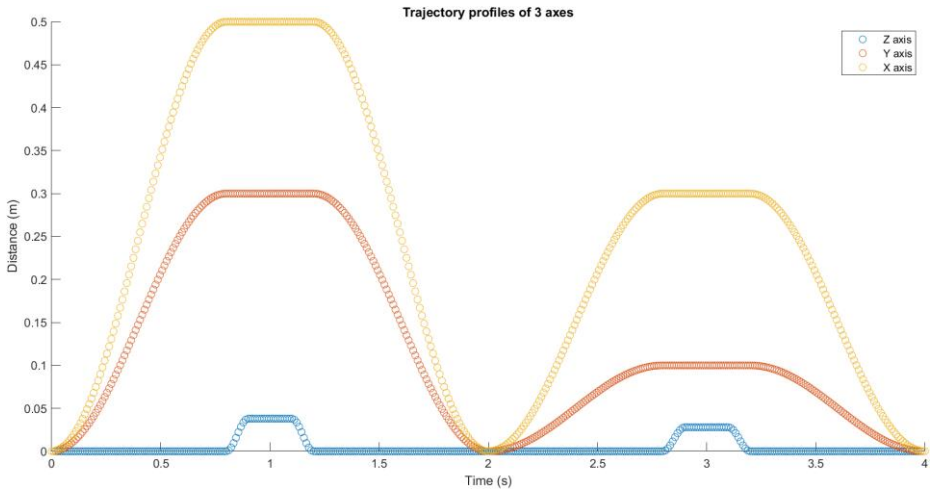

Figure 5.3: Trajectory profile for all 3 axis

Table 5.1 shows the respective values for each axis profile where A denotes amplitude, d denotes rise and fall time, D denotes deadtime.

Table 5.1: Parameters to generate trajectory profile for each axis controller

Parameters	X axis	Y axis	Z axis
A1	0.5	0.3	0.038
A2	0.3	0.1	0.028
d1	0.8	0.8	0.1
d2	0.8	0.8	0.1
d3	0.8	0.8	0.1
d4	0.8	0.8	0.1
D1	0.4	0.4	0.8
D2	0.4	0.4	0.2
D3	-	-	1.6
D4	-	-	0.2
D5	-	-	0.8

5.1.1 Tuning ILC Controller

Equation 2.9 and 2.11 are used for next iteration input update and error and are shown below

$$e_{k+1} = r - y_{k+1} \tag{5.3}$$

$$u_{k+1} = u_k + (R + QG^TG)^{-1}QG^Te_k \tag{5.4}$$

where the error vector would be the difference between the trajectory profile shown in Figure 5.3 and the actual distance moved. The plant, G, would be the plant deduced in chapter 4.1.3 for each axis.

There are 2 ways to select R and Q values. The first is to use 'lsim' feature in MATLAB which simulate a time response of a dynamic system to arbitrary input. The second is to pass input from MATLAB to Simulink using 'From workspace' block to generate response and pass the result to MATLAB using 'To workspace' block. The generated response for both is similar as seen in Figure 5.4. But lsim generates result instantly while Simulink takes 4 seconds to simulate each iteration. Therefore, lsim is used to save time.

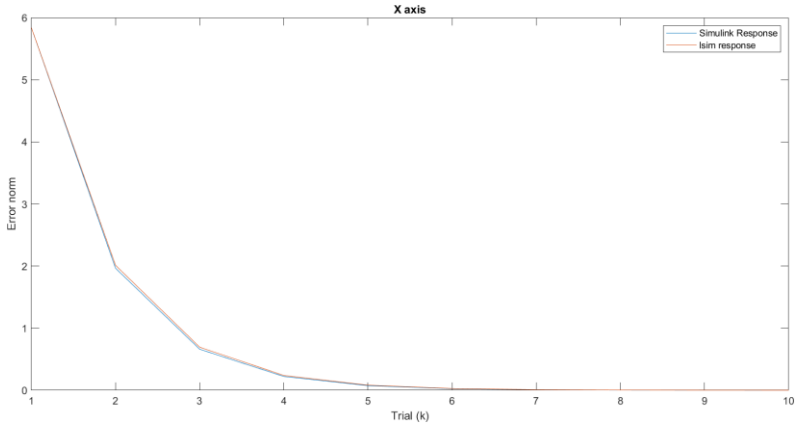

Figure 5.4: Comparison of simulated normalised position error for X axis between using Simulink and lsim

Table 5.2 shows the values of R, Q and iteration number when normalised position error achieve less than 0.01 (DR4). All 3 controllers are able to converge within 10 iterations.

Table 5.2: Some trials conducted to tune R and Q values controllers

Trial	X axis			Y axis			Z axis		
	R	Q	Iteration	R	Q	Iteration	R	Q	Iteration
1	0.5	50	>10	0.01	40	>10	0.001	500	>10
2	0.4	50	>10	0.005	40	>10	0.0005	500	>10
3	0.3	50	10	0.005	300	>10	0.0001	500	5
4	0.2	40	9	0.001	300	9	0.0001	1000	4
5	0.1	30	7	0.001	400	7	0.0001	1500	3

5.2 Trajectory profile generation 2

The issue with the previous algorithm is that the gantry robot moves back to origin after grasping the object which increases the distance travelled as typically, the distance to travel from initial location to destination is shorter than from initial location to origin to destination. Therefore, this could put unnecessary stress to the actuators. Thus, a new trajectory profile is generated and shown in Figure 5.5.

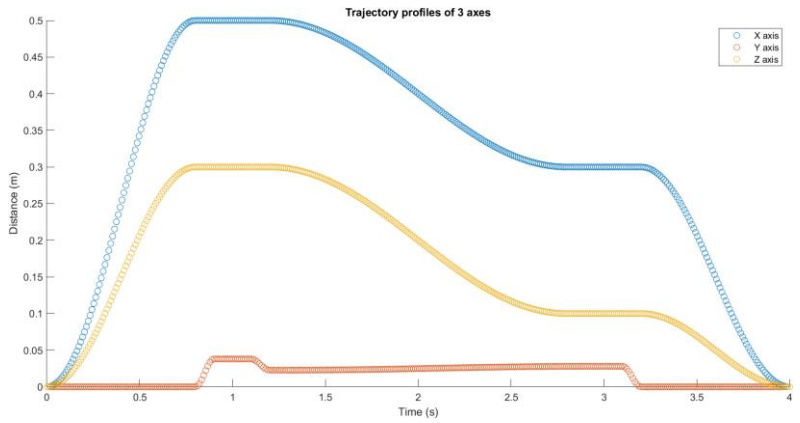

Figure 5.5: Trajectory profile for each axis controller to follow

It can be clearly seen that between 1.2s and 2.8s, the scatter points are closer to each other in Figure 5.5 than in Figure 5.3, this indicates that the changes between each time sample is less and thus put less stress on the actuators.

To avoid the grasped object from being 'dragged' along the floor when the X and Y axis moves, the Z axis will lift the object up slightly before the deadtime of X and Y axis ends. A close up view of Z profile is shown in Figure 5.6, where each part is colour coded. The new values for the trajectory profile can be found in Table 5.3, where A denotes amplitude, d denotes rise/fall time, D denotes deadtime.

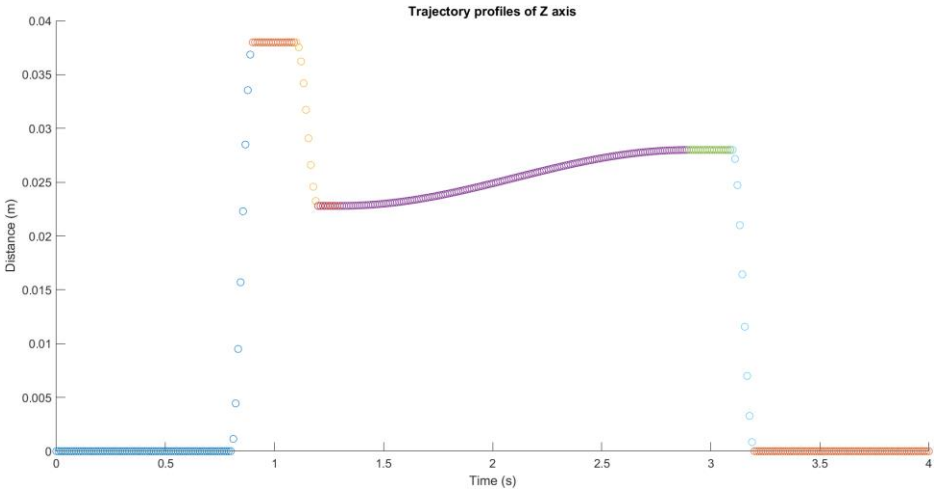

Figure 5.6: Trajectory profile of Z axis, each colour shows different parts of the trajectory profile generation, and the timing is given in Table 5.3

Table 5.3: Values for trajectory profile generation

Parameters	X axis	Y axis	Z axis
A1	0.5	0.3	0.038
A2	0.3	0.1	0.038*60%
A3	-	-	0.028
d1	0.8	0.8	0.1
d2	1.6	1.6	0.1
d3	0.8	0.8	1.6
d4	-	-	0.1
D1	0.4	0.4	0.8
D2	0.4	0.4	0.2
D3	-	-	0.1
D4	-	-	0.2
D5	-	-	0.8

This algorithm is capable of grasping the object and releasing at its destination accurately. However, Z axis will start to operate in the first iteration. This causes issues where the Z axis converges before X and Y axis, hence caused the gripper to collide and damage the object as captured at the 4th iteration shown in Figure 5.7.

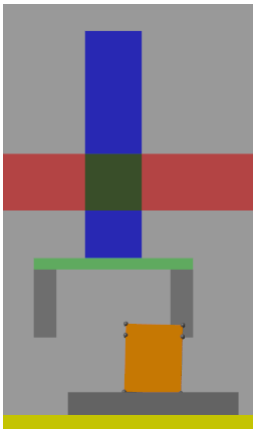

Figure 5.7: Gripper colliding with object due to Z axis converging before X and Y

5.3 Trajectory profile generation 3

In light of the issue experienced in previous subchapter, a new control algorithm was designed where the Z axis shall 'wait' until X and Y axis have relatively small tracking error moving. The new algorithm is illustrated using flow chart shown in Figure 5.8.

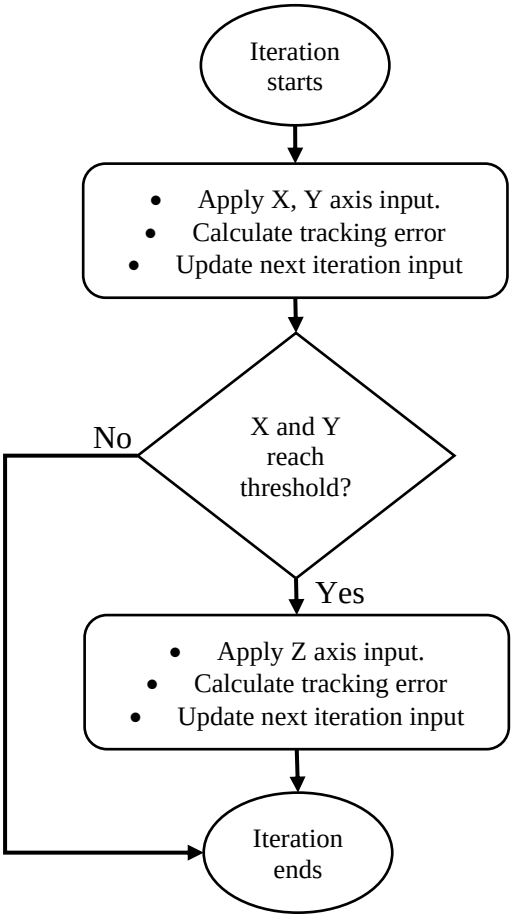

Figure 5.8: Flow chart of new control algorithm

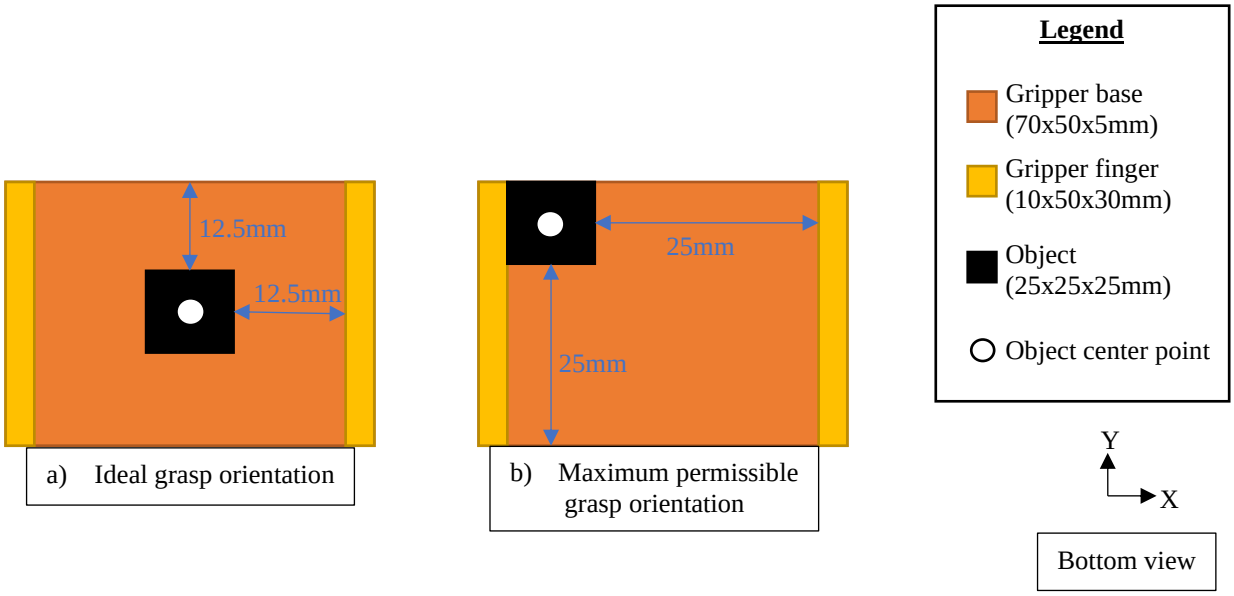

Figure 5.9: Illustration of gripper and object location for ideal grasping orientation and maximum permissible orientation

The best location to grasp the object is when it reaches the centre of the gripper as illustrated in Figure 5.9a. But for the controller to converge to zero tracking error would take infinite iterations. Therefore, as long as the object is within the gripper grasping area shown in Figure 5.9b, the object can be regarded as safe the grasp, hence the Z axis can start to lower the gripper. The earliest safe distance/threshold to allow Z axis to operate is calculated by subtracting 25mm from A1 of X and Y values shown in Table 5.3.

To get the most reliable reading to compare with the threshold, an average data of the position feedback during each axis deadtime is considered (between 0.8s and 1.2s, and 2.8s and 3.2s as shown in Figure 5.5).

Figure 5.10 shows the normalised error of the 3 axes. The Z axis normalised error remains constant during the first 4 iterations because X and Y axis are still not within the threshold. The normalised tracking error of Z axis reduces down to less than 0.01 in the 6th iteration which is still within the 10 iteration limit mentioned at the beginning of the chapter.

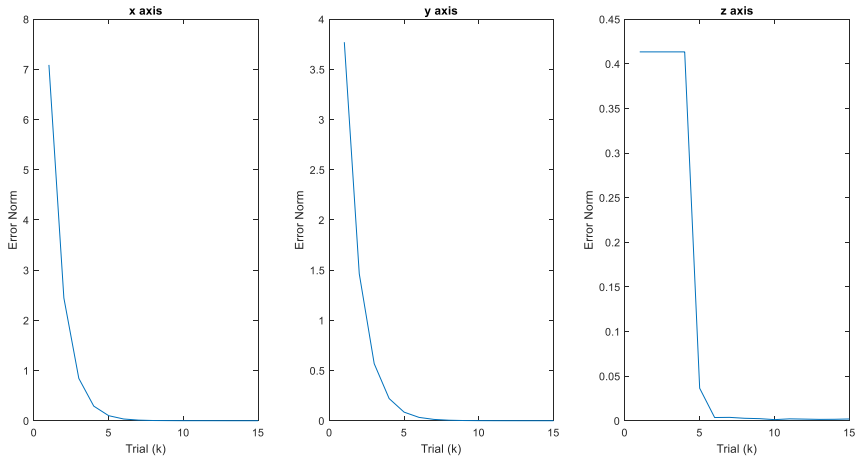

Figure 5.10: Normalised error for X, Y and Z axis with the new control algorithm

Figure 5.11 shows the position feedback of the 3 aixs during different iterations while Figure 5.12 shows the changes of input signal to realise the ideal tracking trajectory. This is evident that ILC learns from previous iteration mistakes and corrects itself.

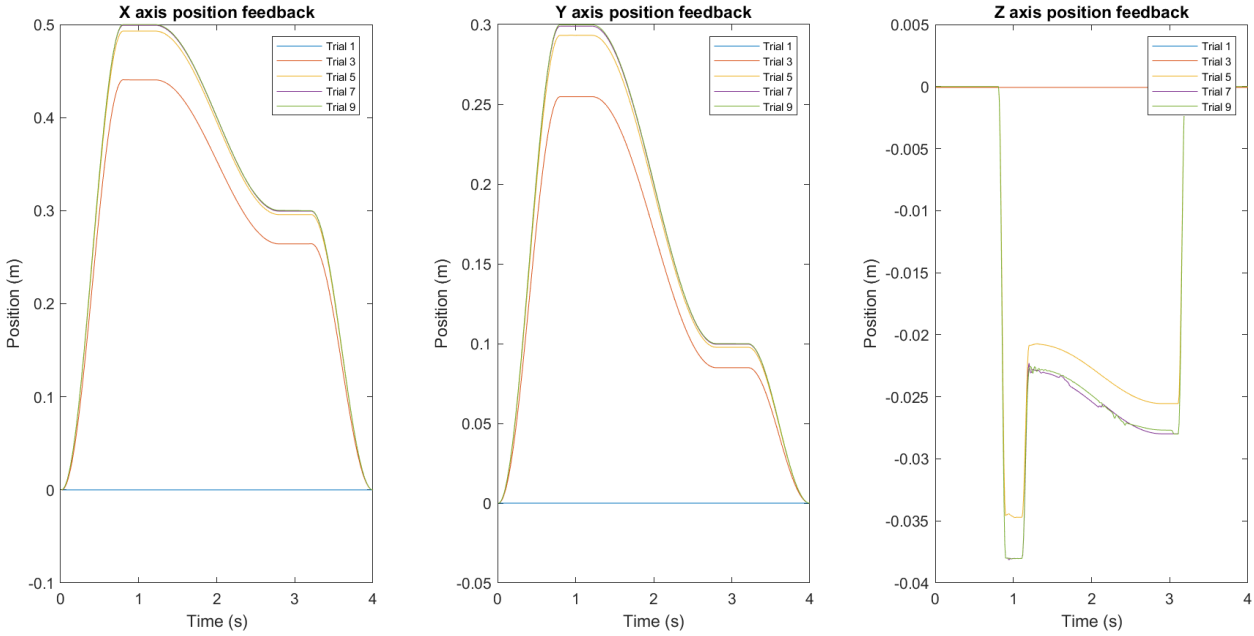

Figure 5.11: Position feedback of X, Y and Z axis for different iterations

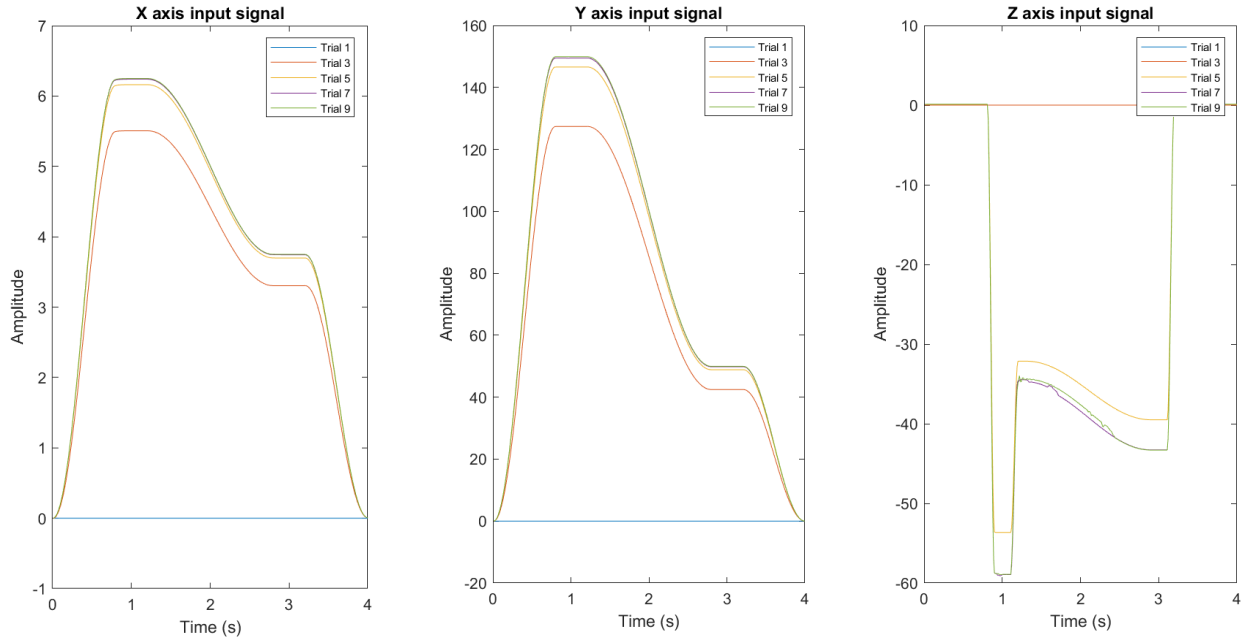

Figure 5.12: Input signal for X, Y and Z axis for different iterations

6 Gripper Controller Design

The rise and fall period of Z axis shown in Figure 5.6 is relatively short. Therefore, to reduce the strain put on the system, the total time period has increase from 4s to 5s and reducing middle transition period. This allows Z axis to operate over a longer period. The profile would still have 400 samples giving it a sampling rate of 0.0125s. The new profile is shown in Figure 6.1.

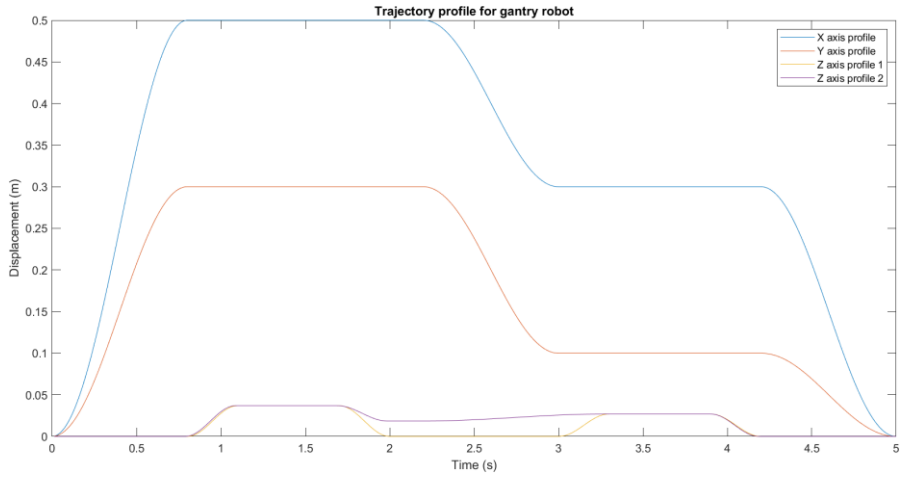

Figure 6.1: Gantry new profile with longer deadtime and longer iteration cycle

The previous Z axis profile is shown in figure 6.1 as profile 2. This profile will be discarded as it is safer to fully retract Z axis prior moving in X and Y direction as this ensures the object will not collide with anything in the environment. The values to generate the profiles can be found in Table 6.1.

Table 6.1: Values to generate profiles seen in Figure 6.1. D denotes deadtime, d denotes rise/fall time and A denotes amplitude

Parameters	X axis	Y axis	Z axis 1	Z axis 2
A1	0.5	0.3	0.037	0.037
A2	0.3	0.1	0.027	0.037*50%
A3	-	-	-	0.027
d1	0.8	0.8	0.3	0.3
d2	0.8	0.8	0.3	0.3
d3	0.8	0.8	0.3	0.8
d4	-	-	0.3	0.3
d5	-	-	-	0.3
D1	1.4	1.4	0.8	0.8
D2	1.2	1.2	0.6	0.6
D3	-	-	1.0	0.2
D4	-	-	0.6	0.6
D5	-	-	0.8	0.8

6.1 Impedance Gripper

The schematic for impedance controller is shown in Figure 3.4 and 3.5. The design will be split into 2 subsections where one focuses on the PD controller and the other Impedance.

6.1.1 Position Control

To ensure the gripper fingers reaches their desired location, a simple PD controller is added to correct any position error. Since the gripper fingers are identical to each other, it is only necessary to tune the values of one of the controllers and the other will take the same value. The schematic for the PD controller is shown in Figure 6.2.

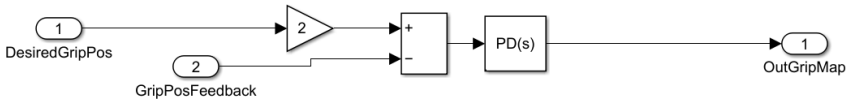

Figure 6.2: PD controller schematic for position control of gripper fingers

The PD controller aim is to correct position error as fast as possible. This can be achieved by ensuring the step response has small transient time. Figure 6.3 shows the response of the gripper finger dynamics using PID tuner. The values can be found in table 6.2.

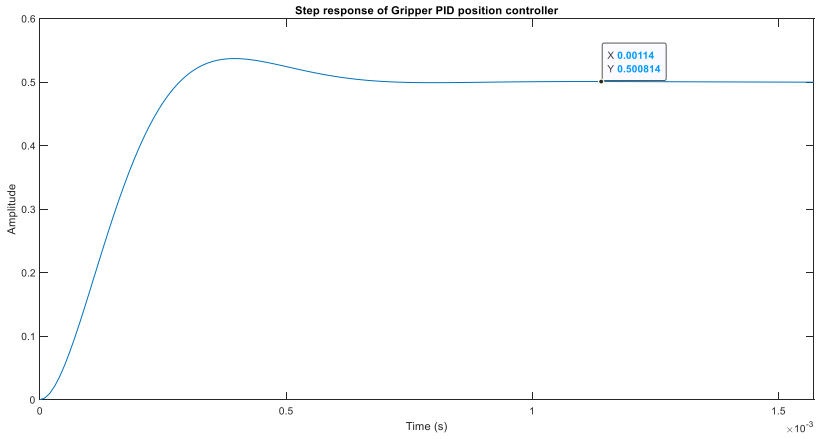

Figure 6.3: Step response of PD controller connected in series with gripper finger plant

Figure 6.3 identifies a problem where the steady-state value remains at 0.5. Therefore, a scalar gain of 2 is added to the signal to increase the steady-state value to 1.

Parameter	Value
P	1493.03
D	0

6.1.2 Force Control

There is a direct relationship between the gripper grasping position and force applied on the object. To change the force applied, the controller has to change the reference trajectory for PD controller to follow. Impedance control can be used for this operation by using the schematic is shown in Figure 6.4 which is adapted from the general schematic shown in figure 2.2.

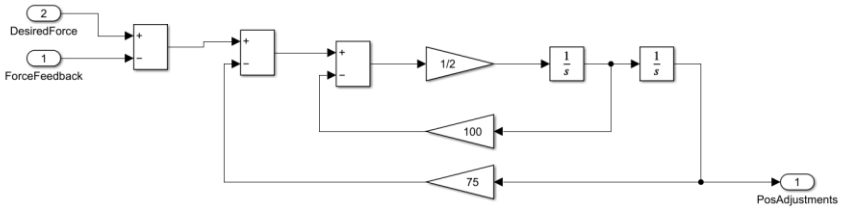

Figure 6.4: Schematic of Impedance Control

For the gripper to skim the surface of the object, it has to travel 0.0115m. This calculation can be done by referring to figure 5.9. A conservative approach is taken where the gripper is set to close a further 0.003m to grasp the object firmly. This reference profile shown in figure 6.5.

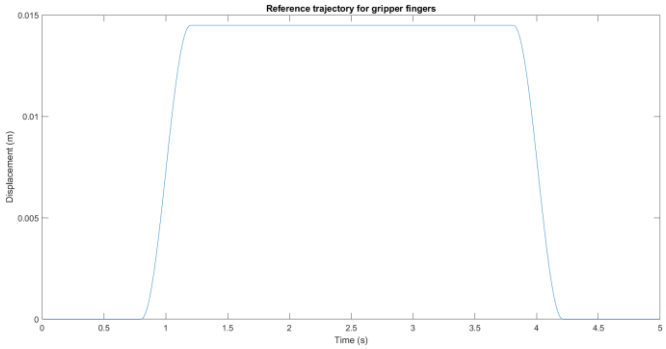

Figure 6.5: Reference trajectory for gripper fingers to follow

The minimum force to grasp an object is calculated using equation 4.11. This is increase by 20% to account for any modelling and calculation uncertainties and is known as desired force. The force feedback would be measured by force sensors placed at the fingers. The resultant force adjustment will be added to the reference profile shown in figure 6.6.

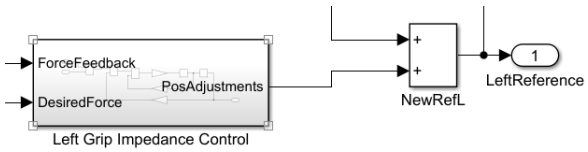

Figure 6.6: Input and output of impedance controller

The values of M, B and K needs to be tuned to get the best response. Table 6.2 shows a summary of values tested. Some of the gripper force graphs are plotted in figure 6.7.

Table 6.2: Values for Impedance control and remarks via observing simulation and graph

Trials	M	B	K	Remarks
1	2	300	200	Huge spike, stable grasp
2	2	100	50	Smaller spike, small valley but still good grasp
3	2	50	50	Small spike reduction, multiple valleys, slip slightly
4	2	75	50	Amplitude of valley is smaller, slip slightly
5	2	100	75	Good grip, minimal to no valley

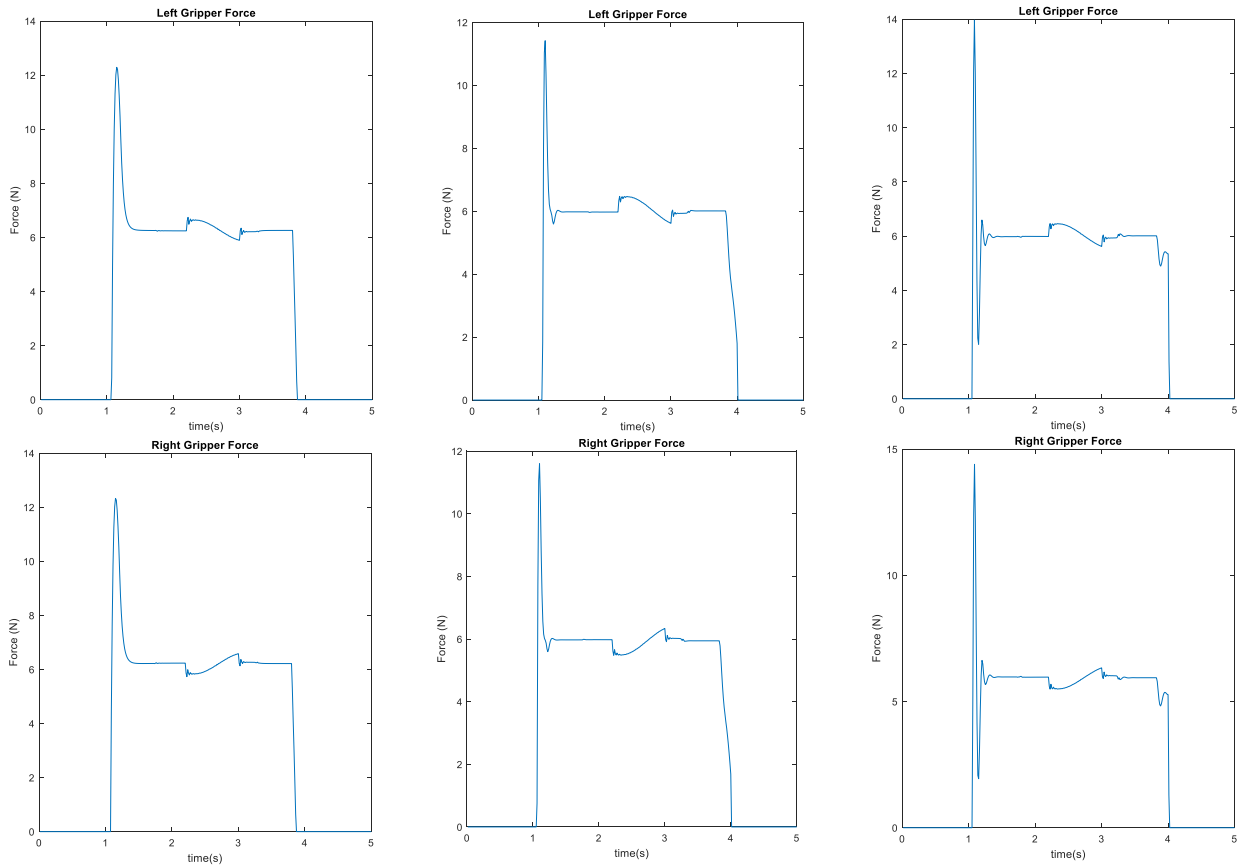

a) M = 2, B = 300, K = 200 b) M = 2, B = 100, K = 50 c) M = 2, B = 50, K = 50

Figure 6.7: Interaction forces between gripper finger and object under different B and K values.

As the reference profile takes a conservative approach, it will always initially apply excessive force before force control kicks in as evident in figure 6.7. The sine wave like phenomenon happening around 2s to 3s is caused by the acceleration and deceleration effect explained in chapter 4.2.2. Care has to be taken when selection the values, as demonstrated by Figure 6.7a to 6.7c, although the max amplitude of the spike decreases, the controller is less stiff and damped hence produces some sharp valleys where the gripper to behave like a jelly and could potentially cause the gripper to drop the object.

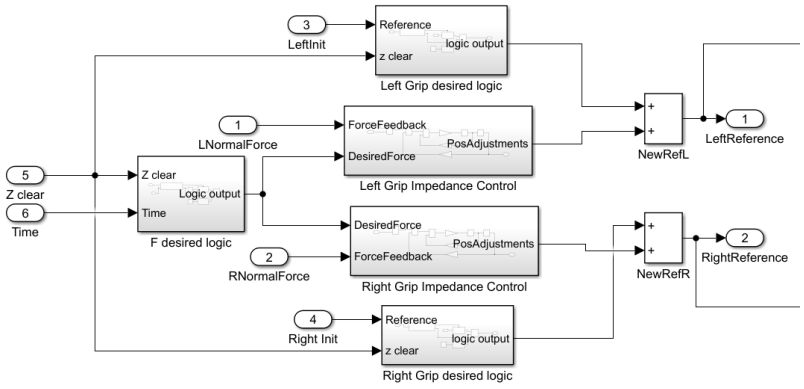

Figure 6.8: Full schematic of Impedance Control, without PD controller

To ensure the gripper is able to grasp the object firmly, the X, Y and Z axis should be at a reasonable position (within certain grasping volume) before the gripper is allowed to grasp. Therefore, a logic system is implemented as shown by the flowchart in figure 6.9 which proceed the one in figure 5.8. The full schematic of impedance controller is shown in Figure 6.8. Details can be found in Appendix C.

The calculation for Z axis threshold is similarly to chapter 5.3, where the threshold is set to 97% of the final value.

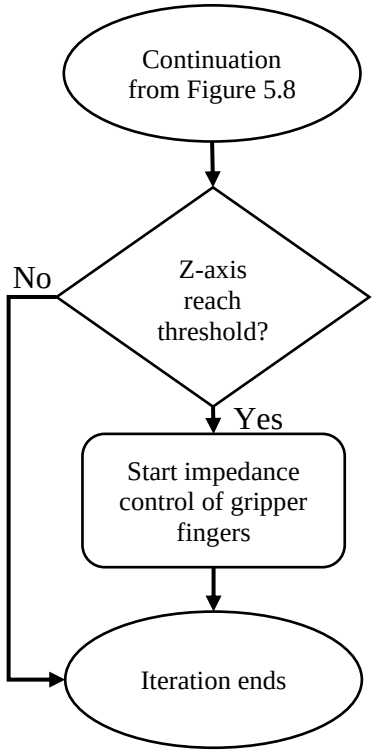

Figure 6.9: Flow chart of full impedance control algorithm

6.2 ILC Gripper

The ILC algorithm will largely follows the one shown in Figure 6.9 with some modification to suits the task better. This section will be split into 3 subsections with the following aim

- Ensure gripper fingers move to the correct location.
- Ensure gripper uses the least amount of force.
- Investigate the effect of updating plant model with the weight of grasped object.

6.2.1 Position Control

The gripper fingers will use equation 5.3 and 5.4 for next iteration input vector update calculation. The plant has been identified chapter 4.1.3. To tune the values of R and Q, similar steps used in chapter 5.1.1 are used and the best value are R = 0.00005, Q = 2000.

Figure 6.10 shows the normalised error for each part of the system. From there, the gripper can be seen to converge to 0.01 normalised error at 10^{th} iteration which meets DR4.

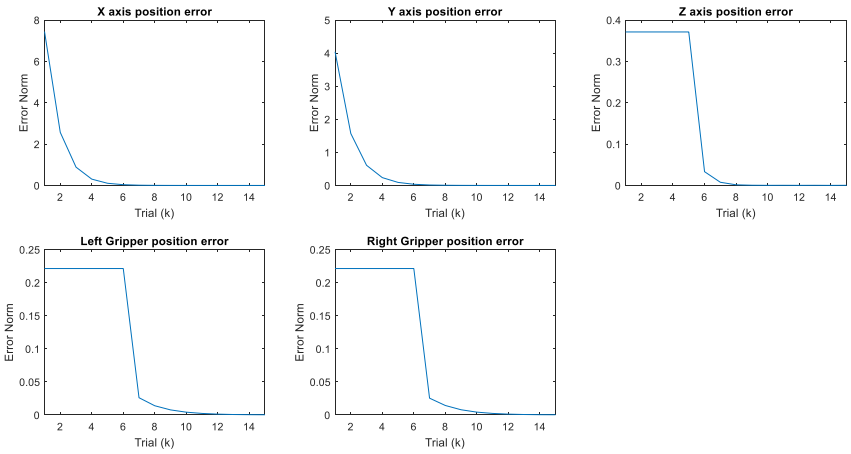

Figure 6.10: Normalised position error for whole gantry system

ILC would use the same schematic as shown in figure 6.9 but with some minor modification. As ILC only updates the input vector at the end of the iteration, the information passed to the controller to make decision can be seen as delayed by 1 iteration, therefore, it is crucial that the gripper has a firm grasp of the object before transporting. As a result, 2 reference trajectory profile is generated. The first would grasp and release the object to ensure the average force is within the desired force value. Only if the average exceeded the desired force, should the second profile be used. The second profile is the same as seen in Figure 6.5, where it will grasp the object during the whole operation. The overall profile for the whole system is shown in Figure 6.11, while the comparison between the 2 gripper profiles is shown in Figure 6.12.

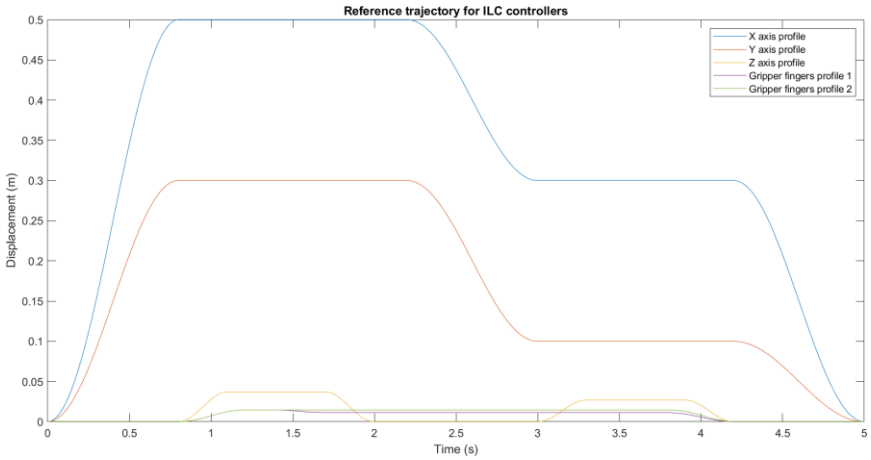

Figure 6.11: Reference trajectory profiles for X, Y, Z axis and gripper fingers to follow

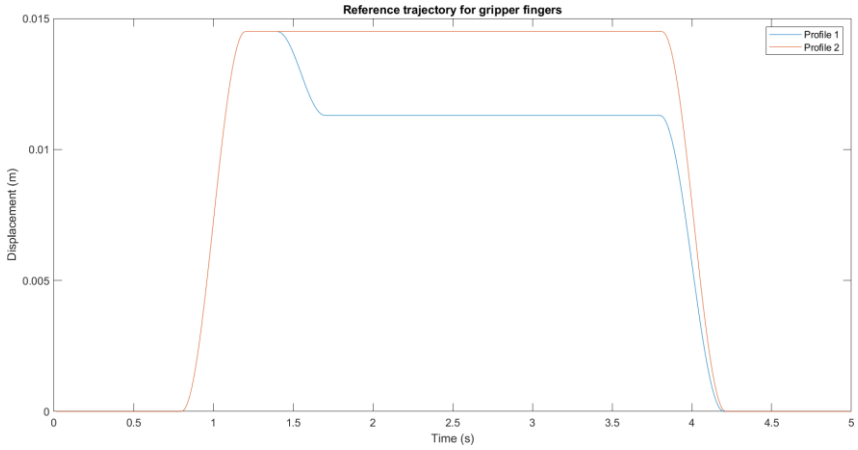

Figure 6.12: Two different reference trajectory for gripper fingers controller to operate under different conditions

The modified flow chart of the new algorithm is illustrated in Figure 6.13.

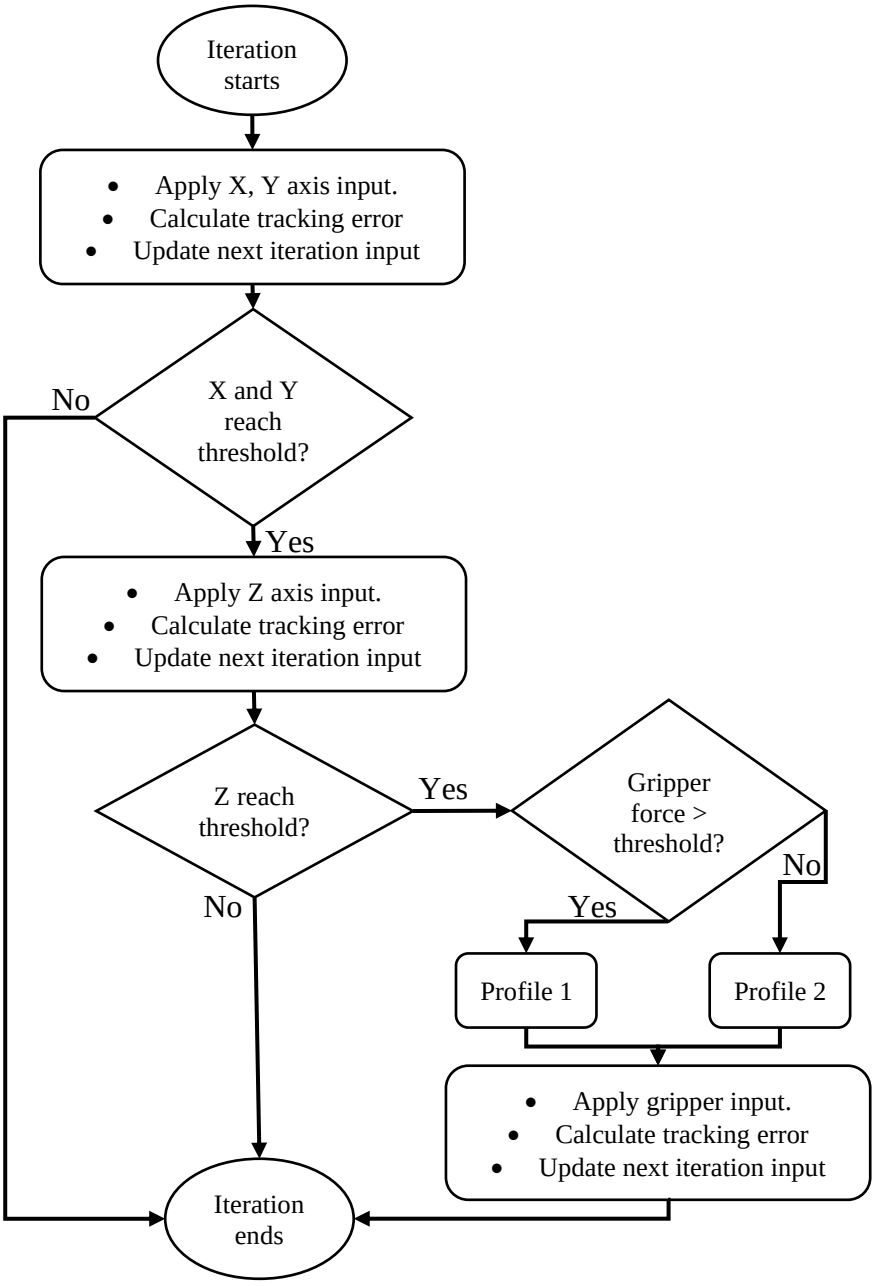

Figure 6.13: New control algorithm with different grasping profiles

For the threshold of X, Y and Z axis to be fulfilled, they have to be within a 97% accuracy when comparing the average difference between position feedback value and reference trajectory. The force threshold is set to be 20% higher than the minimum force (F_{min}) calculated using Equation 4.11 to account for any uncertainties or modelling errors that may arise.

6.2.2 Force Control

In order to ensure the gripper does not use excessive force, a force control is needed. As discussed, and justified in chapter 3.3.2, a simple gain ILC update would be used. This updated flow chart is shown in Figure 6.14.

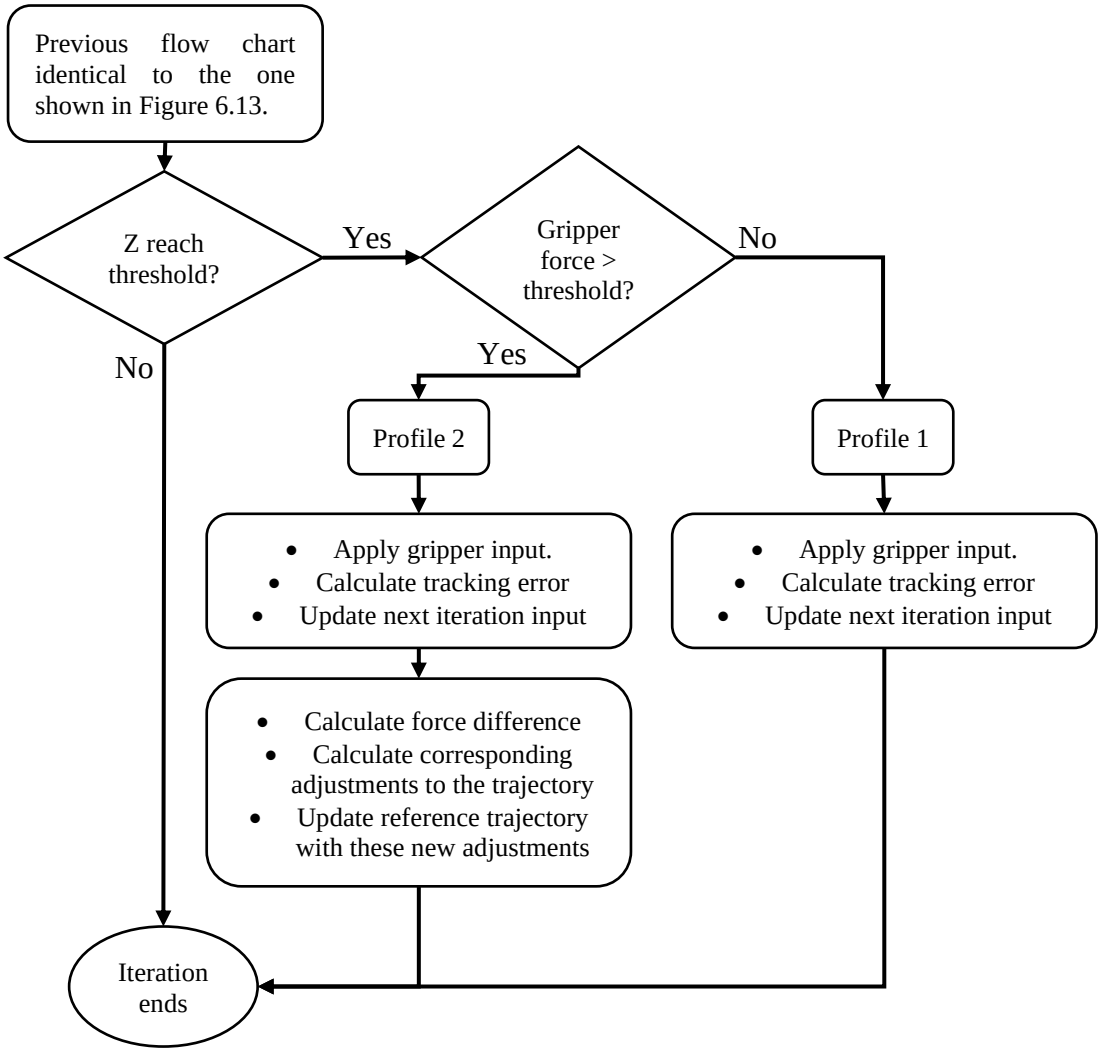

Figure 6.14: New flow chart showcasing new algorithm with features reducing grasping force

There are a few steps to calculate the changes to reference trajectory for the gripper to grasp with minimal excessive force.

The first step is to calculate the force difference (F_{diff}) using the following equation

$$F_{diff} = (F_{min} * 120\%) - F_{measured} \tag{6.1}$$

where F_{min} is the minimum force, $F_{measured}$ is the measured force.

The interaction force is modelled using a spring-mass system explained in Chapter 4.2, the force is directly proportional to the distance two bodies overlap ($d_{overlap}$). This can be calculated using the following formula

$$F_{applied} = d_{overlap} * stiffness \tag{6.2}$$

The stiffness is set to be 10000N/m. For an object of mass 2kg, using equation 4.11, the F_{min} to lift the object is 4.91N.

Combining equation 6.1 and 6.2, it is possible to calculate the changes to the trajectory (d_{diff}) for the fingers to reduce the force applied on the object and is shown in equation 6.3.

$$d_{diff} = \frac{F_{diff}}{stiffness} \tag{6.3}$$

d_{diff} can be regarded as an error signal and thus the update of profile 2 reference trajectory can be carried out using ILC using equation 3.4, forming equation 6.5.

$$\boldsymbol{ref}_{k+1}(t) = \boldsymbol{ref}_{k}(t) + \beta(t)\boldsymbol{d}_{diff}(t) \tag{6.5}$$

where $\beta(t)$ is set as a scalar gain of 0.5 to ensure the correction is smooth and not destructive.

However, as the force calculation is only done during the deadtime (between 1.2s and 3.8s), the value of d_{diff} before and after this deadtime is 0. This causes an issue shown in Figure 6.15, where it is not smooth all the way.

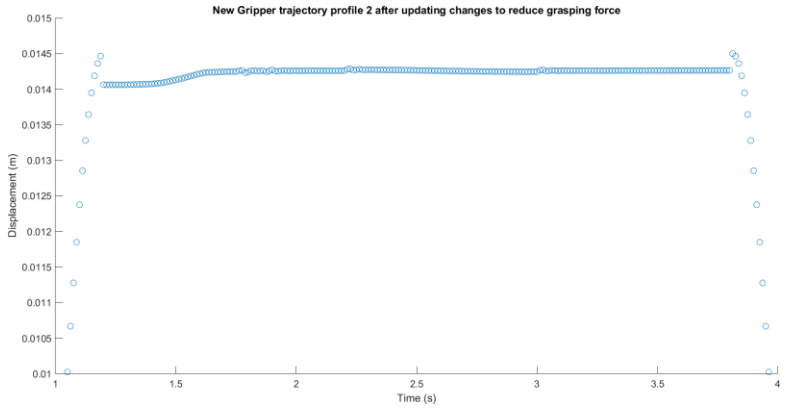

Figure 6.15: Non-smooth edge of the new reference profile via ILC

Therefore, to produce a new grasping profile for the gripper, the whole profile has to be regenerate with the new magnitude at 1.2s and 3.8s using equation 5.1 and 5.2 producing profile seen in Figure 6.16.

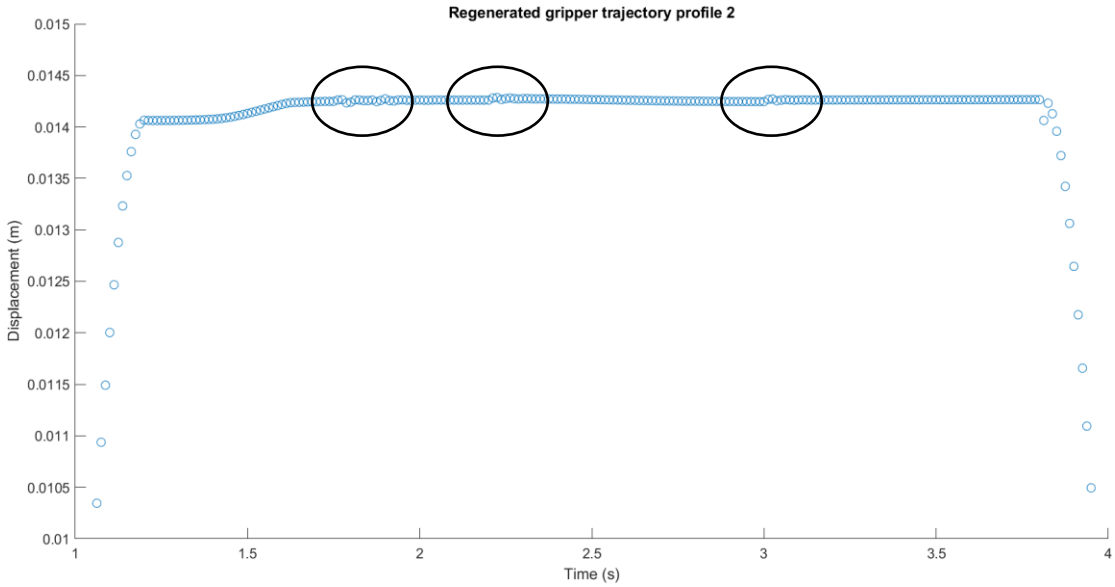

Figure 6.16: Non-smooth data within the deadtime of the grasping trajectory profile

Unfortunately, part of the profile (circled) in Figure 6.16 is not smooth. This can be the result of discretising the data. If left unfix, it should cause the system to become more and more unstable.

One of the solutions to resolve this issue is to increase the sampling rate to get more accurate data, however this comes at a cost of increase computational complexity. Fortunately, another solution is to apply a non-casual filter to the signal. This can be done using MATLAB built in function call 'smoothdata' which returns a moving average using a fix window size. Figure 6.17 shows the data before and after smoothing.

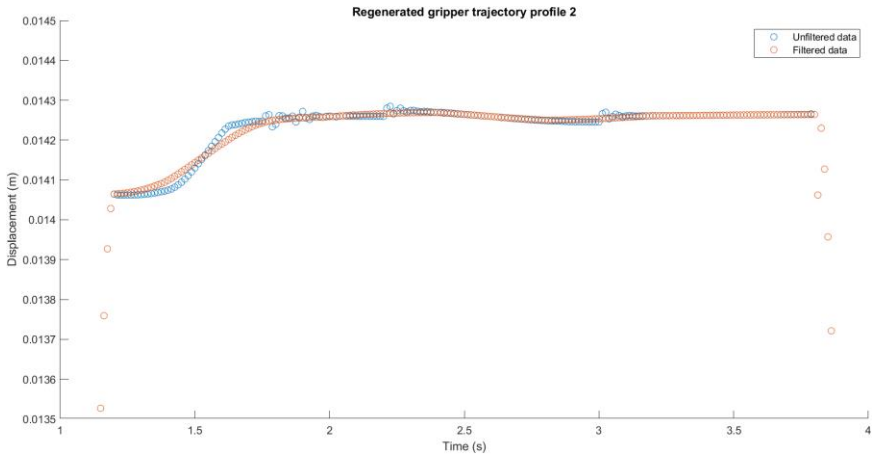

Figure 6.17: New trajectory profile before and after passing through a non-casual filter

Figure 6.18 shows the normalised position and force error. All the position controller converges at roughly 10th iteration with minimal error. The average force the object experienced is shown in Figure 6.19. Recall that DR6 requires the gripper to use no more than 25% of minimum force to grasp the object within 20 iterations after the gripper starts grasping, the simulation shows that the gripper starts grasping at 7th iteration and after 17 iterations, both fingers are below that value.

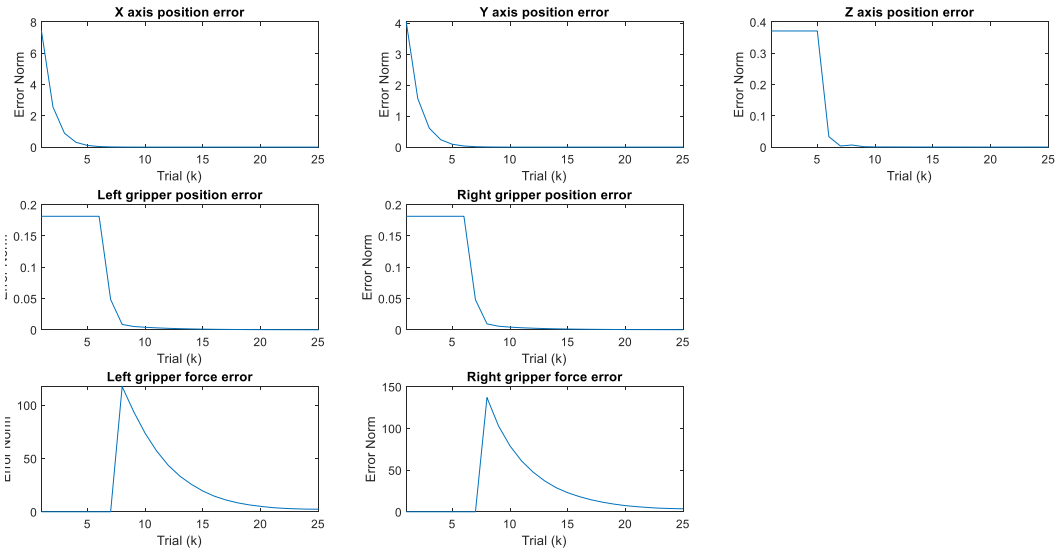

Figure 6.18: Normalised position and force error for each part of the gantry robot controller by ILC controllers

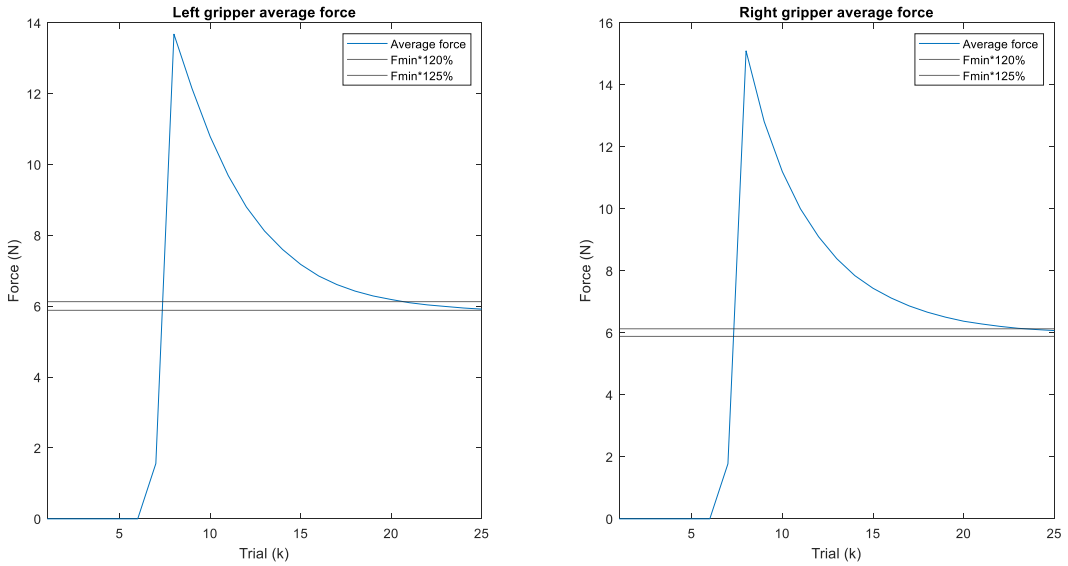

Figure 6.19: Average forces experienced by the object and the 20% and 25% increase in force over minimum force

It can be seen in Figure 6.20 that when the gripper starts grasping at 7th iteration, profile 1 is used. Once concludes the gripper has a solid grasp in the 8th iteration, profile 2 is used. It can also be seen that the controller has learn and adapted the grasping profile. The effect of the phenomenon of acceleration and deceleration force identified in chapter 4.2.2 can be seen at the 40th iteration peak and valley, where the gripper profile changes to considers those forces.

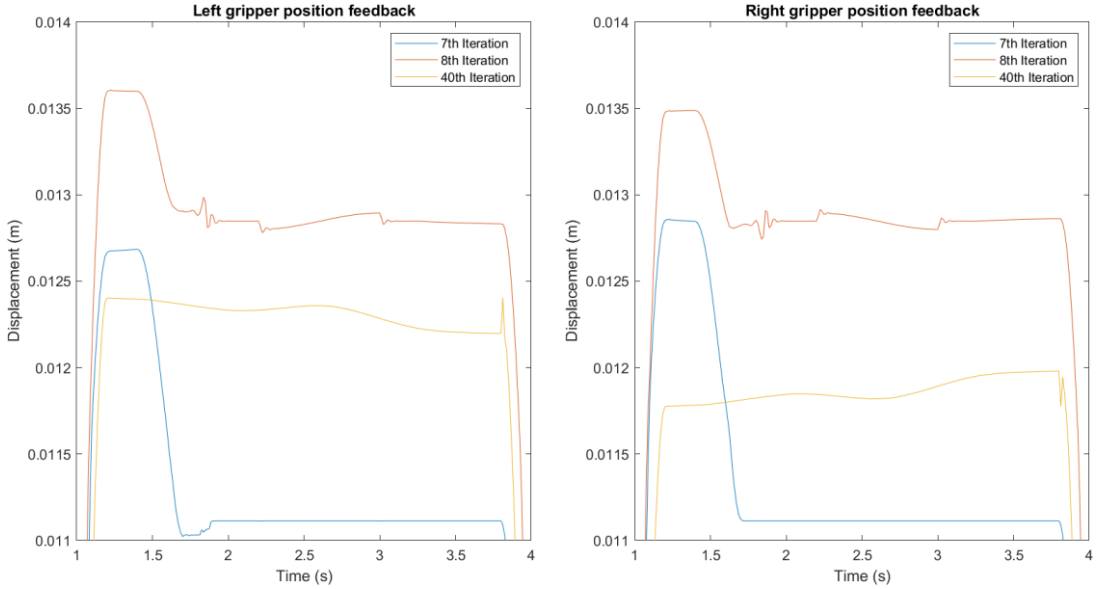

Figure 6.20: Left and Right gripper position feedback for 7th, 8th and 40th iteration

Figure 6.21 shows the force feedback which is not flat as compared to the impedance counterpart shown in figure 6.7. This could be due to applying non-casual filter to make the new trajectory smooth at the expense countering the unwanted dynamics or could be due to the controller not converging to exactly 0 normalised error which requires infinite number of iterations. Despite this issue, the gripper is able to grasp the object firmly thanks to the 20% margin given and resultant force applied is still identical to the desired force shown in Figure 6.21c.

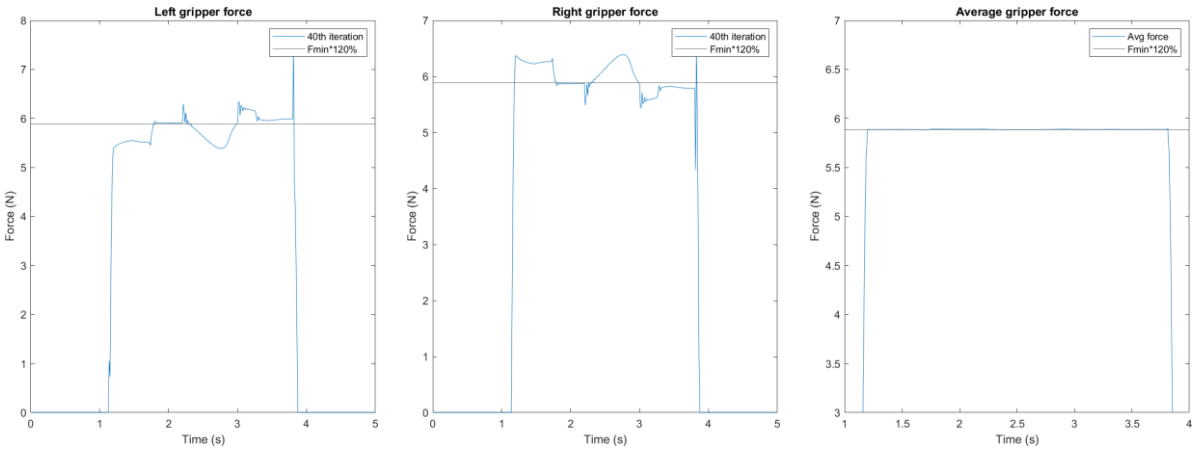

a) Left gripper force plot b) Right gripper force plot c) Sum and average force of left and right gripper

Figure 6.21: Gripper forces at 40th iteration

6.2.3 Updating Controller Model

As the aim of the gantry robot is to grasp object ranging from 0.2kg to 2kg. The bound is object weighing 0.2kg and 2kg. Thus, investigation of the effect of updating the plant will be carried out at the upper and lower bound as the effect of the rest would lie in between these two bounds. The plant is updated by recalculating the transfer function using equation 4.7 after taken into account the mass of the object.

Since Z axis (3kg) and gripper (1kg) are much lighter compared to X (47.7kg) and Y (21kg) axis [39]; the additional mass could cause these system dynamics to change significantly. Figure 6.22 show the grasping force experienced by the object of 2kg when the plant is updated versus not updated. The force feedback can be seen to be oscillating for non-updated plant, this is caused by extreme mismatch of the plant and actual system, causing the next iteration input vector to be significantly incorrect.

Figure 6.23 shows there is little to no effect of updating the plant for 0.2kg case as the mass is too small to cause significant mismatch.

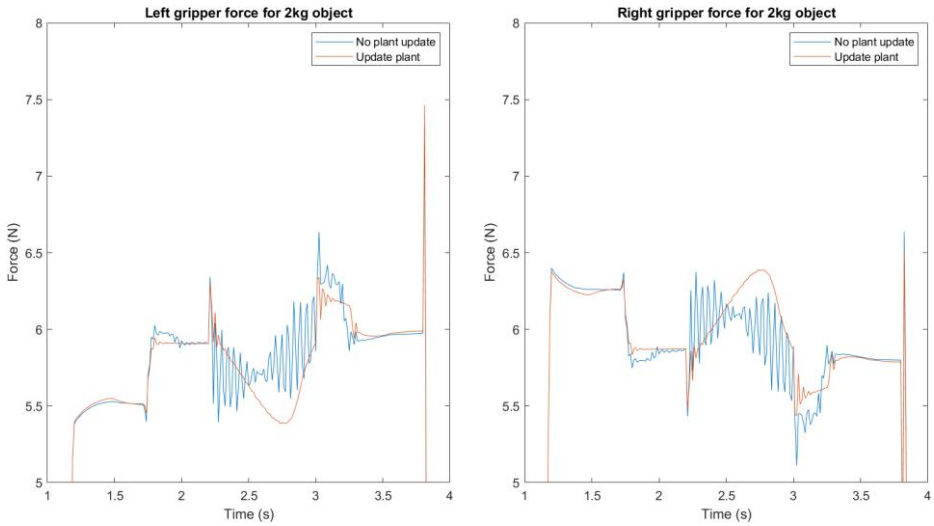

Figure 6.22: Forces experienced by the object when for scenario where plant is updated and not updated with the object mass of 2kg

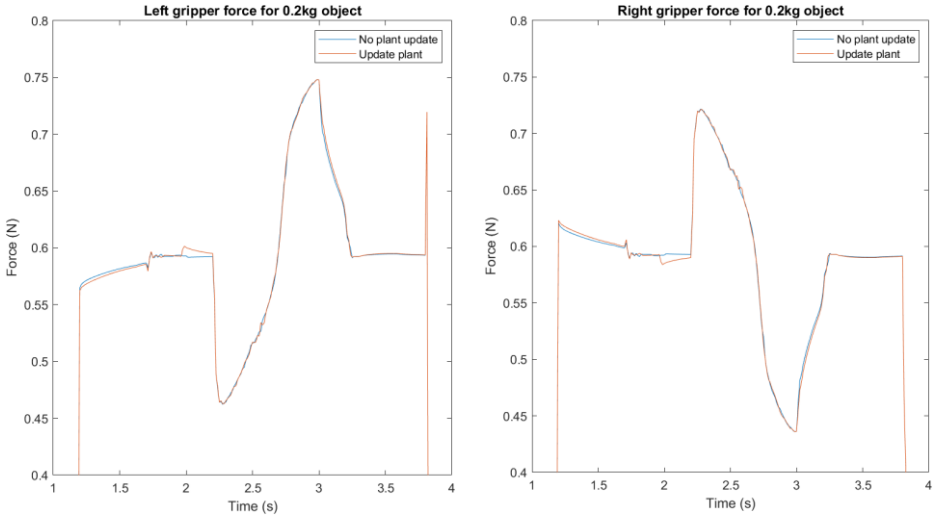

Figure 6.23: Forces experienced by the object when for scenario where plant is updated and not updated with the object mass of 0.2kg

Figure 6.24 shows the effect of updating plant model on position feedback on Z axis. Similar to the force scenario, there is significant consequences for not updating the model with 2kg object as the Z axis vibrates, essentially shaking the object. This phenomenon can be seen in figure 6.25 as the object starts to slid.

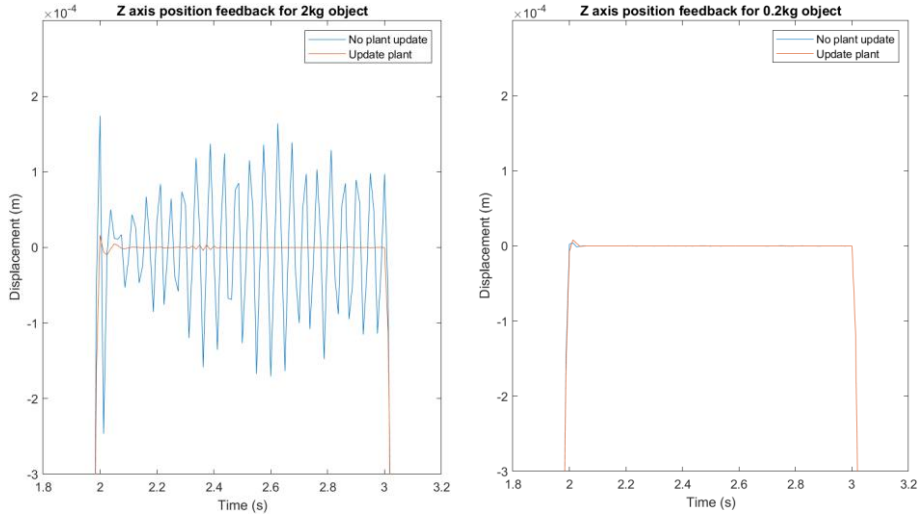

Figure 6.24: Z axis position feedback for 0.2kg and 2kg object for updated and non-updated plant

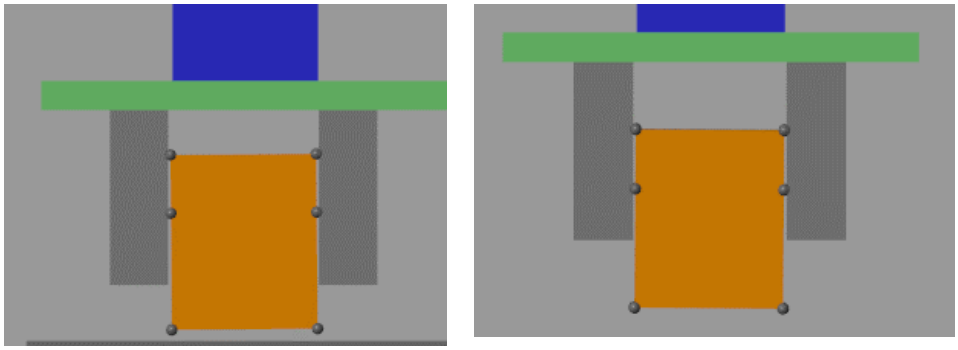

a) At 1.75s b) At 3.15s

Figure 6.25: 2kg object sliding when being transported using non-updated ILC controller. Both figures are to the same scale.

6.3 Summary

Both Impedance and ILC controllers are able to grasp object of mass ranging from 0.2kg to 2kg with little excessive force and fulfils DR4 to DR7. However, the disadvantage of Impedance control as shown in Figure 6.7 is the huge initial spike which could cause damage to the goods. ILC is able to eliminate this spike at the expense of taking more iteration to converge. The force feedback of ILC (figure 6.21) is relatively not ‘flat’ compared to the impedance counterpart (figure 6.7). As ILC uses model-based algorithm, it is crucial to update the plant to account for the object mass to avoid oscillation which could result in the object sliding off or dropped by the gripper.

7 Controller Disturbance Test

7.1 Test Setup

The disturbance will be introduced to the system via method discussed in Chapter 3.4. In total, there are 3 different disturbances.

1. Constant error added to the 1st iteration to mimic initial error.
2. Constant error added to the 30th iteration mimicking error occurring during operation.
3. Impulse error showing the effect of external force interacting with the system.

The magnitude of 5% and 10% disturbance shown in Table 7.1 are taken from the highest input signal amplitude under ideal condition shown in Figure 7.1. Impulse error will have short rise and fall time seen in Figure 7.2 with values found in Table 7.1.

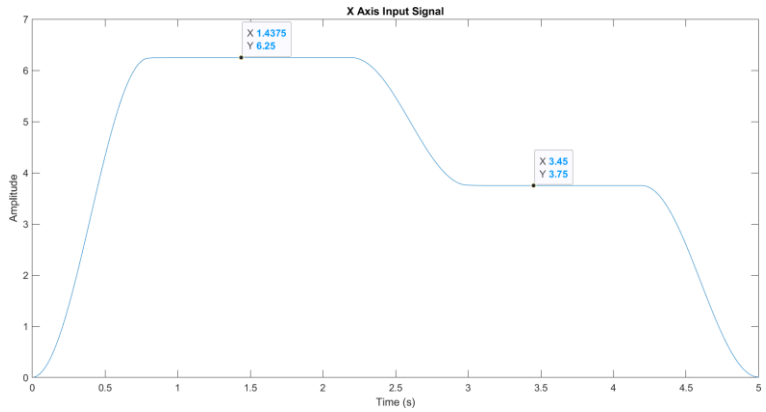

Figure 7.1: X axis input signal at 40th iteration under no disturbance scenario

Table 7.1: Values used to generate both constant and impulse disturbance for each part of the gantry system

	Constant error				Impulse error			
	X	**Y**	**Z**	**Gripper**	**X**	**Y**	**Z**	**Gripper**
5% amplitude	0.3125	7.5	-2.87	1.2	0.3125	7.5	-2.87	1.2
10% amplitude	0.625	15	-5.74	2.4	0.625	15	-5.74	2.4
Rise time	-	-	-	-	0.2	0.2	0.2	0.1
Dead time	-	-	-	-	0.2	0.2	0.2	0.2
Fall time	-	-	-	-	0.2	0.2	0.2	0.1

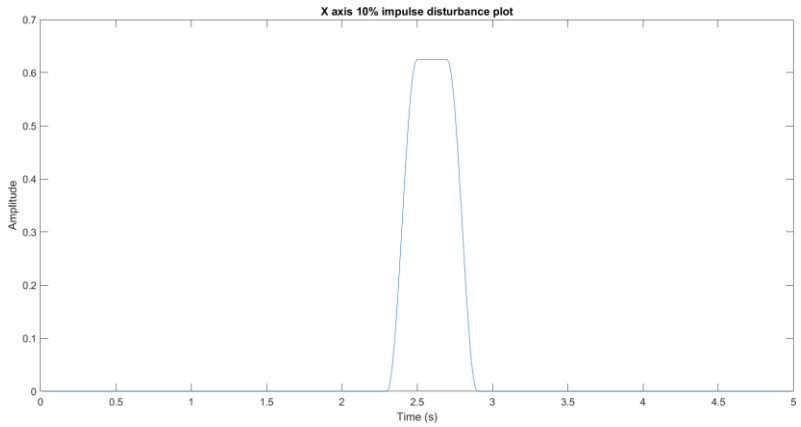

Figure 7.2: Example of Impulse disturbance, where in this case it is 10% for X axis

For ILC based controllers, the disturbance will be added to the input prior to passing the value to Simulink as demonstrated in Figure 7.3a, while for impedance-based controller, the disturbance will be added in Simulink prior to passing the value to PD controller as seen in Figure 7.3b.

```
if (i >= error_start)
    u_z_d = u_z+disturbance_z;
else
    u_z_d = u_z;
end
 inputz = timeseries(u_z_d,t);
```

a) Code showing disturbance added to ILC controller input

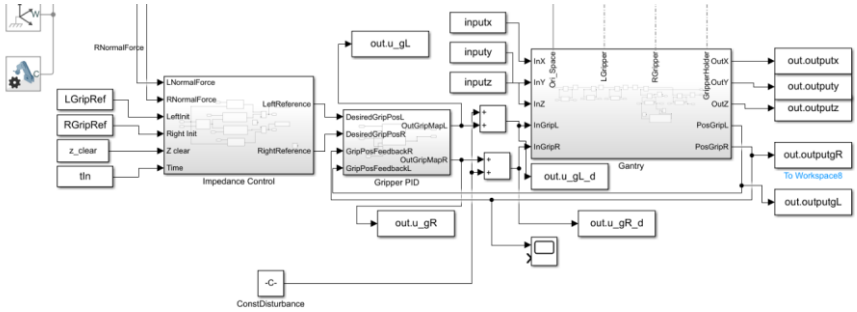

b) Simulink schematic where disturbance is added using blocks prior to the signal passing to the PD controller

Figure 7.3: Schematic for adding disturbance to ILC and Impedance based controllers

The following sections will investigate and analyse the outcome of the controllers when subjected to these disturbances.

7.2 Constant Error

7.2.1 Error at 1st Iteration

Table 7.2 highlights the observations from the test using various graphs such as normalised error, force feedback, etc and visual inspection of the simulation in Simulink.

Table 7.2: Observation of the behaviour of gripper and affect part of the gantry system under constant disturbance of various magnitude occurred at the 1st iteration

Remarks	ILC				Impedance
	X axis	Y axis	Z axis	Gripper	Gripper
5%	• Normalised error same as ideal at 4th iteration • Object grasped at 8th iteration	• Normalised error same as ideal at 4th iteration • Object grasped at 8th iteration	• Normalised error same as ideal at 6th iteration • Object grasped at 8th iteration	• Normalised error same as ideal at 7th iteration • Object grasped at 8th iteration	• Behaves identically to Ideal case
10%	• Normalised error same as ideal at 4th iteration • Object grasped at 8th iteration	• Normalised error same as ideal at 4th iteration • Object grasped at 8th iteration	• Normalised error same as ideal at 6th iteration • Object grasped at 8th iteration	• Normalised error same as ideal at 7th iteration • Object grasped at 8th iteration	• Behaves identically to Ideal case
Ideal	• Object firmly grasped at 8th iteration				• Object firmly grasped at 7th iteration
	• Gripper starts grasping object at 7th iteration • Z axis starts operating at 5th iteration				

Recall that X, Y, Z axis and gripper controller converges quickly as discussed in Chapter 5 and 6. Therefore, any initial error occurring at the 1st iteration will have been corrected in a few iterations.

This can be seen in Figure 7.4 where the normalised error between ideal and disturbed scenario are similar at 4th iteration for X axis. Figure 7.5 shows that the error between ideal and disturbed scenario is quickly corrected in 1 iteration. This concludes that initial error does not hinder the performance of the gripper.

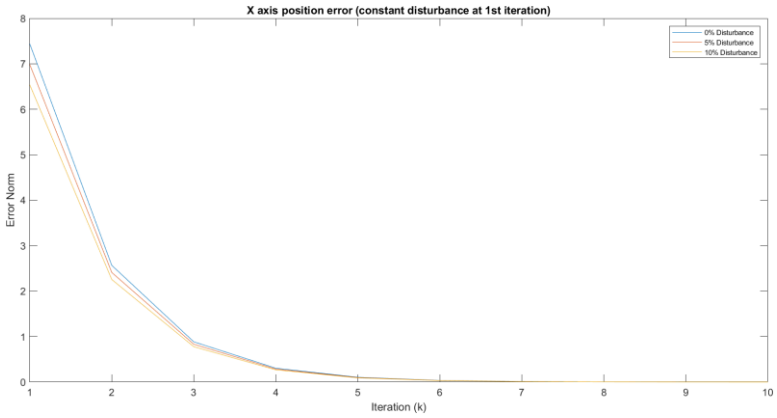

Figure 7.4: Normalised error of X axis for case of ideal, 5% error and 10% constant error occurring at the 1st iteration

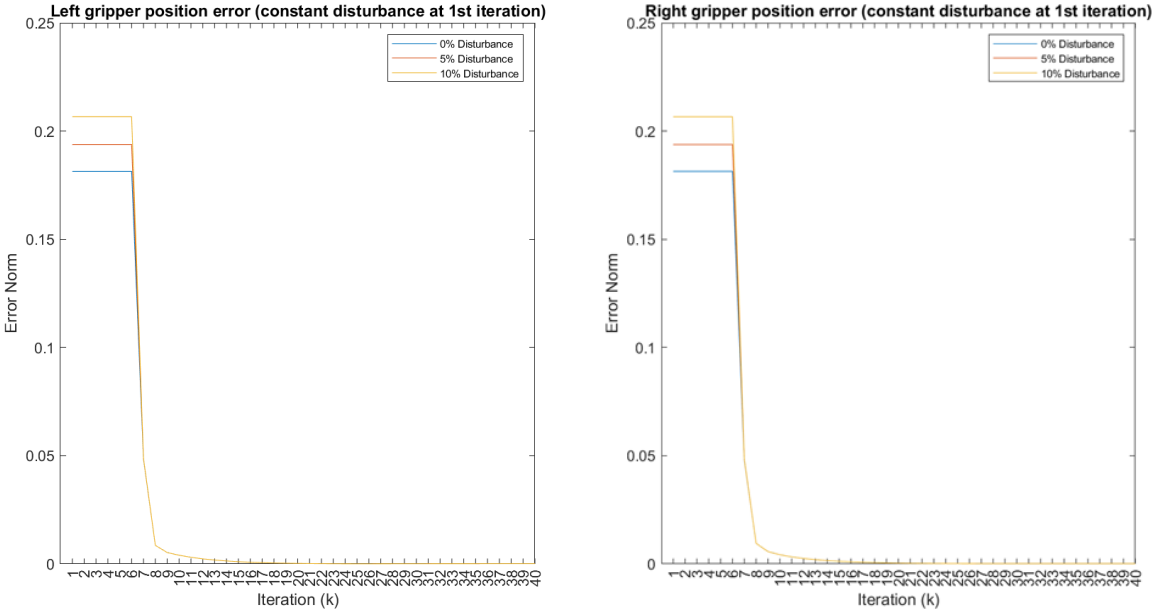

a) Left gripper normalised error for different magnitude of disturbance

b) Right gripper normalised error for different magnitude of disturbance

Figure 7.5: Normalised error for gripper when subjected to different magnitude of constant disturbance occurring at the 1st iteration using ILC controller

7.2.2 Error at 30th Iteration

A simple logic system is implemented to only add disturbance at the 30th iteration which is included in the schematics shown in Figure 7.3. 30th iteration is chosen because the force control converges to minimal error after 25th iteration as shown in Figure 6.19, therefore, this would mimic a system which is in operation for a sufficiently long period of time and now suffering from the effect of wear and tear.

Table 7.3 shows the observation on Impedance and ILC controlled gripper when part of the gantry system is subjected to a constant disturbance occurring at 30th iteration.

Table 7.3: Observation of affected axis/part of the gantry system and gripper when each part of the gantry system is subjected to constant disturbance occurring at 30th iteration

		Observations							
Amplitude	**Iteration**	**Disturbance on X axis**		**Disturbance on Y axis**		**Disturbance on Z axis**		**Disturbance on Gripper**	
		Impedance gripper	**ILC Gripper**	**Impedance gripper**	**ILC Gripper**	**Impedance gripper**	**ILC Gripper**	**Impedance gripper**	**ILC Gripper**
5%	30th	• Overshoot grasping volume • Attempted but failed grasp	• Overshoot grasping volume • Attempted but failed grasp	• Overshoot grasping volume • Attempted but failed grasp	• Overshoot grasping volume • Attempted but failed grasp	• Same as ideal operation	• Same as ideal operation	• Stable grasp	• Failed grasp
	31st	• Overshoot grasping volume • Unstable grasp	• Overshoot slightly • Success grasp (off centre)	• Overshoot slightly • Success grasp, slid slightly	• Overshoot slightly • Object 'push' before grasping				• Failed grasp
	32nd	• Same as ideal operation	• Overshoot slightly • Success grasp (off centre)	• Same as ideal operation	• Same as ideal operation				• Initial success grasp, drop in transportation
	33rd		• Same as ideal operation						• Success grasp, slid slightly
	34th								• Same as ideal operation
10%	30th	• Overshoot grasping volume • Failed grasp	• Overshoot grasping volume • Failed grasp	• Overshoot grasping volume. • Failed grasp	• Overshoot grasping volume. • Failed grasp	• Same as ideal operation	• Same as ideal operation	• Success grasp • Slid slightly.	• Failed grasp
	31st	• Overshoot slightly • Attempted but failed grasp	• Overshoot slightly • Attempted but failed grasp	• Overshoot slightly • Failed grasping	• Overshoot slightly • Unstable grasping				• Failed grasp
	32nd	• Overshoot slightly • Success grasp (off centre)	• Overshoot slightly • Success grasp (off centre)	• Overshoot slightly • Stable grasp	• Overshoot slightly • More stable grasp				• Failed grasp
	33rd	• Overshoot slightly • Success grasp (off centre)	• Overshoot slightly • Success grasp (off centre)	• Same as ideal operation	• Overshoot slightly • More stable grasp				• Failed grasp
	34th	• Same as ideal operation	• Same as ideal operation		• Same as ideal operation				• Failed grasp
	35th								• Initial success grasp, drop in transportation
	36th								• Success grasp, slid slightly
	37th								• Same as ideal operation

The observations are support by figures similar to the one shown in figure 7.6 where the effect of both scenario is reduced to a minimal at roughly 34th iteration despite one having double the magnitude. From these observations, it can be concluded that for disturbances occurring at X, Y or Z axis, both impedance and ILC gripper converges at roughly the same iteration when X, Y and Z axis controller

converges. Figure 7.7 shows the position feedback received and the corresponding changes to the input signal to counter the disturbance.

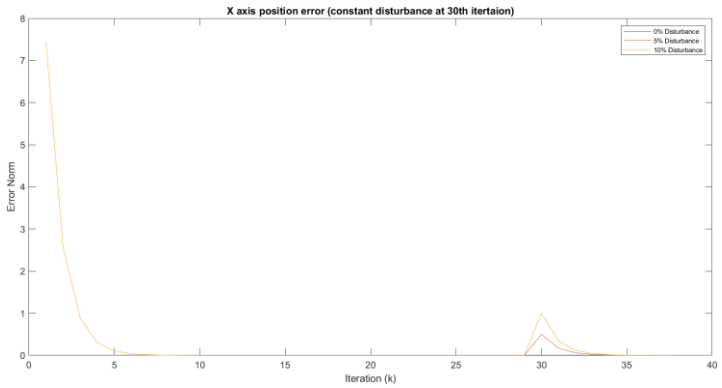

Figure 7.6: X axis normalised position error for case of no disturbance, constant 5% and 10% amplitude disturbance occurring at 30th iteration

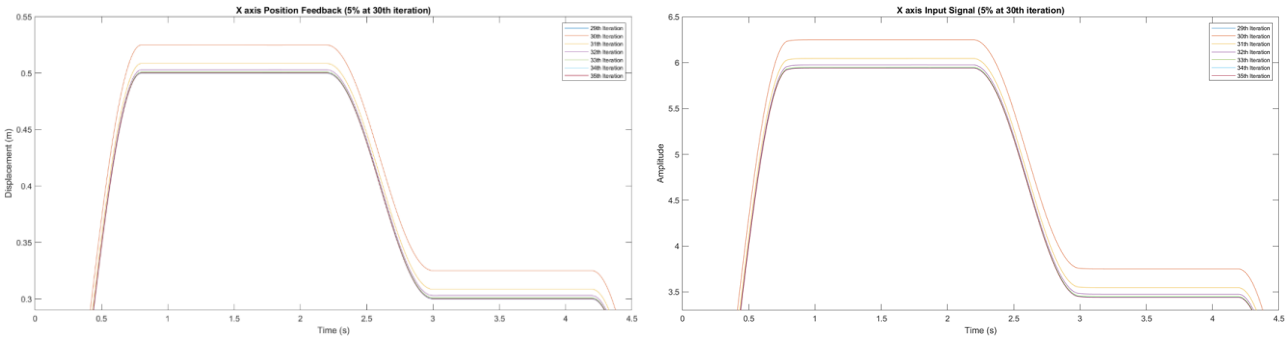

Figure 7.7: X axis position feedback for 5% disturbance occurring at 30th iteration and the corresponding changes to input signal

As seen from Table 7.3, the impedance-controlled gripper always is able to grasp the object, whereas the ILC controlled gripper takes a few iterations before it is able to grasp. However, since impedance control does not learn from previous iterations, for the 10% amplitude disturbance, the object will always slid. ILC on the other hand, is able to grasp the object firmly under the same disturbance after just a few iterations. To capture the sliding effect, tactile sensors are normally placed at the fingers, however, since the model does not include tactile sensors, it is identified visually illustrated in figure 7.8.

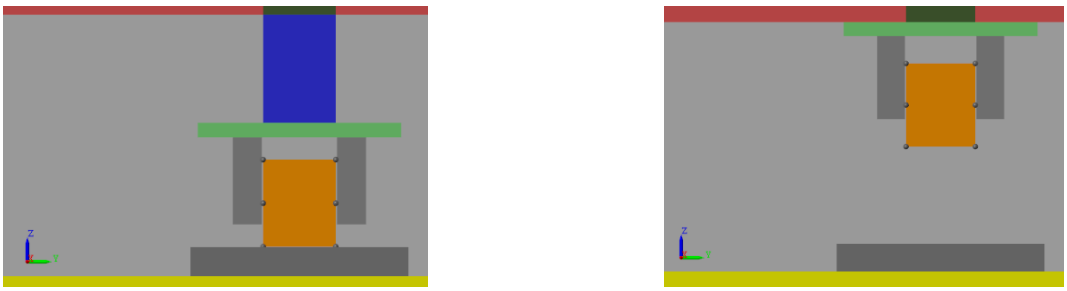

a) Initial grasp (1.25s) b) Object slid (2.2s)

Figure 7.8: Visual simulation of grasping point when impedance-controlled gripper is subjected to 10% constant disturbance (To scale)

Figure 7.9 and 7.10 shows the position and force feedback of the ILC grippers when it is subjected to disturbance. At 30th iteration, the gripper position feedback is lower than the one at 29th iteration showing disturbance has occurred, this causes the gripper to drop the object as insufficient force is applied resulting in the force feedback reduces to 0 at roughly 1.9s. This causes the next iteration input signal to experience a significant change thus resulting in excessive force used compared to at 29th

iteration. After the object has been grasped (32nd iteration), it will start correcting itself and finally residing to similar applied force seen at 29th iteration.

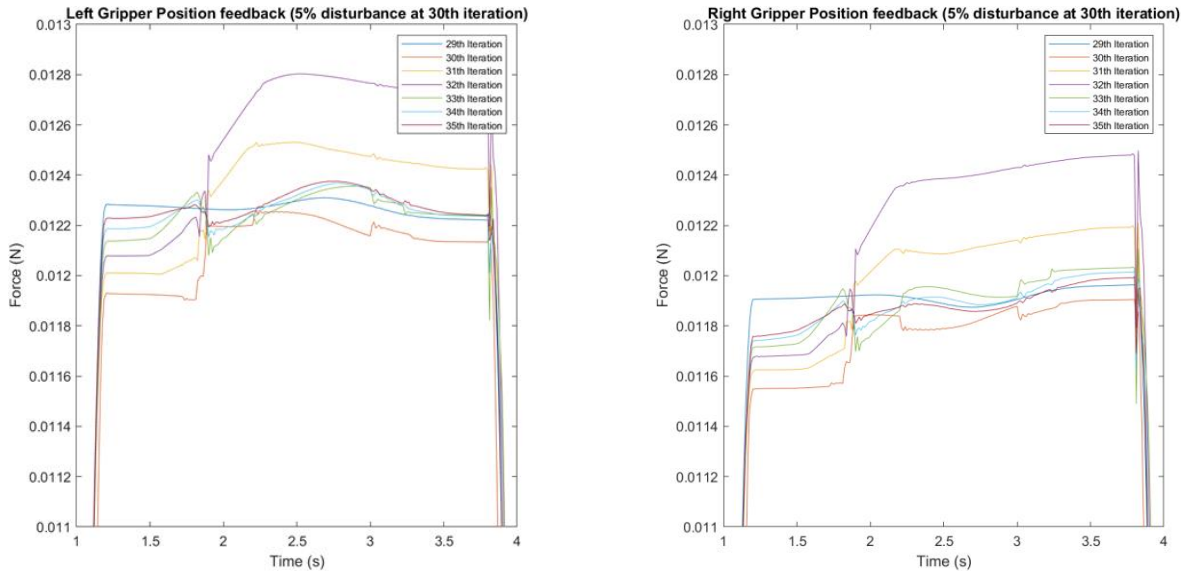

Figure 7.9: Graph showing gripper position feedback when the ILC controlled gripper is subjected to 5% constant disturbance at 30th iteration

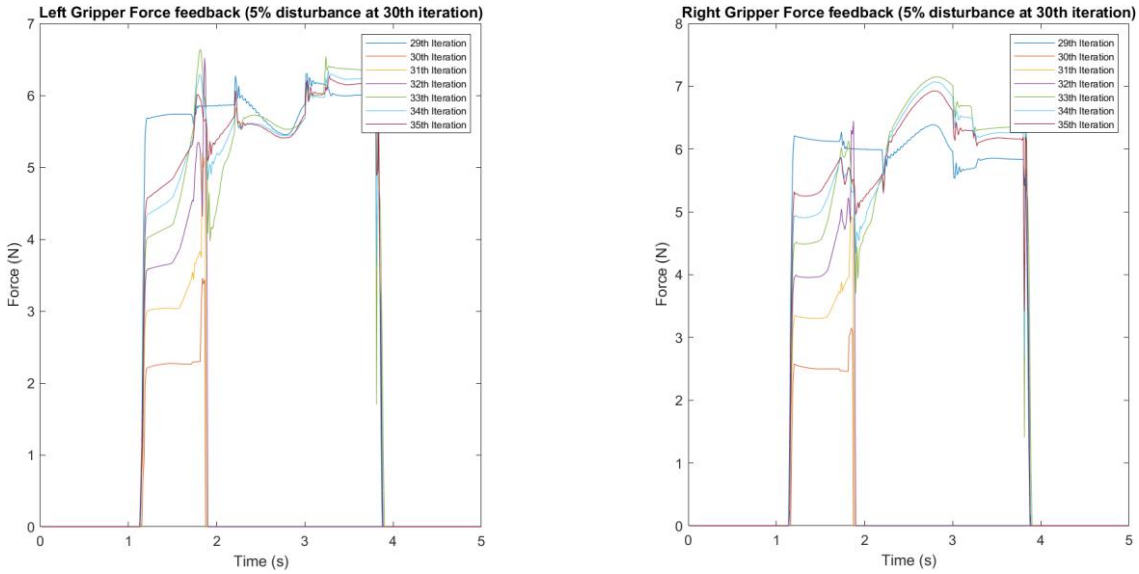

Figure 7.10: Graph showing force applied when the ILC controlled gripper is subjected to 5% constant disturbance at 30th iteration

7.3 Impulsive Error

Table 7.4 shows the observation when the gantry system is subjected to impulse disturbances. Similar to the constant disturbance case, impedance and ILC gripper performance relatively similar to teach other when X, Y and Z axis are subject to disturbance.

Table 7.4: Observation of affected axis/part of the gantry system and gripper when each part of the gantry system is subjected to impulse disturbance occurring at 30th iteration

		Observations							
Amplitude	**Iteration**	**Disturbance on X axis**		**Disturbance on Y axis**		**Disturbance on Z axis**		**Disturbance on Gripper**	
		Impedance gripper	**ILC Gripper**	**Impedance gripper**	**ILC Gripper**	**Impedance gripper**	**ILC Gripper**	**Impedance gripper**	**ILC Gripper**
5%	30th	• Failed grasp	• Object slid	• Failed grasp	• Object slid	• Stable grasp	• Stable grasp	• Object slid	• Fail grasp
	31st	• Stable grasp	• Stable grasp	• Stable grasp	• Stable grasp				• Fail grasp
	32nd								• Stable grasp
10%	30th	• Failed grasp	• Failed grasp	• Failed grasp	• Object slid more	• Stable grasp	• Stable grasp	• Failed grasp	• Fail grasp
	31st	• Object slid	• Object slid	• Object slid and dropped	• Object slid slightly				• Fail grasp
	32nd	• Stable grasp	• Stable grasp	• Stable grasp	• Stable grasp				• Fail grasp
	33rd								• Stable grasp

Since X, Y and Z axes uses ILC controller, the effect caused by the disturbance is minimised in a few iterations. Figure 7.11a shows that at 30th iteration, there is a massive error but by 34th iteration, the error has been corrected. Figure 7.11b shows the resultant changes to input signal for X axis to account for the disturbance. Y and Z axis can be analyse similarly.

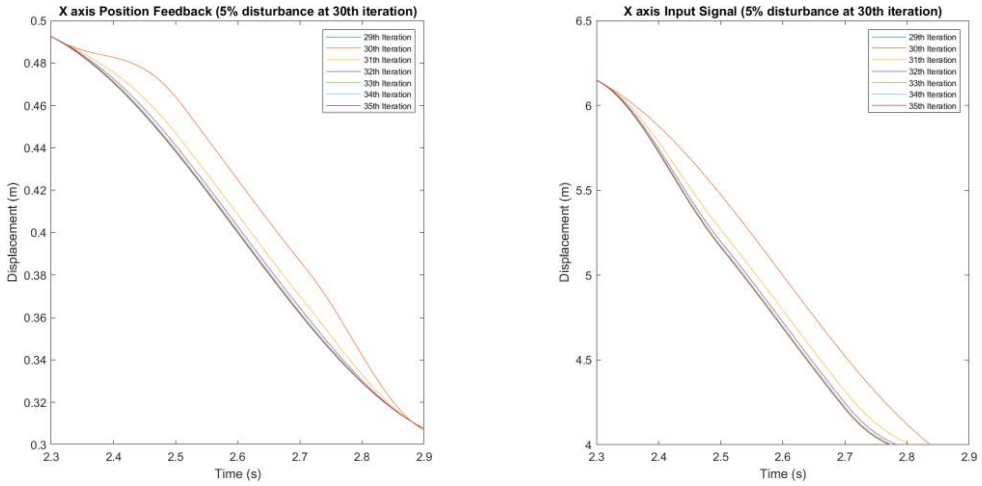

Figure 7.11: Adaptation of ILC algorithm on X axis position feedback and input signal when subjected to 5% Impulse disturbance

The corresponding force and position feedback of the impedance and ILC gripper when X axis is subjected to 5% impulse disturbance is shown in figure 7.12 and 7.13. For Impedance gripper, it can be seen that at 30th iteration, the force drops to roughly 0 around 2.6s indicating that the object has

been dropped, in line with the observation in Table 7.4. During this time, the impedance controller does not have knowledge that the object has been dropped where it to assume that there is not enough force causing it to close the gripper further causing a huge spike.

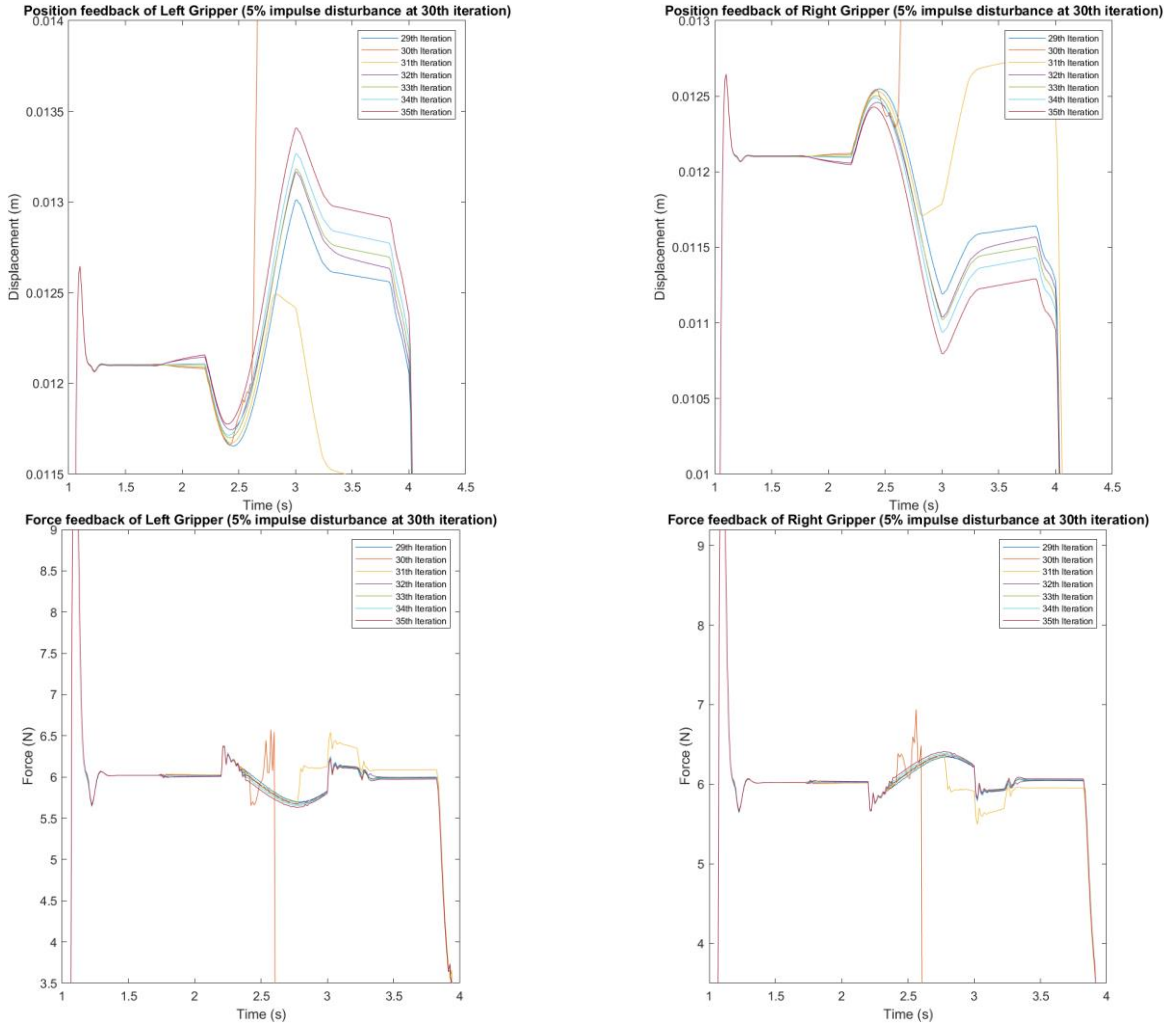

Figure 7.12: Impedance controlled gripper position feedback and force plots when X axis is subjected to 5% impulse disturbance

The ILC gripper does not drop the object when subjected X axis with 5% impulse disturbance, but rather slip. Due to the lack of tactile sensor, it is not possible to identified slippage, but the force plot seen in Figure 7.13 shows that there is a minor spike, indicating something has happened.

Both grippers performance superbly when the Z axis is subjected to impulse disturbance. This is because when Z axis encounters impulse disturbance, it is similar to shaking the object vertically and the 20% margin helps to mitigate the effect.

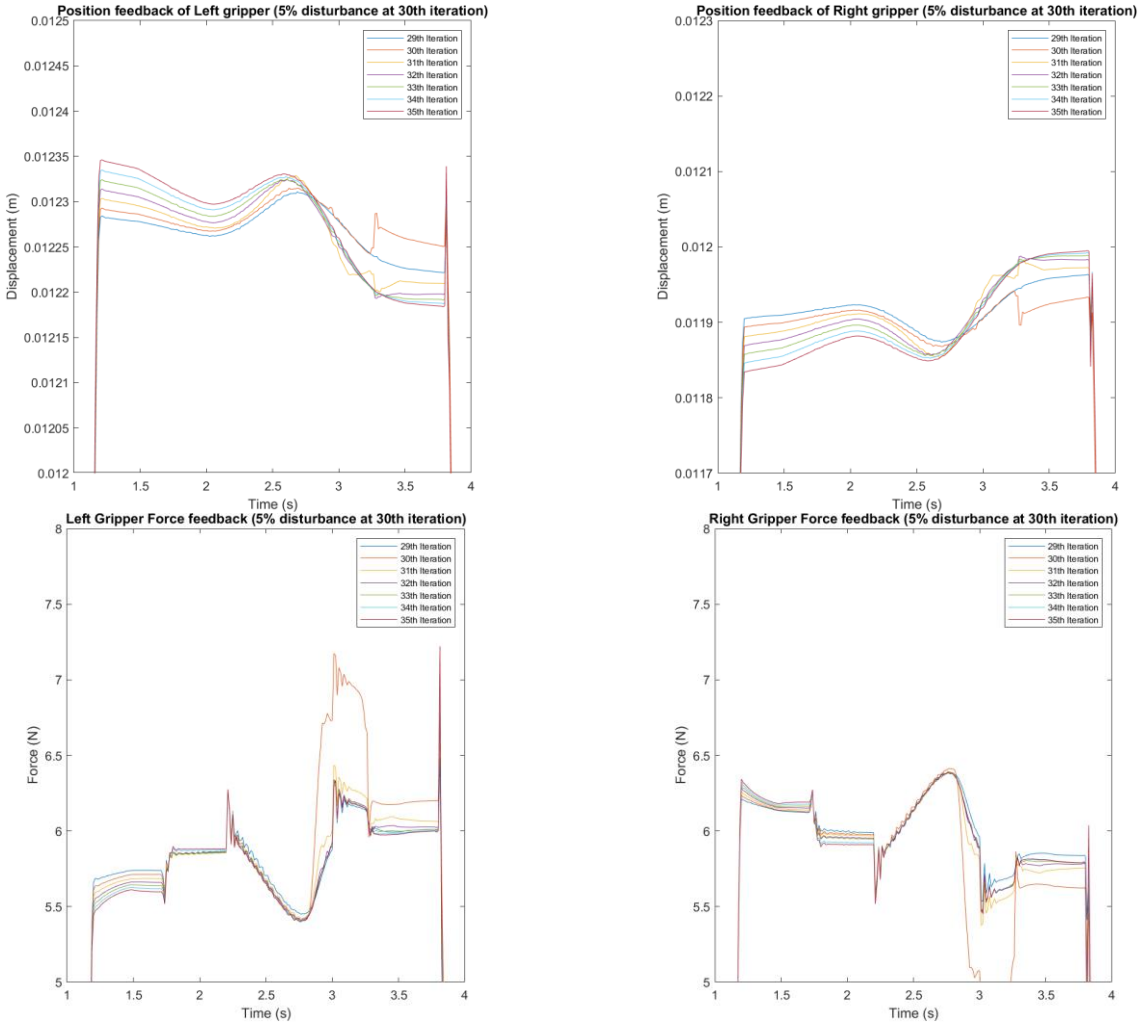

Figure 7.13: ILC controlled gripper position feedback and force plots when X axis is subjected to 5% impulse disturbance

In this scenario, since impedance does not learn from previous iteration, once the gripper becomes unstable and drop the object, it will never recovers as highlighted in Table 7.4 . Figure 7.14 shows the sequence visually. ILC controller on the other hand initially performs worse by dropping the object, but after 2-3 iterations, it converges and is able to grasp the object.

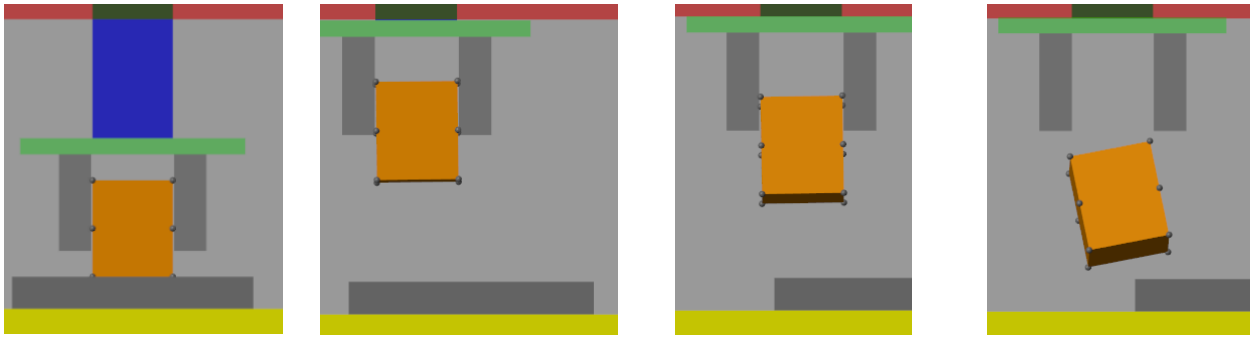

a) 1.25s b) 2.35s c) 2.4s d) 2.45s

Figure 7.14: Sequence of gripper using impedance controller subjected to 10% impulse disturbance

The effect of impulse disturbance on ILC gripper can be seen at the 30th iteration in Figure 7.15. The position feedback of 29th and 35th iteration is almost identical, showcasing the ability of ILC to correct repetitive error. The force experienced by the object is also shown in Figure 7.16. Recalling that if the force feedback drops to 0, the object is dropped.

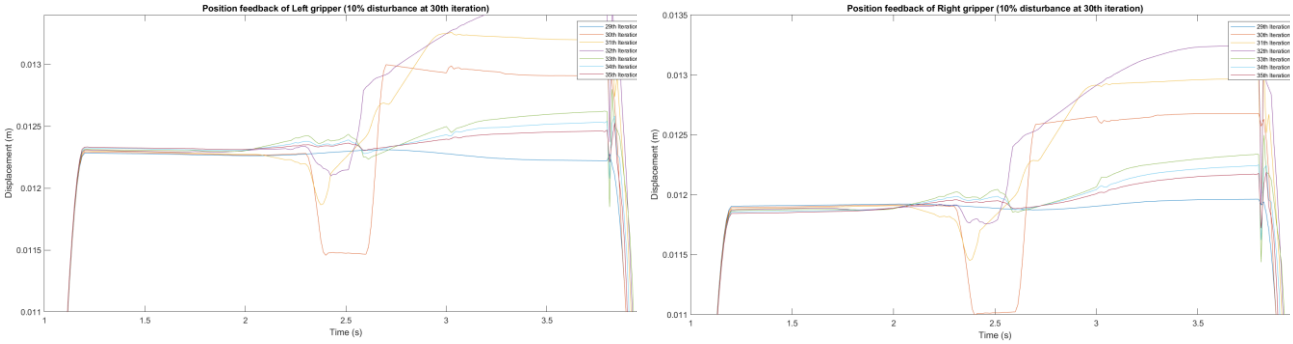

Figure 7.15: Gripper position feedback when subjected to 10% impulse disturbance

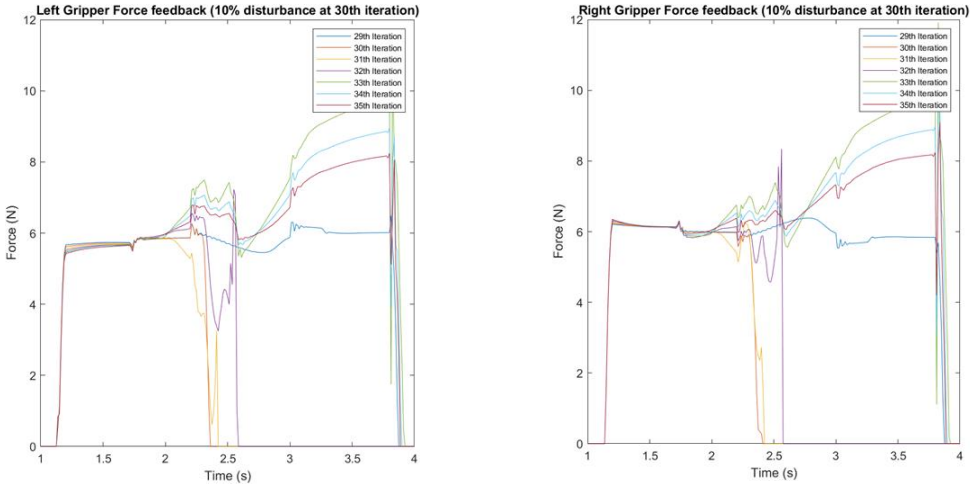

Figure 7.16: Force experienced when gripper is subjected to 10% impulse disturbance

7.4 Summary

Both impedance and ILC controlled gripper performance relatively similarly when the gantry system is subjected to constant and impulse disturbance. Particularly, due to the additional 20% force margin specified in the control algorithm, Z axis disturbance does not cause any damage.

The advantage of ILC over impedance control is its learning ability. As demonstrated with impulse disturbance, impedance-controlled gripper has a limit to how large disturbance it can be subjected to before dropping the object indefinitely. Although ILC gripper initially dropped the object, after a few iterations, it is able to correct itself and grasp the object securely.

Unfortunately, both controllers are not able to detect slippage and correct them accordingly.

8 Conclusions and Future Work

A model industrial gantry robot and interaction forces between robot and environment is modelled successfully in MATLAB Simulink using Simscape Multibody toolbox.

A new control algorithm was designed to fulfil the requirements set at chapter 2. The ILC controller is able to reduce the spike in force issue encountered by impedance control after a few iterations. However, the force profile is not as smooth as impedance control owing to the fact that ILC updates its input after every iteration. As the ILC controller in this project uses a model-based algorithm, it is crucial to update the plant model to include the added grasped object mass to ensure the changes in system dynamics is encountered for. ILC controller has proven itself to be great at eliminating repetitive disturbances that the impedance counterpart could not.

To fully evaluate the success of the project, the specification layout in chapter 2 is compared against the result and analysis conducted in Chapters 4-7.

8.1 Review against Design Requirement

Table 8.1 contains numbered Design Requirements set out previously, a brief description of the aim and how well it is met out of 10.

Table 8.1: Comparison of design requirement against the ILC controller algorithm and quality of simulation model

Design Requirement	Brief description	Achievement
1	Simulation model related to industrial robot	7/10
2	Accurate simulation model	9/10
3	Simulation can be seen visually	9/10
4	Gantry robot reaches final location in a few iterations	10/10
5	Fast reach and grasp sequence	10/10
6	Minimal excessive force used	9/10
7	Grasp range of objects	10/10
8	Robust to commonly encountered disturbances	9/10
Total score		73/80

A detailed breakdown of the scores can be found in Table 8.2.

Table 8.2: Detailed breakdown of the scores given in Table 8.1

Design Requirement	Achievement	Additional notes
1	The model selected was a simple 3 axis gantry robot.	However, a more flexible robotic arm robot with multiple direction of freedom (DOF) is gaining popularity in industry.
2	The simulation model is capable of modelling the dynamics of the system and any interaction force it may encounter.	Unfortunately, the chosen gantry robot dates back to 2005, the mass used in the simulation does not reflect the actual mass but an estimation. The gripper fingers are quite large as the contact point is modelled as spheres.
3	The 3 axis of the gantry robot and the gripper can be visually seen, and it is possible to see what is happening when it is simulating.	Box-like structure is the easiest to implement using Simscape multibody. To improve the visual aspect, 3D models can be generated from elsewhere such as Solidworks and imported in.
4	The gantry robot is able to complete close to ideal reach and grasp action in roughly 10 iterations.	-
5	The whole reach and grasp profile is completed in just 5s under the assumption that the gantry robot is capable of producing the required torque.	Most industrial robot deals with bigger and heavier object and thus the duration for 1 iteration might increase.
6	The gripper uses around 20% more force when grasping an object after it converges.	Initial few iterations use quite excessive force depending on the initial profile generated for the gripper
7	The gripper is able to safely transport object ranging from 0.2kg to 2kg	Further research should aim at grasping object of various shapes and size
8	The gripper is able to correct itself and grasp the object when there is repetitive disturbance presence.	The gripper might initially drop the object when the disturbance is first encountered.

8.2 Future Work and Research

A few areas that could be improved and investigated are highlighted below.

8.2.1 Hybrid of ILC and Impedance

Impedance controller is great at reducing the amount of excessive force applied to the system whereas ILC is superb at removing any repetitive disturbances. Therefore, to get the best of both worlds, it would be worth investigating the overall gain of combining these two algorithms.

8.2.2 Test on Physical System

The project has only focus on evaluating the performance of the new ILC controller in a simulation environment. To fully test the controller, it is necessary to subject the controller to test on the actual gantry robot to fully justify the improvements gain of ILC over Impedance controller.

8.2.3 Increase Complexity of Gripper Hardware

This project uses a basic two parallel plate fingers gripper with force sensors. To avoid object falling out during operation, it is necessary to detect any slippage that occurs and correct it immediately. This requires multiple tactile sensors to be placed carefully at the fingers.

As identified by Chapter 1, there are multiple more advance gripper structure. To fully exploit ILC capability and improve grasping, these more advance grippers shall be used and compare the result with ones using impedance controller.

8.2.4 Improve ILC Algorithm to Grasp Object of Different Shapes and Sizes

Objects in the real world comes not only in different mass, but also different shapes and sizes. To be able to grasp different types of objects, some sort of visual sensors should be used. With the help of machine learning, different tracking profiles should be used to grasp different objects. ILC can be used to improve the tracking profiles which theoretically should use less computational resources than machine learning methods.

8.2.5 Research Into Minimisation Equations

The ILC controller algorithm focuses on minimising two cost function. This could potentially cause the update to conflict with each other. Research should be conducted to find the relationship between force applied and grasping distance and minimise these two components to produce only just one update equation instead of the current two.

References

[1] Dima, "Short history of manufacturing: from Industry 1.0 to Industry 4.0", KFactory, 2021. [Online]. Available: https://kfactory.eu/short-history-of-manufacturing-from-industry-1-0-to-industry-4-0/#:~:text=The%20Third%20Industrial%20Revolution%20(Industry,memory%2Dprogrammable%20controls%20and%20computers.

[2] "Robotics Market Size, Share (2022 - 27)", Mordorintelligence.com. [Online]. Available: https://www.mordorintelligence.com/industry-reports/robotics-market.

[3] R. Hodson, "A gripping problem", Nature, vol. 557, 2018.

[4] T. Scott, "How many robots does it take to run a grocery store? ", [Online]. Available: https://www.youtube.com/watch?v=ssZ_8cqfBlE.

[5] J. Mahler et al., "Learning ambidextrous robot grasping policies," Science Robotics, vol. 4, no. 26, p. eaau4984, 2019, doi: doi:10.1126/scirobotics.aau4984.

[6] O. Ryuta and T. Kenji, "Grasp and dexterous manipulation of multi-fingered robotic hands: a review from a control view point," Advanced Robotics, vol. 31, no. 19-20, pp. 1030-1050 , year = 2017, doi: 10.1080/01691864.2017.1365011.

[7] NAPIER JR. The prehensile movements of the human hand. J Bone Joint Surg Br. 1956 Nov;38-B(4):902-13. doi: 10.1302/0301-620X.38B4.902. PMID: 13376678.50

[8] Kamakura N, Matsuo M, Ishii H, Mitsuboshi F, Miura Y. Patterns of static prehension in normal hands. Am J Occup Ther. 1980 Jul;34(7):437-45. doi: 10.5014/ajot.34.7.437. PMID: 6446851.

[9] M. R. Cutkosky, "On grasp choice, grasp models, and the design of hands for manufacturing tasks," in IEEE Transactions on Robotics and Automation, vol. 5, no. 3, pp. 269-279, June 1989, doi: 10.1109/70.34763.

[10] B. Abbasi, E. Noohi, S. Parastegari and M. Žefran, "Grasp taxonomy based on force distribution," 2016 25th IEEE International Symposium on Robot and Human Interactive Communication (RO-MAN), 2016, pp. 1098-1103, doi: 10.1109/ROMAN.2016.7745245.

[11] Y. Li, Q. Lei, C. Cheng, G. Zhang, W. Wang, and Z. Xu, "A review: machine learning on robotic grasping," 03, 2019.

[12] T. Yamashita, 'Engineering approaches to function of fingers', 1963.

[13] Mouri, T., Kawasaki, H., and Ito, S., "Unknown Object Grasping Strategy Imitating Human Grasping Reflex for Anthropomorphic Robot Hand", Journal of Advanced Mechanical Design, Systems, and Manufacturing, vol. 1, no. 1, pp. 1–11, 2007. doi:10.1299/jamdsm.1.1

[14] M. Teichmann and B. Mishra, "Reactive Robotics I: Reactive Grasping with a Modified Gripper and Multifingered Hands," The International Journal of Robotics Research, vol. 19, no. 7, pp. 697-708, 2000, doi: 10.1177/027836490001900706

[15] K. G. Shin and C. -p. Lee, "Compliant control of robotic manipulators with resolved acceleration," 1985 24th IEEE Conference on Decision and Control, 1985, pp. 350-357, doi: 10.1109/CDC.1985.268883.

[16] P. R. Pagilla and M. Tomizuka, "Adaptive control of two robot arms carrying an unknown object," Proceedings of 1995 IEEE International Conference on Robotics and Automation, 1995, pp. 597-602 vol.1, doi: 10.1109/ROBOT.1995.525349.

[17] J. -. E. Slotine and Li Weiping, "Adaptive manipulator control: A case study," in IEEE Transactions on Automatic Control, vol. 33, no. 11, pp. 995-1003, Nov. 1988, doi: 10.1109/9.14411.

[18] S. Pertuz, C. Llanos, and D. Muñoz, "Simulation and Implementation of Impedance Control in Robotic Hand," 04, 2018

[19] S. Pertuz, C. Llanos, and D. Muñoz, "Simulation and Implementation of Impedance Control in Robotic Hand," 04, 2018
[20] D. A. Bristow, M. Tharayil and A. G. Alleyne, "A survey of iterative learning control," in IEEE Control Systems Magazine, vol. 26, no. 3, pp. 96-114, June 2006, doi: 10.1109/MCS.2006.1636313.
[21] T. Nakayama, S. Arimoto and T. Naniwa, "Coordinated learning control for multiple manipulators holding an object rigidly," Proceedings of 1995 IEEE International Conference on Robotics and Automation, 1995, pp. 1529-1534 vol.2, doi: 10.1109/ROBOT.1995.525492.
[22] S. SHAIKH and M. SHAIKH, "IMPORTANCE OF MODELING AND SIMULATION: A VITAL SYSTEMS ENGINEERING TECHNIQUE," International Journal of Advances in Science Engineering and Technology, vol. 5, no. 1, pp. 121–124, Feb. 2017.
[23] H. Elci, R. W. Longman, Minh Phan, Jer-Nan Juang and R. Ugoletti, "Discrete frequency based learning control for precision motion control," Proceedings of IEEE International Conference on Systems, Man and Cybernetics, 1994, pp. 2767-2773 vol. 3, doi: 10.1109/ICSMC.1994.400292.
[24] W. Messner, R. Horowitz, W. -. Kao and M. Boals, "A new adaptive learning rule," in IEEE Transactions on Automatic Control, vol. 36, no. 2, pp. 188-197, Feb. 1991, doi: 10.1109/9.67294.
[25] Dong-Il Kim and Sungkwun Kim, "An iterative learning control method with application for CNC machine tools," in IEEE Transactions on Industry Applications, vol. 32, no. 1, pp. 66-72, Jan.-Feb. 1996, doi: 10.1109/28.485814.
[26] S. Arimoto, S. Kawamura and F. Miyazaki, "Bettering operation of dynamic systems by learning: A new control theory for servomechanism or mechatronics systems," The 23rd IEEE Conference on Decision and Control, 1984, pp. 1064-1069, doi: 10.1109/CDC.1984.272176.
[27] S. Arimoto, S. Kawamura, F. Miyazaki and S. Tamaki, "Learning control theory for dynamical systems," 1985 24th IEEE Conference on Decision and Control, 1985, pp. 1375-1380, doi: 10.1109/CDC.1985.268737.
[28] M. Q. Phan and J. A. Frueh, "Learning control for trajectory tracking using basis functions," Proceedings of 35th IEEE Conference on Decision and Control, 1996, pp. 2490-2492 vol.3, doi: 10.1109/CDC.1996.573465.
[29] O. Markusson, H. Hjalmarsson and M. Norrlof, "Iterative learning control of nonlinear non-minimum phase systems and its application to system and model inversion," Proceedings of the 40th IEEE Conference on Decision and Control (Cat. No.01CH37228), 2001, pp. 4481-4482 vol.5, doi: 10.1109/CDC.2001.980908.
[30] M. Togai and O. Yamano, "Analysis and design of an optimal learning control scheme for industrial robots: A discrete system approach," 1985 24th IEEE Conference on Decision and Control, 1985, pp. 1399-1404, doi: 10.1109/CDC.1985.268741.
[31] N. Amann, D. H. Owens, and E. Rogers, "Iterative learning control for discrete-time systems with exponential rate of convergence," IEE Proceedings - Control Theory and Applications, vol. 143, no. 2, pp. 217-224. [Online]. Available: https://digital-library.theiet.org/content/journals/10.1049/ip-cta_19960244
[32] N. Amann, D. H. Owens and E. Rogers, "Iterative learning control for discrete time systems using optimal feedback and feedforward actions," Proceedings of 1995 34th IEEE Conference on Decision and Control, 1995, pp. 1696-1701 vol.2, doi: 10.1109/CDC.1995.480384.
[33] G. Lahr, J. V. Rocha Soares, H. Garcia, Adriano, A. A. G. Siqueira, and G. Caurin, "Understanding the Implementation of Impedance Control in Industrial Robots," 10, 2016
[34] S. Pertuz, C. Llanos, and D. Muñoz, "Simulation and Implementation of Impedance Control in Robotic Hand," 04, 2018.

[35] José and K. Frank, "Modelling and Simulation of Robot Arm Interaction Forces Using Impedance Control," IFAC Proceedings Volumes, vol. 41, no. 2, pp. 15589-15594, 2008, doi: https://doi.org/10.3182/20080706-5-KR-1001.02636
[36] F. Caccavale, C. Natale, B. Siciliano and L. Villani, "Integration for the next generation: embedding force control into industrial robots," in IEEE Robotics & Automation Magazine, vol. 12, no. 3, pp. 53-64, Sept. 2005, doi: 10.1109/MRA.2005.1511869.
[37] J. Ratcliffe, "Iterative Learning Control Implemented on a Multi-Axis System", June 2005.
[38] J. Collins, S. Chand, A. Vanderkop and D. Howard, "A Review of Physics Simulators for Robotic Applications," in IEEE Access, vol. 9, pp. 51416-51431, 2021, doi: 10.1109/ACCESS.2021.3068769.
[39] Aerotech sales website, “AGS1000 Direct-Drive Gantry”. Available at: https://uk.aerotech.com/product/gantries-en-uk/ags1000-direct-drive-gantry/

Appendix A. Project management

Project management including time and progress management is an important part of ensuring the project is completed in an organised and timely manner. The following sections identified several risks and methods to minimise them and plans to realise a smooth project progress.

A1 - Contingency Planning, Minimising risk, reduce impact

Setbacks and issues due to unexpected events, failures and changes are unavoidable in projects. An effective solution involves the following steps:

1. Identify potential setbacks/issues.
2. Plan out methods of minimising the chances or damage of these setbacks/issues.
3. Create contingency plans to overcome them.

Setbacks/issues can be classified as risks encountered during a project lifetime. Some risks can be foreseen while others can't. Similarly, some risks are controllable and effective risk management can reduce the impact while others are uncontrollable and can only be manage. Appendix A1 highlights any identified risks. As not all risks are able to be identified at first glance, the list is modified when any unidentified risks become apparent.

Appendix A1 classified each risk by how likely it is to occur, the severity of the risk, methods that could reduce the risk and any contingency plans should the risk becomes apparent.

A2 - Time and Progress Management

Effective progress and time planning can be done with the help of Gantt charts. Gantt charts in this project are split into 2 timelines Semester 1 (Appendix A2) and semester 2 (Appendix A3). Semester 1 plans were mostly completed during the first half of the project timeline.

Semester 1 Gantt chart provides a buffer region which allows any uncompleted works to be carried out without causing domino effect to the rest of the project progress. Part of building the gripper model and contact modelling was not carried out during this buffer region and the rest of the progress was carried out during Semester 2.

Since it takes longer than expected to complete the models, part of the Semester 1 was carried forward to Semester 2. Therefore, there is not sufficient time to test the controller design onto the physical system and compare the performance with the simulation results and evaluate the controller. It has been discussed in Chapter 8 as a potential future work area.

A3 - Risk Management Strategy

The risks are rank out of 5, where 5 is very likely/severe and 1 is unlikely/low severity. A small explanation of each risk is provided below the table

Risk	Risk likelihood	Risk severity	Risk reduction methods	Contingency plans
Loss of files	1	5	N/A	Daily backup of files to both pen drive and OneDrive
Simulation model does not work	3	5	N/A	Use MATLAB built in Simulink model
Simulation takes too many resources/too long	2	3	Reduce the step size of the simulation or run section by section	Request to use university computational resources
Simulation files incompatible with other versions	3	2	Ensure MATLAB does not get upgraded/downgraded during the project duration	Locate computer from university/friend which uses that version

Loss of files – Files might be corrupted or lost due to issues arising from computer/malware/theft.

Simulation model does not work – The attempts on building a working model which mimics the interested robot system fails or it takes much longer than expected to complete.

Simulation takes too many resources/too long – MATLAB has been known to consume a significant portion of resources to simulate, this can cause the simulation to be slow and takes a long time to complete.

Simulation files incompatible with other versions – MATLAB files are version dependent; it is not possible to run files created in newer versions on older ones. This could be a factor when simulating using university machines while using personal to write codes.

A4 - Semester One Gantt Chart

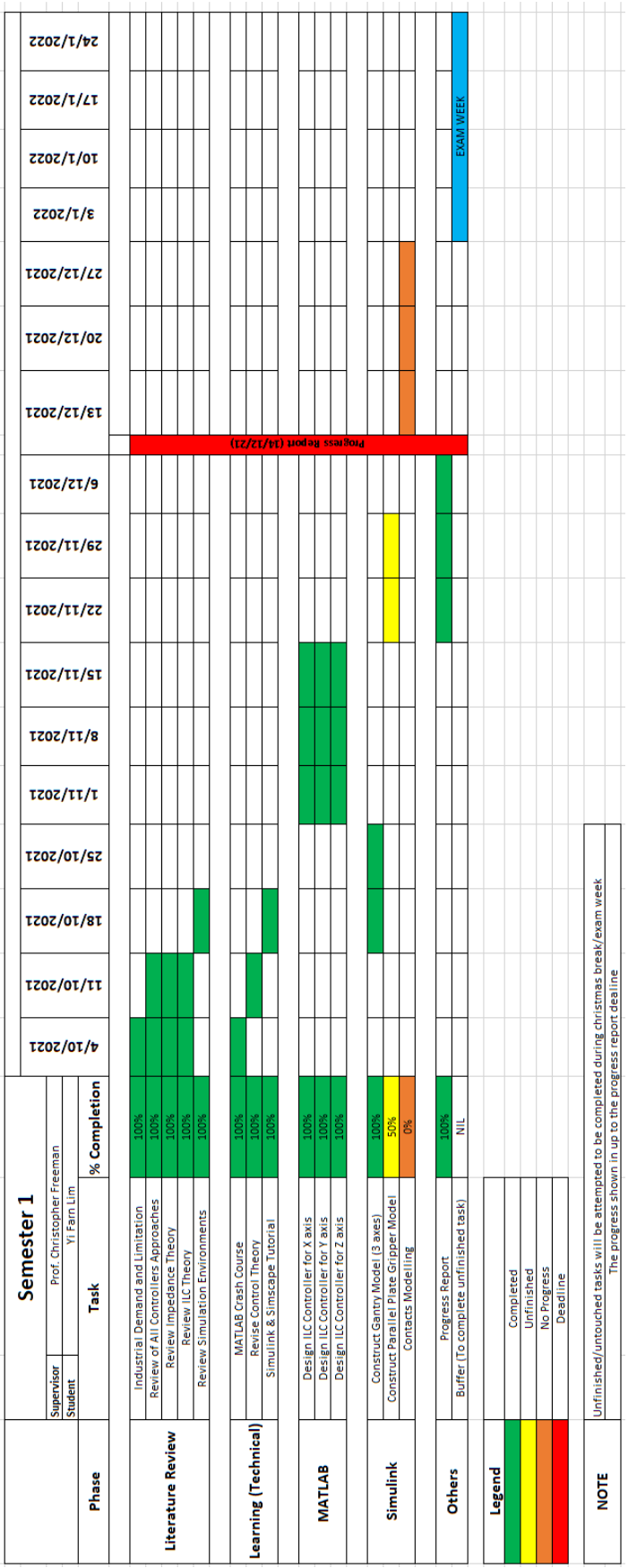

A5 - Semester Two Gantt Chart

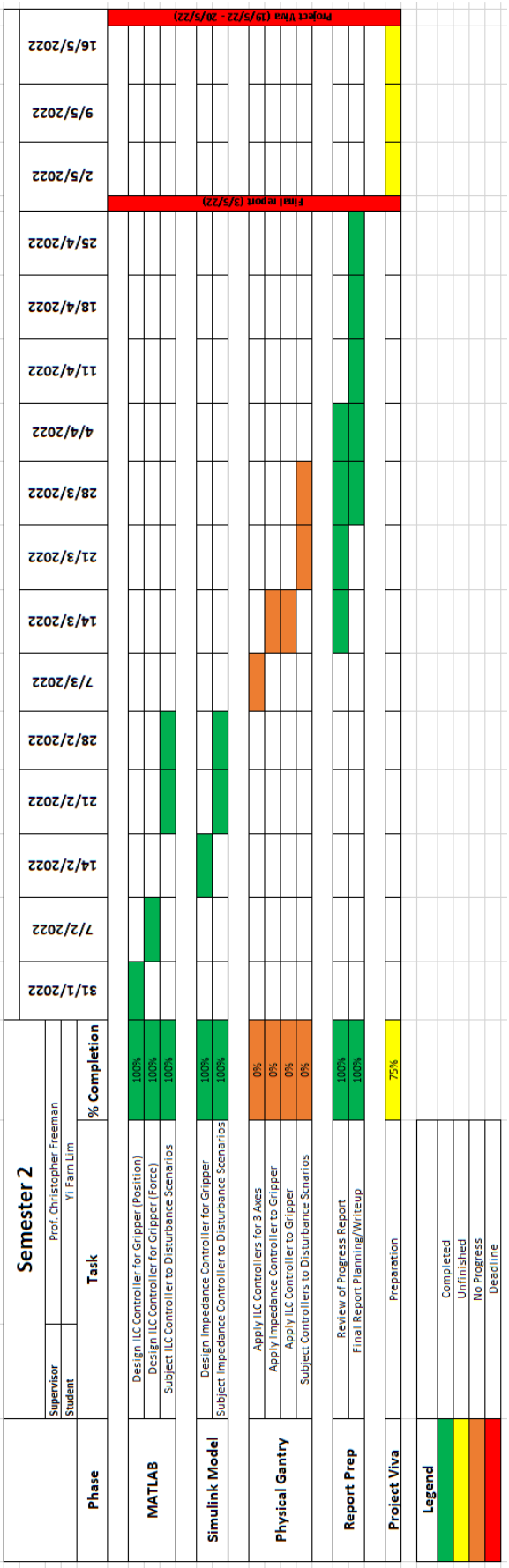

Appendix B. Project Assumptions

B1 - Position and Force Feedback

It is assumed that the position and force feedback provided to the controller is accurate. Although wear and tear are expected to build up and cause inaccurate data being fed into the controller. A frequent inspection of force sensors or encoder should ensure the error caused by damaged equipment is kept to a minimal. Hence, this is a valid assumption for simulation.

B2 - Force Applied by Gantry Robot

Unfortunately, the specification of the linear motor used by Ratcliff when constructing the Gantry robot is no longer available on the manufacturer website. The closest system that the specification is currently available is AGS1000 series by Aerotech. The maximum load the gantry robot can carry is 15kg.

The gripper of choice is a 0.2kg universal 2-finger parallel gripper (JGP-P 50-2-As) from Schunk which recommends grasping workpiece of 2kg. This gives a total load to be transported by the gantry robot to be 2.2kg which is within the 15kg recommendation.

According to the gantry manufacturer, the peak force to move in X direction is 916N while to move in Y direction is 458N. With a gentle rise and fall time of 0.8s for X and Y axis and 0.3s for Z axis, it is safe to assume that the force required would not exceed the recommendation provided by the manufacturer.

Appendix C. Simulink Model Schematic

This section will be dedicated to showing the full schematic for the model built in Simulink as well as detailed explanation of each part. The aim is to provide full information regarding how the simulation model is built.

C1 - Overview

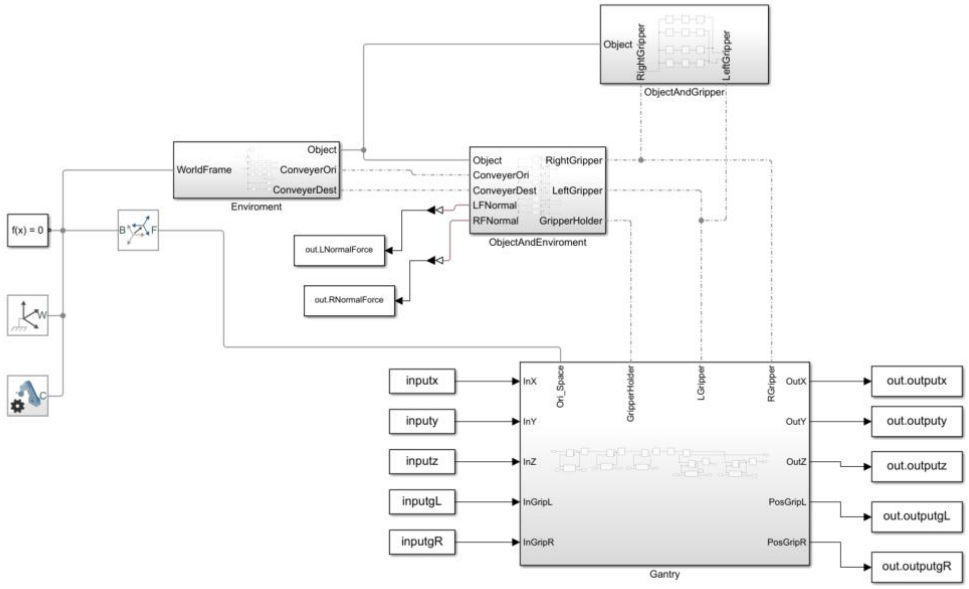

This shows the highest level of the schematic which is used for both ILC and Impedance controller. There are 4 major blocks that made up the whole simulation model: 'Environment', 'Object and Environment', 'Object and Gripper', and 'Gantry'. Each will be broken down further in the following subsections.

The definition for each ToWorkspace and FromWorkspace block is found at the table below.

Name	Type	Description
inputx	FromWorkspace	Pass X axis input vector from workspace (ILC)
inputy	FromWorkspace	Pass Y axis input vector from workspace (ILC)
inputz	FromWorkspace	Pass Z axis input vector from workspace (ILC)
inputgL	FromWorkspace	Pass Left Gripper input vector from workspace (ILC)
inputgR	FromWorkspace	Pass Right Gripper input vector from workspace (ILC)
out.outputx	ToWorkspace	Pass X axis position feedback to workspace
out.outputy	ToWorkspace	Pass Y axis position feedback to workspace
out.outputz	ToWorkspace	Pass Z axis position feedback to workspace
out.outputgL	ToWorkspace	Pass Left Gripper position feedback to workspace
out.outputgR	ToWorkspace	Pass Right Gripper position feedback to workspace
out.LNormalForce	ToWorkspace	Pass Left Gripper force feedback to workspace
out.RNormalForce	ToWorkspace	Pass Right Gripper force feedback to workspace

The schematic for Impedance controlled gripper is slightly different. This is due to implementing full impedance control in Simulink instead of passing values from workspace as done with ILC. The schematic can be found below. The major difference is the addition of 'Impedance control' and 'PD control', these will be further decomposed in the following subchapters.

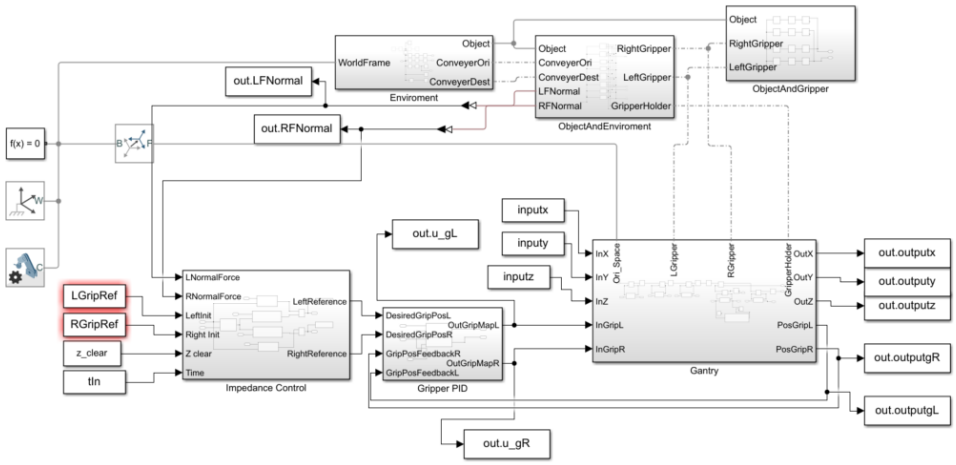

The definition for new ToWorkspace and FromWorkspace blocks can be found below

Name	Type	Description
LGripRef	FromWorkspace	Initial trajectory profile for Left Gripper
RGripRef	FromWorkspace	Initial trajectory profile for Right Gripper
z_clear	FromWorkspace	Logic signal to signal X, Y and Z axis has reach threshold
tIn	FromWorkspace	Discrete time samples
out.u_gL	ToWorkspace	Pass Left Gripper input signal to Workspace
out.u_gR	ToWorkspace	Pass Right Gripper input signal to Workspace

Data passed to workspace are either use as feedback for controllers or to plot, analyse and evaluate the controller performance.

A visual representation of the model is shown below along with labels.

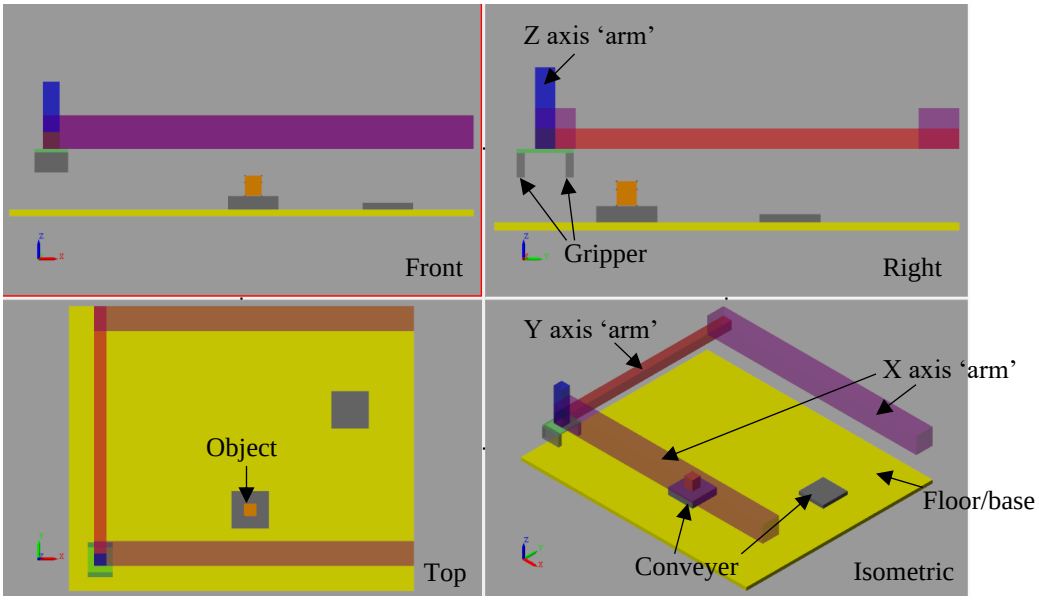

The following subsections will breakdown each individual subsystem of the model.

C2 - Environment

This subsystem contains all visual elements that do not affect the operation of the gantry robot which includes the object to be grasped (ObjectBlock), conveyer 'blocks'(ConveyerBlock and ConveyerBlock2), floor (BBB) and X axis arm to match the actual gantry (XArm1 and XArm2). The schematic is shown below

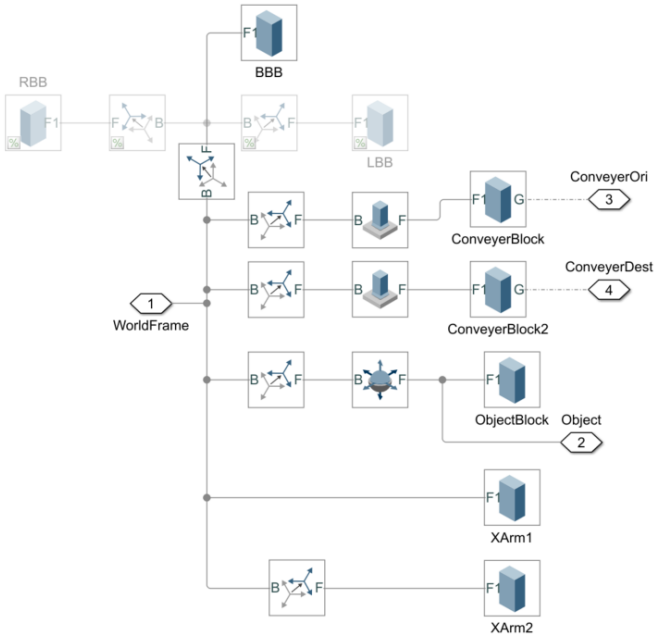

C3 - Gantry

This subsystem houses the blocks required to model the dynamics of the gantry robot and grippers.

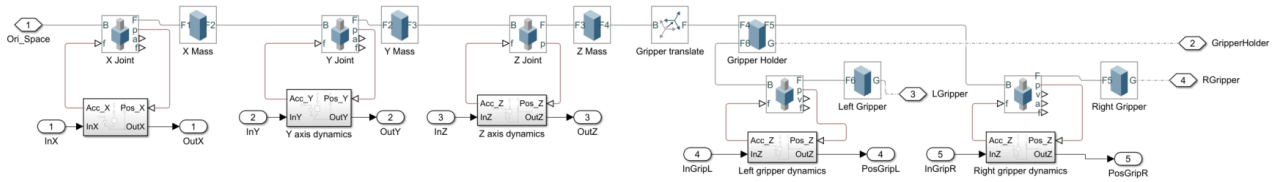

The dynamics of each part of the robot is modelled using a PD controller each with a similar schematic as follows.

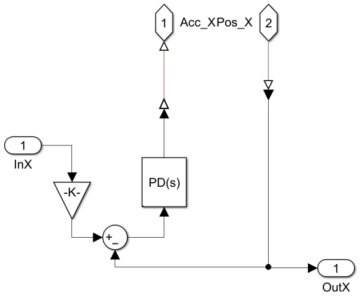

C4 - ObjectAndEnvironment

This subsystem focuses on the interaction forces and condition between the object and the environment which includes the conveyer where the object is located at and the top of the gripper (not finger). This makes up each top and bottom 4 spheres as circled below. As the object is a cube, A contact sphere located at each edge of the object ensures the object interact with the environment adequately and would not topple/rotate without external intervention.

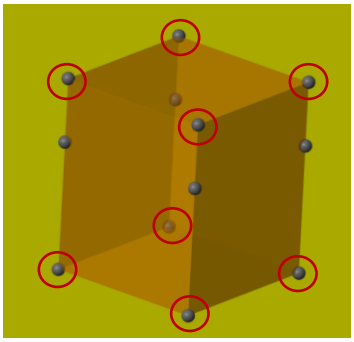

The schematic for such system is shown below. The contact schematic is slightly different for the top 4 spheres compare to

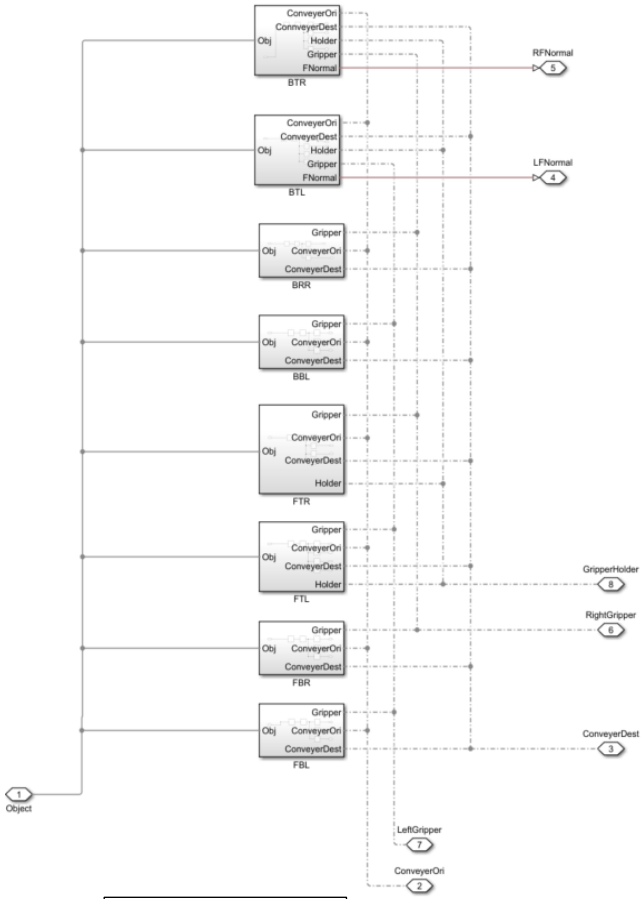

Main Subsystem

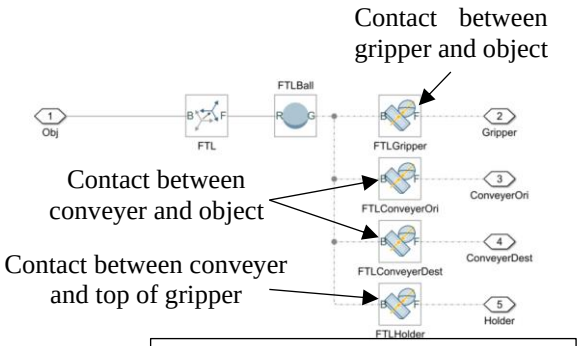

Top sphere subsystem (FTL, FTR, BTL, BTR)

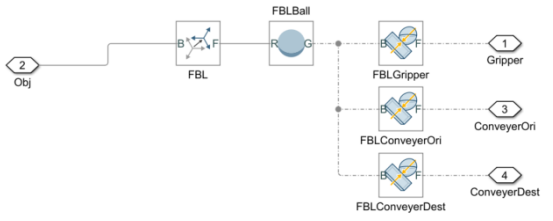

Bottom sphere subsystem (FBL, FBR, BBL, BBR)

C5 - ObjectAndGripper

This subsystem is similar to the previous one, where this focuses on the contact sphere located at roughly the centre of the object.

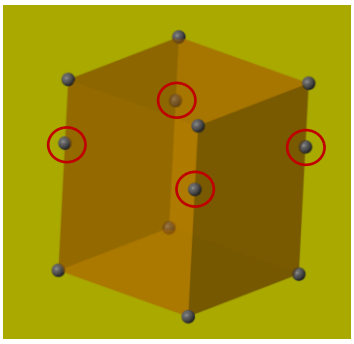

As this contact sphere is located roughly at the centre, it only has to interact with the gripper. Therefore, the schematic is relatively simple and is shown below.

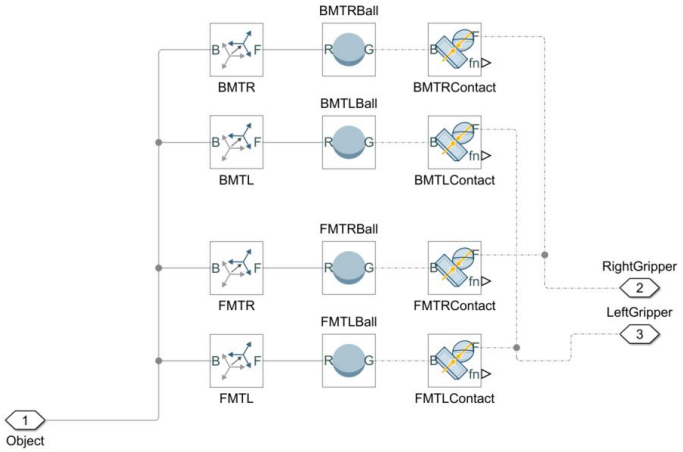

C6 - Impedance Controller

The impedance controller can be split into 2 sections. One is the force correction impedance control schematic and the other is the position correction PID schematic.

The position correction PID schematic is a simple feedback PID controller.

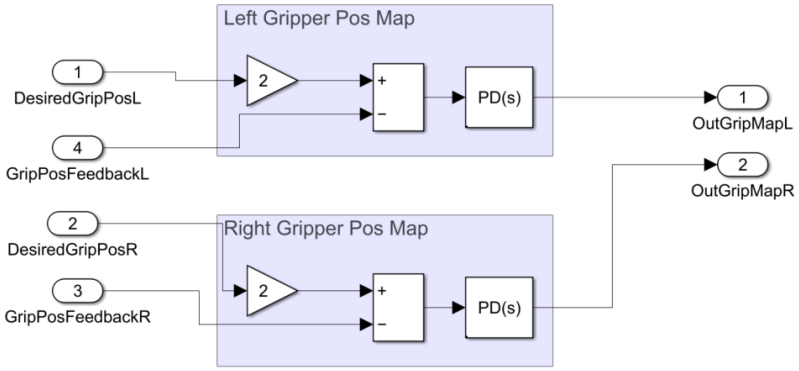

The force correction impedance control schematic is more complicated. Each finger controller is made up of 3 additional subsystems namely ‘F desired logic’, ‘Grip desired logic’, and ‘Grip Impedance Control’

F desired logic tells the impedance-controlled gripper when the X, Y and Z axis has reached the threshold and thus it is safe to grasp the object. Grip desired logic passes the initial grasping trajectory profile when the gripper is safe to grasp. Grip Impedance Control on the other hand attempts to match the actual force applied by the gripper to the desired value by changing the grasping trajectory.

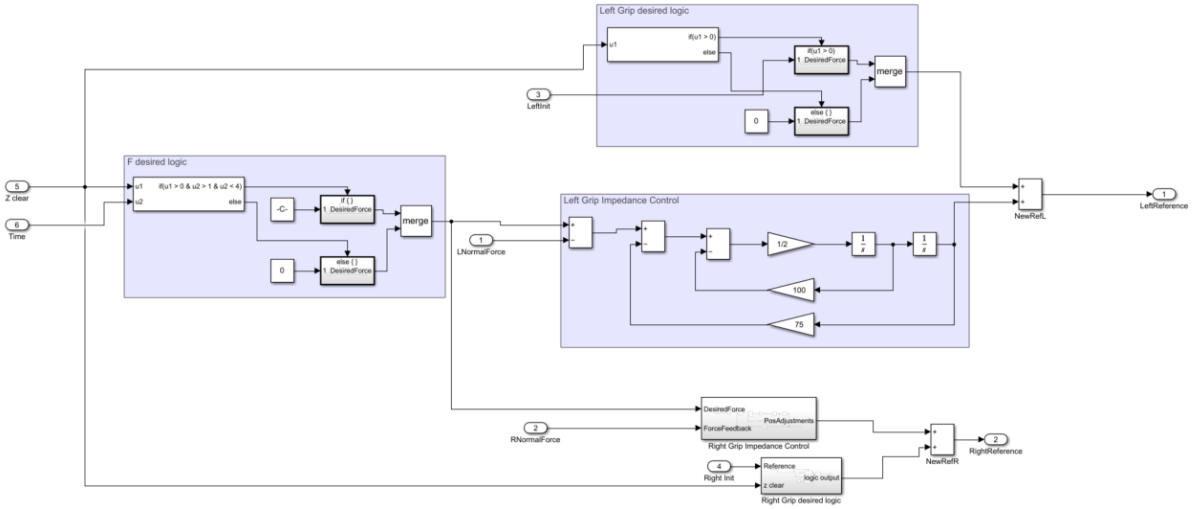

Appendix D. MATLAB Operational Code

This section focuses on the MATLAB part of the project. Two different scripts would be used, one for ILC operation while the other for Impedance.

As the scripts are relatively long, therefore this section will highlight the main features of the code in chronological order as appeared in the actual raw script. Detail of the scripts can be found with the files attached to the submission which are explained in Appendix E.

Simulation parameters
(This shows the parameters that would be use throughout the simulation)

Trajectory profile generation
(This generates the initial tracking profile used by controllers)

Disturbance generation
(This generates the required disturbance signals to be added to ILC input vector)

Grasped object dimensions
(This holds information about the object including number of contact points and calculate minimum grasping force)

Simulation environment details
(This holds information of conveyer height as well as contact modelling)

Logic flags
(Multiple logic flags has been created to be used by ILC and Impedance controller algorithm)

Gantry model
(This holds information about the details of the modelled dynamics using PD controller as well as discretising the modelled transfer function)

Constants for ILC Controller
(This holds information of constants used when updating the next iteration input vectors)

ILC Controller input vector
(This generates an initial all 0-input vector to be initially passed to the system)

Storing of crucial data
(This saves data for each iteration into a big matrix which can later be used to generate response from any iteration for analysis purpose)

Simulation loop
(Iterative simulation for X, Y and Z axis ILC controllers/algorithm and both ILC and Impedance gripper controllers/algorithm. Impedance controller would only require initial grasping profile to be passed)

Post simulation
(Display any important values or plots)

Appendix E. Achieve File Overview

The following flow chart shows the location of each supporting document submitted alongside this report.

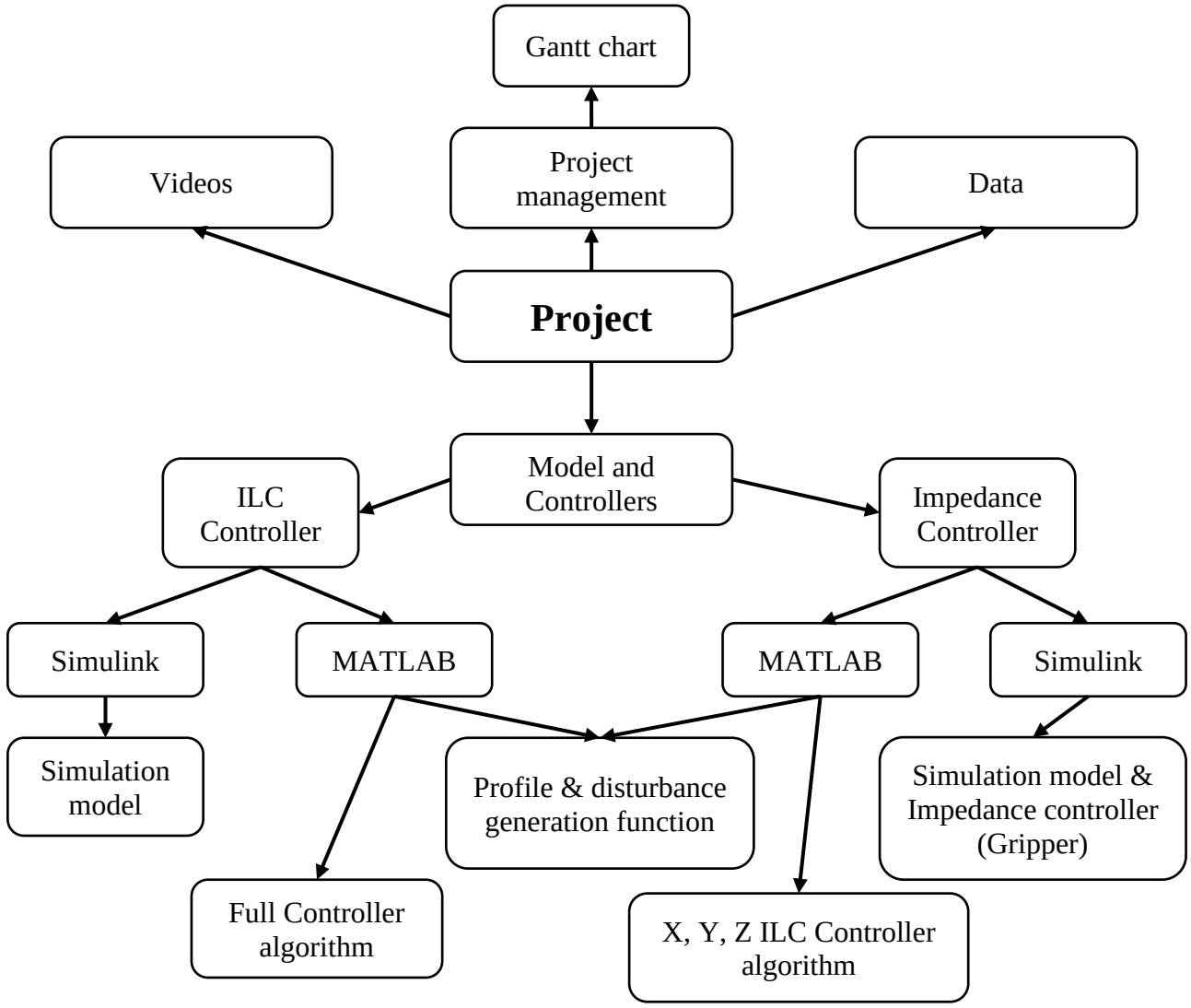

Model and Controllers – Contains all the files to build and run the model and controllers.

ILC Controller – Contains files for Gripper ILC Controller

Simulink – Files built and opened using MATLAB Simulink R2021b, including full simulation model (gantry and contact modelling) and/or gripper impedance controller.

MATLAB – Files built and opened using MATLAB R2021b, including trajectory profile and disturbance generation and/or ILC controller algorithm for X, Y, Z and/or Gripper.

Videos – Contains short videos of simulation for various interesting scenarios/cases

Project Management – Files used to effectively manage the progress and time of the project.

Gantt charts – Excel files for Gantt chart planning and progress tacking.

Appendix F. Project Brief

Problem

In this technologically rich era, our lives are filled with robotics as well as automation. From as simple as an autonomous robot vacuum machine to a more sophisticated multi degree of freedom robotic arm, all these systems required a state-of-the-art controller. As a result, the needs for faster, more precise, and accurate controller are ever more demanding.

There are numerous controllers out there capable of doing 300 picks per hour. On the other hand, the average human can grasp 600 times per hour. This makes robotic grasping twice as slow as an average human. One of the reason robotic grasping is much slower is due to the limited research conducted on robotic grasping, especially ones that incorporates Iterative learning control (ILC). ILC is crucial for robots that does repetitive motions such as a robotic grasping arm as it enables the controller to learn and improves from its own error and mistakes due to imperfection or just environmental factor.

ILC is not a new concept, in fact, it has been successfully applied onto numerous systems such as industrial robots, CNC machines tools, injection-molding machines and many more. However, applying ILC onto robotic grasping is relatively new and to the best of my knowledge there have been no experiments conducted into robotic grasping.

Goal

This project aims to:

- Read up literature, journals to identify different controllers as well as their advantages and points of improvements.
- Model accurately a 3-axis gantry robot as well as a simple gripper arm using Simulink simscape multibody toolbox.
- Attempts to design a new control algorithm which includes ILC to improve the accuracy and speed of the robotic gripper and simulate it using the model built on MATLAB.
- Test the control algorithm onto a real 3-axis gantry robot and identify any improvement or changes to be made to improve the controller and compare the result to the ones obtained via simulation.
- Further test the performance of the controller on a 6-DOF robotic arm.

Scope

My project aims to learn and identify different controller's strengths and weaknesses and adapt or attempts to design a new controller which incorporates ILC to improve the agility of robotic grasping. The project will start off by researching on different controller as well as modeling the gantry robot for simulation testing. The new controller will be tested first on MATLAB via simulation and will later be put to the test onto a real gantry robot. Works done previously on the gantry robot such as the model will be used as a reference and be improved further should any mismatch arises.

Furthermore, as an additional test, the controller will be programed onto a 6-DOF robot and be tested on it after receiving satisfactory results from the gantry robot.

I hope to design a new controller that is optimized for robotic grasping while incorporating ILC to improve its agility.